Title

Li/Ca, B/Ca, and Mg/Ca Composition of Cultured Sea Urchin Spines and Paleo-Echinoderms Measured Using a Secondary Ion Mass Spectrometer

Author

Nguyen, Trung Timothy Do

Publication Date

2013

Peer reviewed|Thesis/dissertation

UNIVERSITY OF CALIFORNIA

Los Angeles

Li/Ca, B/Ca, and Mg/Ca Composition of Cultured Sea Urchin Spines and Paleo-Echinoderms Measured Using a Secondary Ion Mass Spectrometer

A thesis submitted in partial satisfaction

of the requirements for the degree Master of Science

in Atmospheric and Oceanic Science

by

Trung Timothy Do Nguyen

2013

ABSTRACT OF THE THESIS

Li/Ca, B/Ca, and Mg/Ca Composition of Cultured Sea Urchin Spines and Paleo-Echinoderms Measured Using a Secondary Ion Mass Spectrometer

By

Trung Timothy Do Nguyen

Master of Science in Atmospheric and Oceanic Science
University of California, Los Angeles, 2013
Professor Aradhna K. Tripati, Chair

Element-to-calcium (X/Ca) ratios within biogenic calcium carbonate minerals are used as proxies to reconstruct past seawater temperature and composition. This study focuses on examining Li/Ca, B/Ca, and Mg/Ca ratios in sea urchins cultured at different temperatures and pCO_2 levels.

In situ secondary ion mass spectrometry (SIMS) analyses were conducted on two species of sea urchins cultured under controlled conditions and several species of paleo-echinoderms. A temperate species, *Arbacia punctulata,* was cultured at various pCO_2 levels (400, 600, 900, 2850 ppmv) with temperature held constant at 25°C. A tropical species, *Echinometra viridis,* was cultured in variable pCO_2 (400 and 1000 ppmv) and temperature (20°C and 30°C) conditions.

In the tropical species, a positive correlation was found between temperature and the analyzed (Li, B, Mg) element-to-calcium ratios of the spines, while variable responses to pCO_2 were observed. In the temperate species, a variable response to increasing pCO_2 was observed, with B/Ca having a similar trend to the calcification rate found in a previous study by Ries et al. (2009). Paleo-echinoderm samples varied in age from 518 to 53 Ma, and have a global distribution. The X/Ca ratios from paleo-echinoderms were used, along with the full range of observed partition coefficients ($D^{c}X/Ca=X/Ca_{carbonate}/X/Ca_{fluid}$, with X=Li, B, or Mg in this study) from the cultured sea urchins, to model element-to-calcium ratios of paleo-seawater.

The thesis of Trung Timothy Do Nguyen is approved.

Ulrike Seibt

Axel K. Schmitt

Aradhna K. Tripati, Committee Chair

University of California, Los Angeles

2013

Dedication

I would like to dedicate this thesis to my family for their support and encouragement throughout my program. I would also like to dedicate this to Christy.

Table of Contents

Acknowledgements

I would like to thank Dr. Kevin McKeegan and Dr. Axel Schmitt in the department of Earth and Space Sciences, UCLA, for allowing us to perform the SIMS analysis on their equipment. I would also like to thank Dr. Alexander Gagnon and Dr. Ellen Druffel for providing aragonite reference material for Mg/Ca analysis; Dr. Claire Rollion-Bard and Dr. Nathalie Vigier for synthetic calcite reference material for Li/Ca analysis; Dr. Simone Kasemann for coral reference material, as well as for performing the B/Ca analysis. I would like to thank Dr. J.A.D. Dickson and his group for providing the paleo-echinoderm samples. I would also like to thank Dr. Justin Ries and his lab for providing the cultured sea urchin samples for this study, Dr. Rob Eagle for his input, and Vanessa Brillo for her assistance in sample preparation. I would like to thank Dr. Rinat Gabitov, my mentor, for his help and expertise on the SIMS. Finally I would like to thank my advisor, Dr. Aradhna Tripati, for her help throughout the writing of this paper and my program. This work was supported by the Hellman Foundation and the American Chemical Society. SIMS analyses were supported by NSF/EAR: Instrumentation and facilities.

Introduction

Acidification of the Oceans

Throughout Earth's history, carbon dioxide (CO_2) levels in the atmosphere have greatly varied (e.g. Hönisch et al., 2012). Through the use of proxies, geoscientists are able to reconstruct past pCO_2 levels. Air bubbles in polar ice cores show a maximum pCO_2 of ~280 ppmv during interglacial periods, and a minimum pCO_2 of ~180 ppmv during glacial periods (Petit et al., 1999). Although data from ice cores provides scientists with an understanding of atmospheric CO_2 levels over the past 800,000 years (e.g. Laurent et al., 2004), indirect proxies based on the sensitivity of element-to-calcium ratios in biogenic carbonate minerals to the carbonate chemistry of seawater are used to validate the ice core data and reconstruct CO_2 levels during earlier periods (Hönisch et al., 2009; Tripati et al., 2009).

Carbon dioxide readily dissolves in seawater (Equations 1-3). After CO_2 dissolves in seawater, nominally bicarbonate (HCO_3^-), carbonate (CO_3^{2-}), and two hydrogen ions (H^+) are formed (Sarmiento and Gruber, 2006). The release of hydrogen ions lowers pH and results in an increase of seawater acidity. Currently, the atmospheric CO_2 concentration is about 395 ppmv and predictions for future atmospheric CO_2 concentrations vary in different studies. In the worst-case scenario, it is predicted to rise to 1000 ppmv within the next century (Intergovernmental Panel on Climate Change, 2007). It is estimated that this increase would cause the ocean's pH levels to drop to about 7.8, thus causing the ocean to become more acidic than present day levels of ~8.2.

$$CO_{2\ (gas)} + H_2O \Leftrightarrow H_2CO_3 \quad (1)$$

$$H_2CO_3 \Leftrightarrow H^+ + HCO_3^- \quad (2)$$

$$HCO_3^- \Leftrightarrow H^+ + CO_3^{2-} \quad (3)$$

Due to the decrease in seawater pH, many marine invertebrates, that utilize calcium carbonate ($CaCO_3$) as part of their skeleton will be negatively impacted. The decreased pH levels will affect the $CaCO_3$ saturation state (Ω). Due to decreased pH, the availability of CO_3^{2-} will decrease, which in turn affects the calcification rates of marine invertebrates (Fabry et al., 2008; Ries, 2011). The saturation state of calcium carbonate (Ω) is the measure of the potential for calcium carbonate to form or dissolve in seawater (Equation 4). This is based on the solubility product (K_{sp}) and the concentration of the two ions that form $CaCO_3$ ($[Ca^{2+}]$ and $[CO_3^{2-}]$). For values of Ω greater than 1, $CaCO_3$ tends to precipitate in seawater. When values of Ω are less than 1, $CaCO_3$ dissolves in seawater. Future projections of atmospheric pCO_2 also predict the saturation state of the ocean to be less than 1 (Anderson et al., 2005; Feely et al., 2009).

$$\Omega = \frac{[Ca^{2+}][CO_3^{2-}]}{[K_{sp}]} \quad (4)$$

This thesis is focused on investigating the systematics governing the incorporation of lithium, boron, and magnesium into the calcium carbonate of sea urchin spines. Ultimately, this work is relevant to the development of proxies for past seawater compositions and the reconstruction of changing ocean chemistry and carbonate system parameters through time. It may also provide insights into how organisms that secrete $CaCO_3$, are affected when the pCO_2 of their environment is manipulated.

Evolution and Biology of Sea Urchins

Sea urchins are classified under the phylum echinodermata and contain over 70,000 extant species (Barnes, 1963). They began to appear in the Lower Cambrian and have a large geographical distribution (Paul and Smith, 1984). Within the phylum echinodermata, there are over 700 species of sea urchins classified and they can be found living in the tidal and intertidal

zone down to depths of 7 km (Hendler et al., 1995). They feed mostly on algae, although some species feed on a variety of invertebrates such as mussels and sea slugs. Sea urchins' endoskeleton and spines are composed of calcite (Lawrence, 1987).

Sea urchin spines have been extensively studied and are used by the animal in many different ways. The spines main use is for defense against predation and mobility on the ocean floor. It has been observed that a sea urchin knocked over either by ocean turbulence or by a predator can use its spines to push itself upright (Lawrence, 1987). It was also discovered that some species of sea urchins use their spines to dig burrows in rocks to hide from predators (Kozloff, 1990). Sea urchin spines are composed of a single piece of Mg-bearing calcite which has tiny micrometer-sized spaces filled with living cellular tissue called stereom (Politi et al., 2004; Su et al., 2000) (Fig. 1). The spine growth rate depends on several factors such as seawater temperature and age of the sea urchin, but generally urchin spines take up to a year to reach full length (Ebert, 1968; Hendler et al., 1995). When damaged or disturbed by a predator, urchin spines can regenerate within a couple of days (Markel and Roser, 1983; Politi et al., 2004).

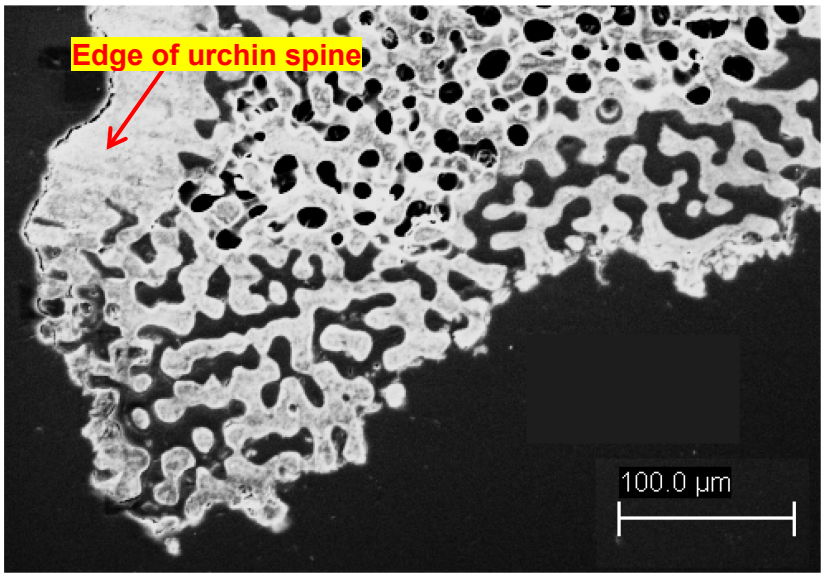

Figure 1: Back-scattered electron (BSE) image of a test urchin spine to see the porous structure (stereom) of the calcite matrix. The edge of the urchin spine (left) to the center of the urchin spine (right)

Sea urchins are extensively studied because they are a model organism in developmental biology; their development from a fertilized egg to a fully-grown adult can be easily studied under an optical microscope (Yokota, 2002). When sea urchins reach maturity, males and females begin to spawn. Spawning is done externally, meaning that the eggs and sperm are released into the water. Sea urchin spawning depends on many factors, such as species and water temperature. Once an egg is fertilized, it can take as little as 12 hours for the single-celled egg to transform into an aggregate of cells. After forming into this aggregate, the cells go through several more phases until being transformed into a cone-shaped echinopluteus larva. This larva is mobile and contains about 12 arms which help catch plankton or food in the ocean water. Over the course of several months, the echinopluteus larva will form test plates around its mouth and anus, and it will transform into an adult at the bottom of the ocean floor (Kozloff, 1990).

Studying the calcification of sea urchins, as well as how their calcium carbonate structure incorporates trace elements may provide clues about how climate has responded in the past, and will respond in the future, to changes in the concentration of CO_2 in the atmosphere.

Sea Urchin Calcification

The development of the sea urchin endoskeleton undergoes three transformations: it begins as a single crystal of Mg-bearing calcite, then amorphous calcium carbonate is formed, and, finally, calcite is formed. During the larval stage, the endoskeleton of the sea urchin contains two spicules which are sharp pointed structures, each one containing a single crystal of Mg-bearing calcite (Wilt and Benson, 1988). This single crystal of Mg-bearing calcite is formed from calcium found in the surrounding seawater (Gilbert and Wilt, 2011). Amorphous $CaCO_3$

dominates during early stages of development in the sea urchin and transforms into calcite over a relatively short time frame (Beniash et al., 1997). A study done on the sea urchin *Paracentrotus lividus* found the transformation from amorphous $CaCO_3$ to calcite occurred within 48-96 hours (Beniash et al., 1997). Amorphous $CaCO_3$ is highly unstable and is a precursor for more stable calcite or aragonite (Beniash et al., 1997). As the sea urchin larva develops into a more mature individual, the amorphous $CaCO_3$ transforms into calcite. Near the end of the life cycle, the endoskeleton of the sea urchin is dominated by calcite, although amorphous $CaCO_3$ may still be present in the regenerating spines (Politi et al., 2004).

Cultured Sea Urchins

Spines of the temperate *Arbacia punctulata* (purple urchin) and the tropical *Echinometra viridis* (reef urchin) were investigated in this study (Ries et al., 2009; Courtney et al., 2013). Approximately twenty cultured individuals were obtained from Justin Ries and Travis Courtney at the University of North Carolina–Chapel Hill (UNC-CH) who collected them in the Atlantic Ocean off the North coast of Florida as adult specimens.

A. punctulata, a temperate urchin, can be found from Cape Cod, Massachusetts to Cuba and the Yucatan Peninsula. The body, or test, is dark brown to purple in color and has spines, up to 100mm (Hendler et al., 1995). They can be found in turtle grass (*Thalassia testudinum*) beds and on coral reefs. *A. punctulata* is mostly an herbivore, feeding on algae and turtle grass, although it occasionally eats sponges, sand dollars, and other small marine invertebrates that it encounters.

The tropical sea urchin *E. viridis* is commonly known as a reef urchin. Its habitat ranges from southern Florida to the West Indies and Venezuela. Unlike other sea urchins, *E. Viridis* does not live inside rocks, but remains hidden in coral reefs. The test is generally reddish-

brown, and the spines are brownish-green, tipped with purple. *E. viridis* is an herbivore and only grazes on algae.

After being transferred from their natural habitat, both temperate and tropical specimens were cultured at the Environmental Systems Laboratory in Woods Hole Oceanographic Institution (WHOI) for 60 days in a 38-liter glass aquaria filled with filtered seawater obtained from the Great Harbor in Vineyard Sound off the coast of Cape Cod, Massachusetts. The temperature was maintained to a constant value (20, 25, or 30°C) using 50-watt electric heaters, and water was filtered using polyester fleece and activated carbon. The air-CO_2 gas mixture was added to the aquaria through 6-inch micro-porous air-stones which were secured to the base of the aquaria following culturing techniques described in Ries et al. (2009). *For more detailed information regarding the culturing experiment refer to Ries et al. (2009).*

Arbacia punctulata was grown at a constant temperature of 25°C with varying pCO_2. The pCO_2 levels ranged from 409 (±6), 606 (±7), 903 (±12), and 2856 (±54) ppmv (corresponding to $\Omega_{calcite}$= 2.06, 1.58, 1.21, 0.54, respectively). Seawater pH was determined using an Orion pH electrode/meter calibrated with certified NBS pH standards of 4.01, 7.00, and 10.01. *Echinometra viridis* was cultured under varying pCO_2 (400 (±27) and 1000 (±45) ppmv and temperature (20°C and 30°C) (Courtney et al., 2013). Salinity was measured from total dissolved solids (TDS) with units in practical salinity units (psu). Alkalinity (μM) was measured biweekly by small or large volume Gran titrations. Parameters for the different culturing conditions the sea urchins were grown in are summarized in Table 1**.**

Table 1: Averaged measured and calculated parameters of the carbonate system from culturing experiment by Ries et al. (2011).

Sea Urchin	Taxa	Common Name	pCO_2 (ppmv)	T (°C)	Salinity (psu)	Alkalinity (μM)	pH
Arbacia punctulata	Temperate	Purple Urchin	400	25	31.9	1744	8.04
			600	25	31.8	1751	7.90
			900	25	31.7	1792	7.77
			2850	25	31.7	1891	7.36
Echinometra viridis	Tropical	Reef Urchin	400	20	31.9	1744	8.04
			400	30	31.9	1744	8.04
			1000	20	31.7	1796	7.70
			1000	30	31.7	1796	7.70

A study from Ries et al. (2009) found that the net calcification rate of *A. punctulata* increased under the intermediate pCO_2 levels (900 ppmv) and then decreased once at the highest pCO_2 (2850 ppmv) relative to the lower pCO_2 treatments One explanation put forth to explain the behavior of *A. punctulata* is that they produce an organic layer that separates their endoskeleton from the surrounding seawater (Ries et al., 2009). Another possible explanation was that *A. punctulata* was able to regulate the pH at the site of calcification, which could help offset the decreased pH in surrounding seawater. The response of the *E. viridis* to variable pCO_2 and temperature showed that the calcification rates of the sea urchin increased under elevated temperature (30°C) and decreased under increased pCO_2 (1000 ppmv) (Courtney et al., 2013). The varied responses found in these marine calcifiers shed light on the complexity of predicting how the future increases in atmospheric pCO_2 will affect marine organisms.

Fossilized Echinoderms

In addition to modern cultured sea urchins, several different species of fossilized echinoderms were examined using the SIMS. These samples were previously analyzed by J.A Dickson (University of Cambridge, Dept. of Earth Sciences) to determine Mg/Ca ratios using an electron microprobe (Dickson, 2004). The fossilized echinoderms were acquired from locations summarized in Table 4, and were prepared as thin cross-sections. Dickson (2004) determined the Mg/Ca content and compared it to the age of the samples to see how the Mg content of the

oceans has evolved since the Carboniferous Era. The paleo-seawater Mg/Ca ratios found in the paleo-echinoderms were similar to those found by other studies based on different materials (Wilkinson and Algeo, 1989; Hardie, 1996; Horita et al., 2002). These same specimens were analyzed by SIMS for Mg/Ca, Li/Ca, and B/Ca as part of this thesis.

Paleo-Climate Proxies

Lithium/Calcium

Dissolved lithium (Li) in seawater is a relatively long lived element with a residence time of about a million years, and a current oceanic concentration of 26 μM (0.194 ppm) (Huh et al., 1998). Most of the lithium found in the ocean comes from river runoff and sedimentation in the form of lithium ions (Li^+) (Chester, 2000). The incorporation of Li into calcium carbonate depends on the precipitation environment, with temperature, growth rate, and carbonate chemistry possibly playing an important role in how much Li can be incorporated into calcium carbonate (Marriott et al., 2004a; Lear and Rosenthal, 2006).

A study by Delaney et al. (1985) examined several species of cultured planktonic foraminifera and investigated how these speices incorporate minor elements (Li, Sr, Mg, and Na) into their calcite structure under varying temperatures. The study did not find a clear relationship between temperature and Li/Ca ratios in foraminfera and the study asserted that there may be an unknown factor controlling the amount of lithium incorporation (Delaney etl al., 1985) (Fig. 2). More recently, Li/Ca ratios in inorganic calcite were determined to be inversely correlated with temperature in a study performed by Marriot et al. (2004a); the results were explained using a model indicating that experiments reflect Li incorporation is due to an exothermic effect, and that Li incorporation is less favored at higher temperatures (Marriot et al., 2004a) (Fig. 2). Thus, during the formation of the inorganic calcite crystals, Li incorporation is expected to be highest at low temperatures, resulting in higher Li/Ca ratios in calcite.

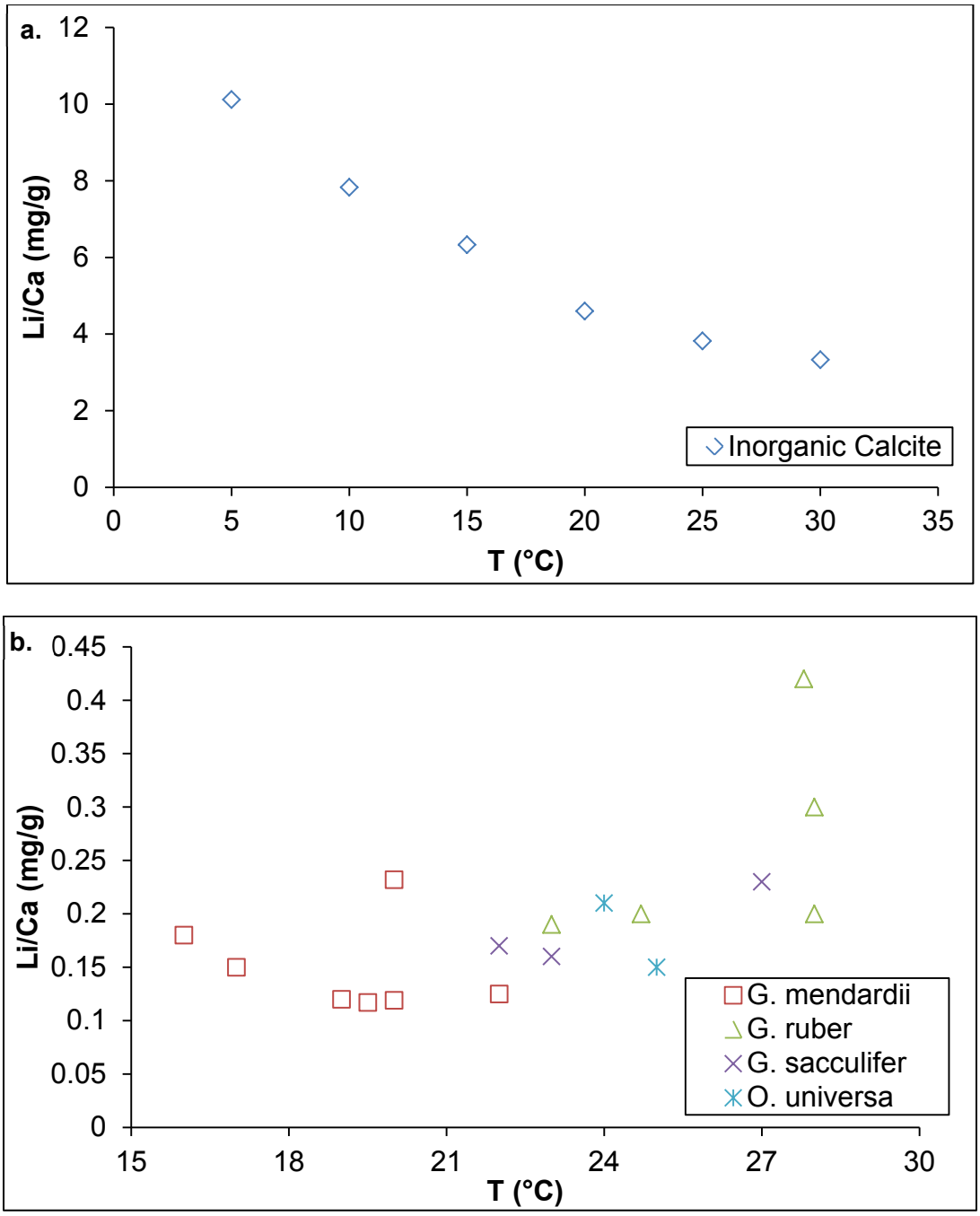

Figure 2: Li/Ca ratios (mg/g) for (a.) inorganic calcite (Marriott et al., 2004a) and (b.) different species of cultured planktonic foraminifera (Delaney et al., 1985). Plot symbols: ◊, Inorganic calcite; ○, *G. mendardii*; △, *G. ruber*; ×, *G. sacculifer*; ✳, *O. universa.* Each point represents the average of 4-5 specimens.

Since lithium incorporation is apparently influenced by temperature during inorganic calcite precipitation, Li/Ca in biogenic calcite can be calibrated as a thermometer of the

temperature of precipitation. Therefore, the Li/Ca ratio in ancient carbonates, such as foraminifera and echinoderms, can be used to reveal past temperatures for a short timescale (typically less than 1 Ma) and/or elemental composition of the oceans, which is linked to the weathering rates and thus to the carbon cycle.

Boron/Calcium

Boron (B) is a conservative element in seawater with a residence time of about sixteen million years (Taylor and McLennan, 1985). The two species of dissolved boron in solution that are dominant in the ocean are borate ion, $B(OH)_4^-$, and boric acid, $B(OH)_3$ (Hershey et al., 1986). Equation (5) shows the typical reaction of boron in seawater.

$$B(OH)_3 + H_2O \Leftrightarrow H^+ + B(OH)_4^- \quad (5)$$

The formation of borate ion or boric acid is dependent on the pH of the seawater. Under high ocean-pH (basic) conditions more borate ions are produced, while under lower ocean-pH (acidic) conditions more boric acid is produced. Since the pH of the ocean water is coupled to atmospheric CO_2 levels, an increase in CO_2 levels will decrease ocean-pH, thereby increasing ocean acidity (Fabry et al., 2008). It has been suggested that HBO_3^{2-} substitutes for CO_3^{2-} in carbonate (Hemming and Hanson, 1992). In Equation (6), the reaction of calcium carbonate with the borate anion and the substitution of boron for CO_3^{2-} are shown.

$$CaCO_{3\,(solid)} + B(OH)_{4(aq)} \Rightarrow Ca(HBO_3)_{(solid)} + HCO_{3\,(aq)} + H_2O \quad (6)$$

Since the pH of the ocean will affect the amount of borate ion or boric acid, these reactions govern the application of B/Ca levels in carbonates as a proxy for paleo-CO_2 levels.

Several studies have aimed to experimentally determine the relationship between boron and calcium under varying pH levels. The results from an early study concluded that the amount

of boron incorporated into benthic and planktonic foraminiferal shells varies from species to species, and some species were able to vary their pH at their site of calcification (Furst et al., 1976). Synthesis experiments of $CaCO_3$ under varying pH established a B/Ca partition coefficient (Hemming et al., 1994). Using the B/Ca partition coefficient of Hemming et al. (1994), the B/Ca ratios in foraminifera species (*Globigerinoides ruber* and *G. sacculifer*) were translated into seawater pH and pCO_2, and correlate well with ice core data for atmospheric CO_2 levels (Tripati et al., 2009).

There are still a number of uncertainties in using boron as a proxy for seawater carbonate chemistry. Studies by Jorgensen et al. (1985) and Nooijer et al. (2009) confirmed by direct pH measurements that some foraminifera species are able to change the pH at the site of calcification. A similar result to Furst et al. (1976) was deducted from boron isotopes measurements within another foraminifera species, *Amphistegina lobifera.* This species was also able to control the pH at the site of calcification (Rollion-Bard and Erez, 2010). The ability to change the pH at the site of calcification will change the amount of boron that is incorporated into the shell and affect the pH values that can be calculated from the boron-to-calcium ratios. This complication is an aspect of B/Ca ratios that needs to be addressed before the proxy can be applied with a reasonable amount of certainty.

Magnesium/Calcium

Dissolved magnesium (Mg) is commonly present in the surface waters as Mg^{2+} and is uniformly dispersed throughout the ocean water column. It is a long-lived trace element in the ocean with a residence time of about 15 million years (Broecker and Peng, 1982). The main source of magnesium in the ocean is from the weathering of igneous rocks, and it is removed from seawater through precipitation into marine sediments and hydrothermal reactions (Berner et al., 1983; Michard and Albarède, 1986; Broecker and Yu, 2011). Previous culturing

experiments of calcifying organisms and synthetic calcite have established a positive correlation between Mg/Ca ratios in calcite and temperature (Chave, 1954; Katz, 1973; Nürnberg et al., 1996; Rosenthal et al., 1997; Lea et al., 1999; Russell et al., 2004) (Fig. 3) Since there is a relationship between magnesium and temperature, the amount of magnesium that is incorporated into calcite can be used as a proxy for past ocean temperature.

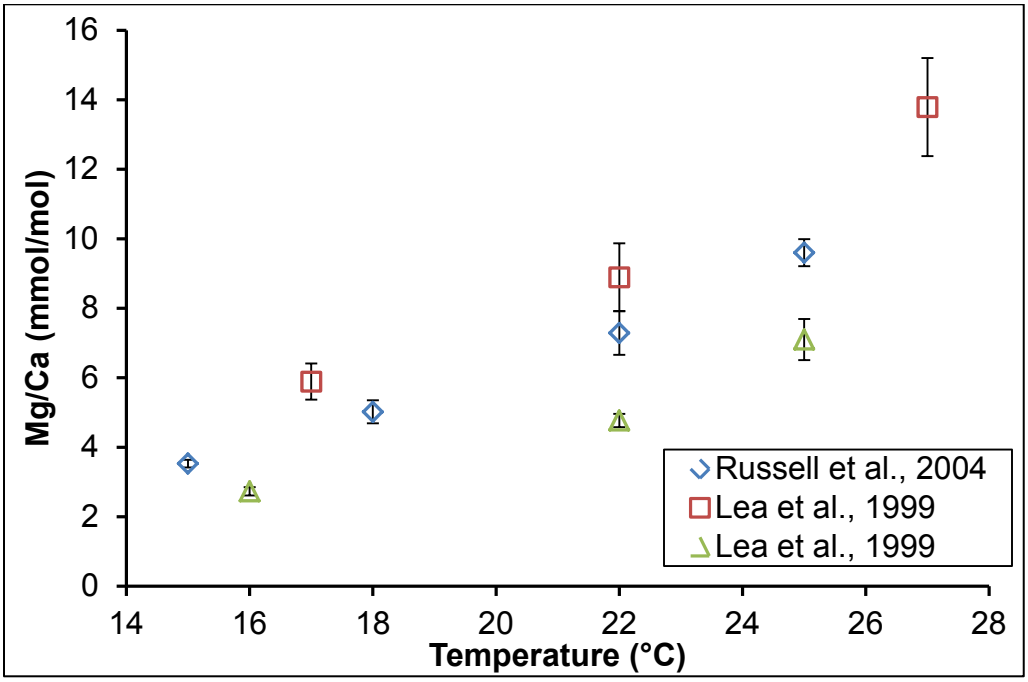

Figure 3: Reproduced data for Mg/Ca ratios (mmol/mol) and temperature in cultured planktonic foraminifera: *O. universa* (open red squares and open blue diamonds) and *G. bulloides* (open green triangles) (Russell et al., 2004; Lea at al., 1999). Each point represents a mean of 4 to 10 individual analysis of pooled shells.

The effect of seawater pH on Mg/Ca ratios in foraminiferas appears to be less pronounced than the effect of temperature (Lea et al., 1999; Russell et al., 2004). The results from the culturing experiments indicate higher Mg/Ca ratios under lower seawater pH (more acidic), and the dependence between Mg/Ca ratios and pH was less significant at the highest pH (Lea et al., 1999). The reason for Mg/Ca ratios being higher under lower seawater pH may be due to complex mechanisms controlling how the calcification rate affect foraminifera shell Mg

incorporation. Temperature, in this case, would be a much stronger control of Mg/Ca ratios in foraminifera with pH being a secondary influencing factor.

Secondary Ion Mass Spectrometery (SIMS)

Secondary ion mass spectrometry (SIMS) is a micro-analytical technique with high sensitivity that can be used to analyze a small portion of a sample (typically several pg), in comparison to conventional bulk mass spectrometry analysis which sometimes requires several micrograms of the sample. In SIMS, the material is removed (1-2 nm deep) from the sample surface through an energetically focused ion beam, then the charged fraction of the ejected material is analyzed in a mass spectrometer (Benninghoven et al., 1987). The process requires the samples to reside in an ultrahigh vacuum ($\leq 10^{-6}$ Torr), so that the generated ions can be effectively collected. For this project, analysis of the samples by SIMS required one day of tuning to achieve instrument conditions suitable for Li/Ca, B/Ca, and Mg/Ca analysis as well as several working days (2-3 days) to analyze the cultured urchin spines and paleo-echinoderm samples. The basic components of a SIMS instrument are: the sample located in a holder, a source of primary ions, primary and secondary ion columns comprising ion optical elements such as lenses, apertures, and slits as well as a double focusing mass spectrometer. The ion optical components steer the primary and secondary ion beams to achieve the optimal spatial and mass resolution, while maximizing ion transmission.

Methodology

Preparation of Cultured Sea Urchin Spines

To analyze sea urchin spines by SIMS, the spines were cast into epoxy requiring several preparation steps described in detail below. Epoxy-mounted spines were placed in a standard steel holder. This holder is designed to take up to 2.5 cm diameter cylindrical samples with a maximum thickness of 0.5 cm.

Subsets of the temperate urchin (*A. punctulata)* spines were selected so that there would be two of the same culturing treatments in one epoxy mount (Table 2). Each epoxy mount for the tropical urchin spines (*E. viridis)* contained two of each of the culturing conditions (pCO_2= 400 and 1000 ppmv and T=20°C and 30°C) (Table 3). There were a total of eight *A. punctulata* spines cast into one epoxy mount and a total of twelve *E. viridis* spines cast into another epoxy mount.

Table 2: List of *A. punctulata* spines that were cast into an epoxy mount. Each spine number corresponds to Figure 4

Spine #	Spp. ID	pCO_2	T (°C)
1	4213	400	20
2	1211	1000	20
3	4311	400	30
4	1311	1000	30
5	4233	400	20
6	1333	1000	30
7	4332	400	30
8	1233	1000	20

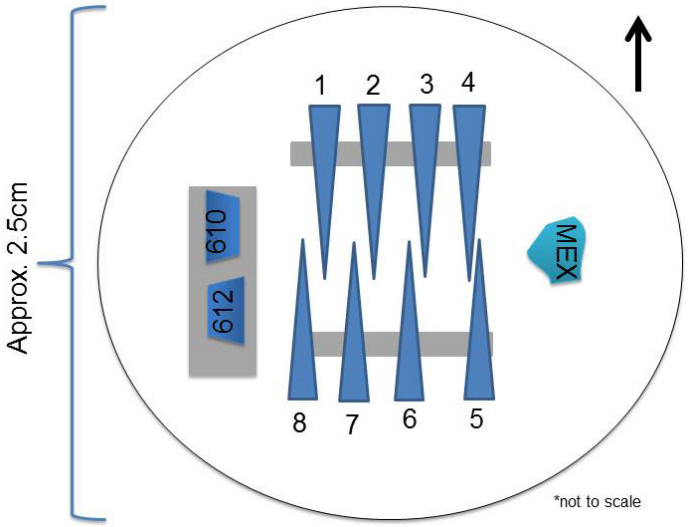

Figure 4: An example of how *A. punctulata* spines were casted in epoxy. The long triangles (blue) represent the urchin spines with the tips pointed downward towards the 3M® 701DL double sided tape. The three rectangles (gray) are the scarp pieces of calcite that the urchin spines rest on. The two standards, NIST-SRM 610 and 612 silicate glass and MEX-calcite are placed to the left and right, respectively, of the spines. The numbers correspond to the urchin samples in the database file.

Table 3: List of *E. viridis* spines that were cast into an epoxy mount. Each spine number corresponds with Figure 5.

Spine #	Spp. ID	pCO_2	T (°C)
1	4221	400	20
2	1212	1000	20
3	4312	400	30
4	1312	1000	30
5	4222	400	20
6	1213	1000	20
7	4321	400	30
8	1313	1000	30
9	4232	400	20
10	1221	1000	20
11	4331	400	30
12	1332	1000	30

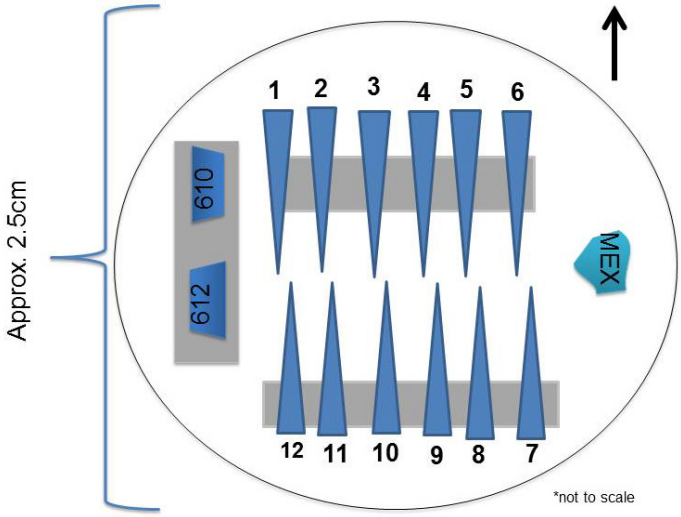

Figure 5: An example of how *E. viridis* spines were casted in epoxy. The long triangles (blue) represent the urchin spines with the tips pointed downward towards the 3M® 701DL double sided tape. The three rectangles (gray) are the scarp pieces of calcite that the urchin spines rest on. The two standards, NIST-SRM 610 and 612 silicate glass and MEX-calcite are placed to the left and right, respectively, of the spines. The numbers correspond to the urchin samples in the database file.

The spines were placed tip side down on a piece of 3M® 701DL double sided adhesive tape mounted flat on 10 cm diameter Al disc. Pre-cast epoxy supports aided in holding multiple spines in place. NIST-SRM 610 and 612 glasses and MEX Calcite (both standards) were added adjacent to the spines (Fig. 4 and 5). A 2.5 cm x 2.5 cm Teflon® ring mold was placed around the assembly of the spines and standards, and filled with epoxy (Fig. 6).

Figure 6: Actual image of how *A. punctulata* spines were mounted onto the Al disc. The blank epoxy (clear blocks) was used as a way to hold up the spines upright. The glass standard (bottom) and MEX-Calcite (top) is also shown.

The epoxy is a two part mixture made by Buehler® and is comprised of the epoxy (Buehler® 20-8130 epoxide resin) and the hardener (Buehler® 20-8132 epoxide hardener). The ratios, by weight, used to make the epoxy were 5 parts epoxy and 1 part hardener. The mixture was weighed in an Al dish and stirred carefully to prevent introducing air bubbles. Once the mixture was homogenized for approximately 10 min, it was poured into the mold and cured overnight at room temperature. The Teflon® ring mold was removed from the adhesive tape and any leftover adhesive from the double-sided tape was mechanically removed. Epoxy discs were labeled with a diamond tip pen.

Subsequently, the spines were sectioned by removing the outermost 2 mm from the tip by using a Buehler IsoMet® low speed diamond saw with 0.5 mm thick blade using distilled water as a cooling medium. Due to the porous natured of the sea urchin spines, a thin layer (~1 mm) of epoxy was applied over the exposed urchin spines in order to achieve a flat surface. The mount was placed in a vacuum chamber for several hours at ~25 kPa, allowing the epoxy to penetrate deep in the calcite matrix of the sea urchin spine.

Polishing

Polishing ensured that the calcite portion of the urchin spine was exposed, flat, and free of scratches (Fig. 7)**.** Scratches or surface roughness on the calcite would be detrimental for SIMS analysis (Benninghoven et al., 1987). Due to the fragile nature of the micropores in the polycrystalline structure of the urchin, fine-grained (800- and 1200-grit) polishing papers were used to prevent grinding damage to the samples. The samples cast in epoxy were first polished with 800-grit SiC paper (Buehler® MicroCut® Discs) to remove any residual epoxy covering exposed urchin spines. The polishing begins by wetting SiC paper with deionized (DI) water and then moving the epoxy in a figure eight pattern. A figure eight pattern for polishing is used because it ensures the maximum area covered while polishing. The polishing was done in one-

minute intervals whereby the polishing progress was checked under an optical microscope to determine how much material was removed.

After the rough sample topography of the calcite was evened out using the 800-grit SiC paper, a finer (1200-grit) SiC paper (Allied® 50-10040) was used. Polishing was done in a similar manner to the 800-grit SiC paper. Once a flat surface was reached, the epoxy mount was ultrasonicated in DI water for one 5-minute cycle, to clean the sample of any polishing debris.

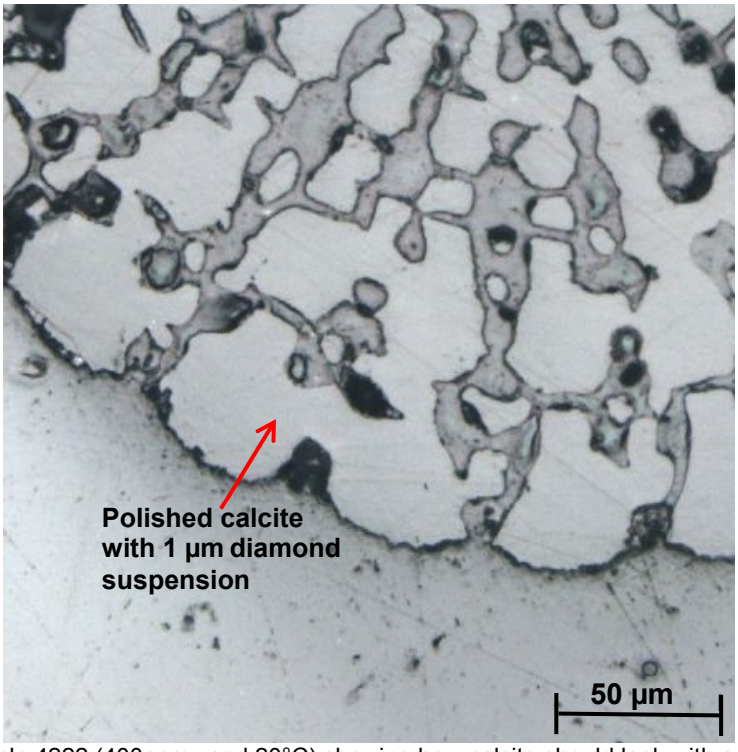

Figure 7: Urchin sample 4222 (400ppmv and 20°C) showing how calcite should look with a final polish with 1 µm diamond suspension.

After ultrasonication, a final polish with 3 µm Buehler MetaDi® Monocrystalline Diamond Suspension was applied to remove any smaller scratches present on the calcite. A small amount of 3 µm diamond suspension was sprayed onto two pieces of white multipurpose paper on top of a flat glass surface. The glass surface was cleared of any dust and debris because this would reintroduce scratches on the calcite and the polishing process would have to be

redone. The same figure eight motion was used to polish the epoxy disc mount. The sample was checked under a reflected light petrographic microscope at high magnification to verify the complete absence of scratches on the calcite (Fig. 7). A final polishing step was applied using 1 µm diamond suspension (Allied® 90-32015) for approximately one minute. After polishing was complete, the sample was cleaned again in the ultrasonicator but with ultra-pure DI water instead of DI water. The sample was left in a drying oven for a couple hours. (See also Fig. 8 for a complete summary of the preparation steps)

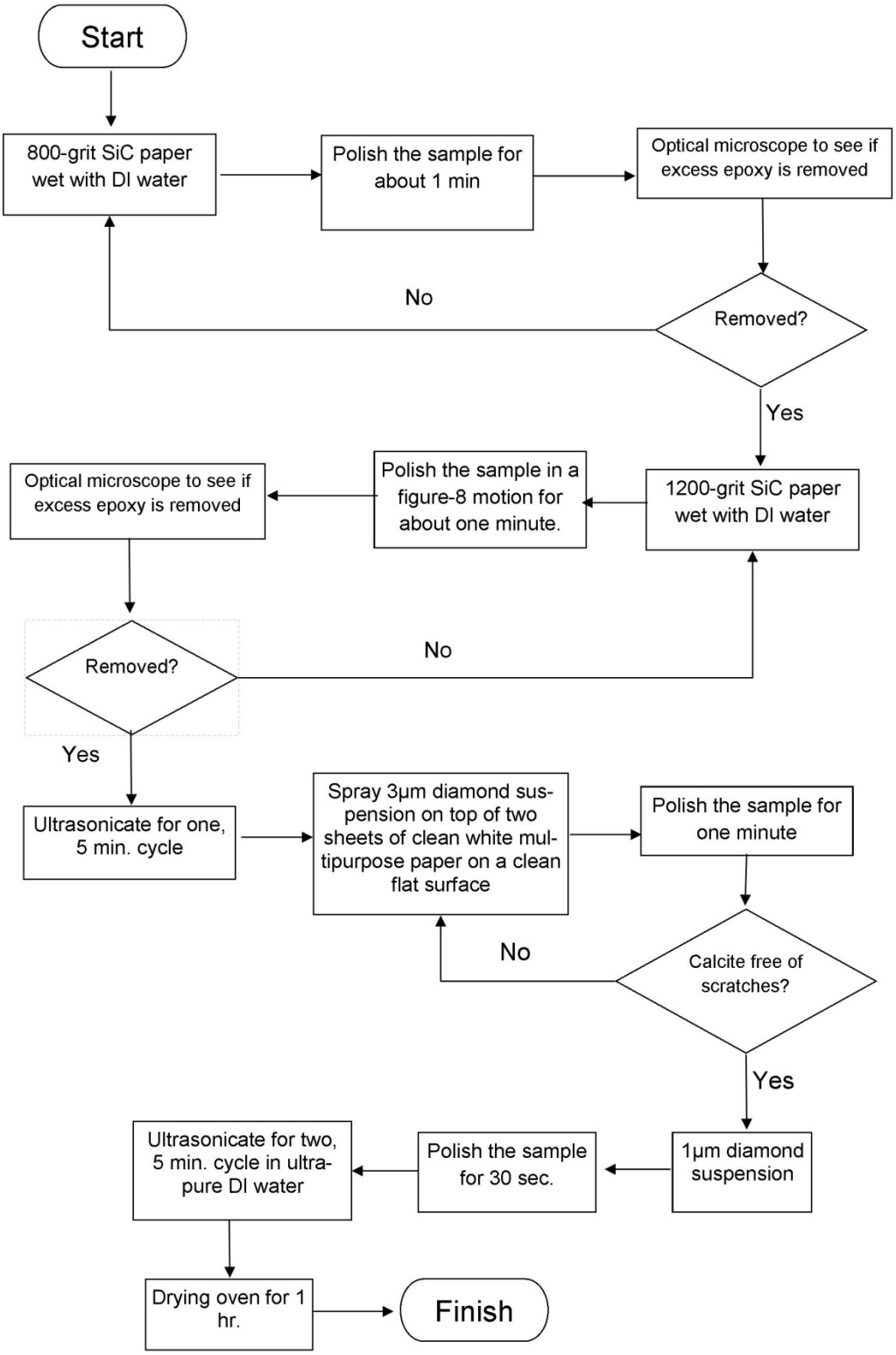

Figure 8: Summary of methods for polishing sea urchin spines embedded in epoxy.

After the polishing was completed, images of the urchin spines were taken with a Nikon® BX51 fluorescence microscope at 2x, 5x, and 10x magnification. These images were used for locating SIMS analysis spots. A composite map (Fig. 9) was made to help navigate over the entire sample holder. Prior to SIMS analysis, the sample mounts were coated with 20-30 nm of gold (Au) to provide an electrically conductive surface for SIMS analysis.

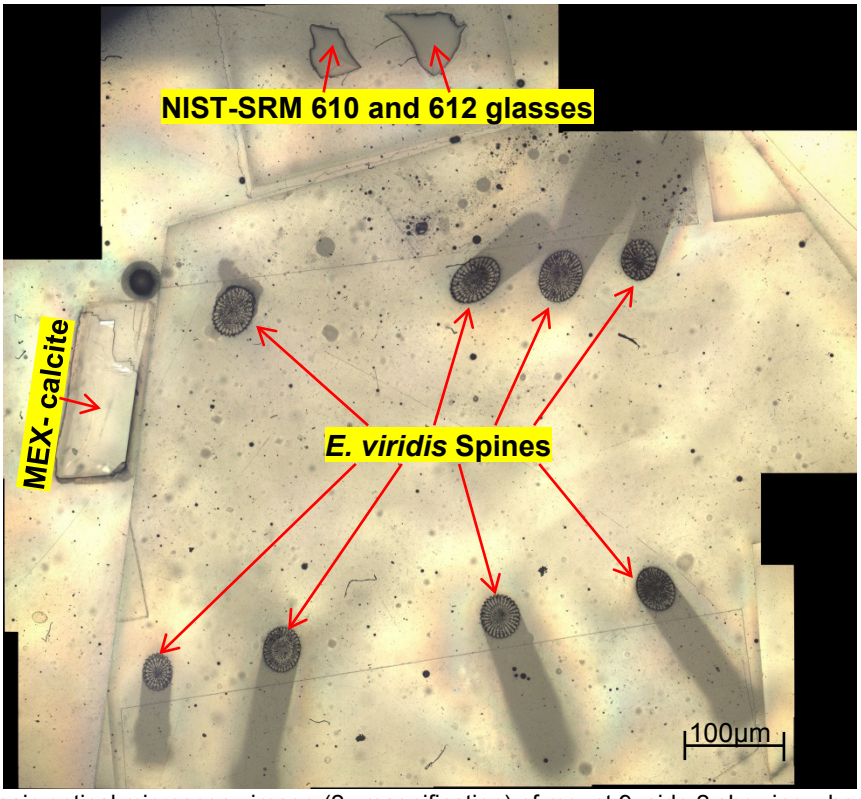

Figure 9: A mosaic optical microscopy image (2x magnification) of mount 9, side 2 showing where the *E. viridis* spines, MEX-calcite, and NIST-SRM silicate glasses were located. It was used as a map for analysis in the SIMS.

Determination of Calcite within Urchin Spine

Since urchin spines are composed of a polycrystalline calcite cortex with tiny micrometer-sized spaces that were filled with stereom or living cellular tissue, it was critical to distinguish the calcite from epoxy that surrounded or penetrated into the spines. To distinguish calcite from epoxy, the epoxy disc was inspected under an optical microscope (Fig. 10).

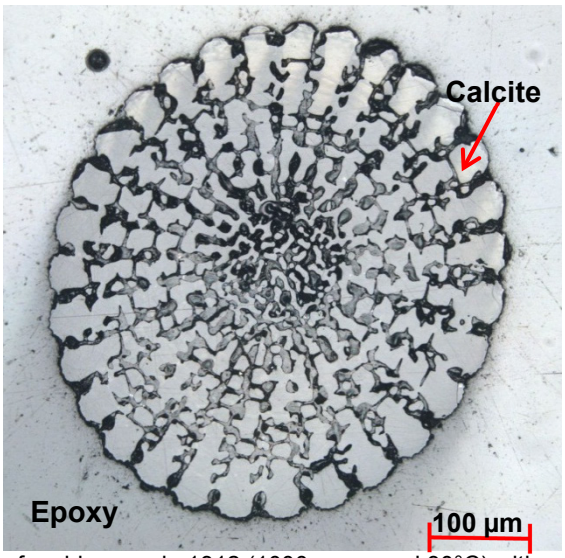

Figure 10: Optical microscope of urchin sample 1312 (1000 ppmv and 30°C) with a final polish with 1 µm diamond suspension. Light areas represent calcite areas and dark areas represent the epoxy filled voids.

To confirm the visual distinction between calcite and epoxy, a LEO 1430 VP SEM scanning electron microscope in the UCLA/NSF Ion Microprobe Facility was used. The epoxy mounts were coated with a conductive (~25 nm) carbon film. Elemental maps of urchin spines were generated using an EDAX energy-dispersive detector, and the Ca Kα intensity. The distrubution of calcium throughout the urchin spine is shown in Fig. 11b in comparison to the optical microscope image in Fig. 11a

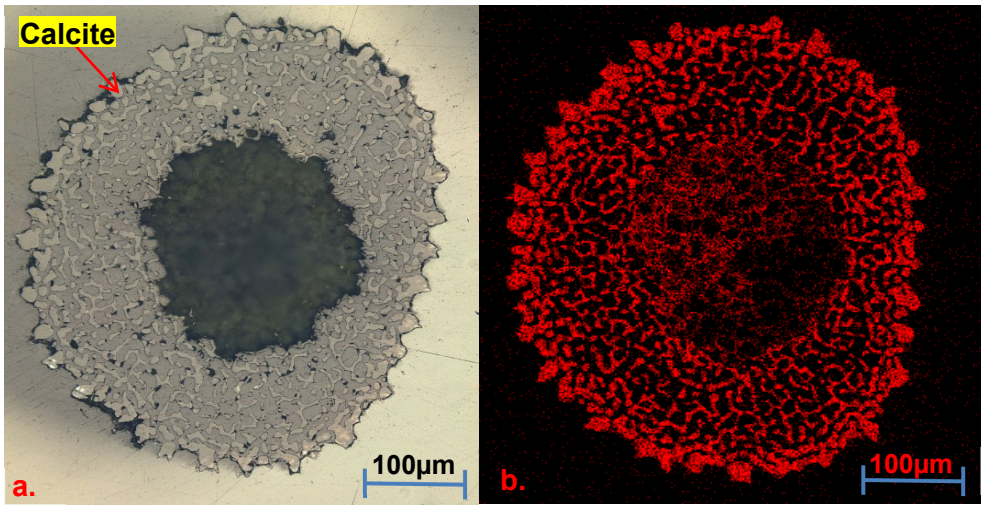

Figure 11: (a) Optical microscope of *A. punctulata* spine JR279 (900 ppmv and 25°C) with a final polish of 1 µm diamond suspension. The calcite area is identified as the cream color area on the sea urchin spine (black arrow). (b) SEM elemental map of the same *A. punctulata* spine, red areas indicate where calcium is detected.

Preparation of Paleo-Echinoderms

The paleo-echinoderms were previously prepared on thin sections that were mounted on 75 x 25 mm glass slides. The available samples are listed in Table 4; the rows highlighted in red were for samples not cast or not analyzed due to time constraints or because they were too large to fit inside the epoxy mold.

Table 4: Lists of the paleo-echinoderms thin sections that were obtained from J.A Dickson. The samples that are highlighted in red were not cast into epoxy because the samples were too large to fit inside the Teflon mold. Sea surface temperatures (SST) were estimated from Dickson (2004). C = Crinoid, E = echinoid, Ag = *Agassizocrinus*, I = *Isocrinus*, B.s. = *Balanocrinus solenotis*, B.p. = *Balanocrinus pentagonalus*, L.m. = *Lepidocantrotus mulleri*, E.c. = *Encrinurus cassianus*.

Sample No.	Description	Location Collected	Stage	Age (Ma)	SST (°C)
62	C	Clapham,London U.K.	Ypresian	53	13
39	I	Speeton,Lincolnshire,U.K.	Hautervian	130	20
17	E	Santa Cruz, Portugal.	Kimmeridgian	152	26
29	B.p	Jarcenay, Doubs, France	Oxfordian	156	22
61	C	Huggits Wood, Yorkshire U.K.	Callovian	164	20
32/33	C	Whatton Cliff Dorset, U.K.	Bathonian	166	22
47	B.s	Staithes, N. Yorkshire U.K.	Domerian	184	22
38	C	Cheltenham, Gloucestersh U.K.	Pliensbachian	190	22
94	E	Black Ven, Dorset U.K.	Sinemurian	200	22
90	E.c	Dolomites, Italy	Norian	220	24
97	C	Djebel Tabago Tunisia	Wordian	253	27
83	C	Callytharra Spings, W. Australia	Artinskian	260	18
99	C	Pittsburg, Kansas U.S.A.	Desmionesian	297	27
98	C	Pontotoclo Co. Oklahoma U.S.A.	Virgilian	291	28
93	C	Palo Pinto County Texas U.S.A.	Virgilian	292	28
70	Ag	Confusion Range, N. Utah. U.S.A	Chesterian	326	28
40/41	C	Clattering Sike, Yorkshire U.S.A	Briganian	330	28
68	C	Liuzhou Guangxi China	Visean	330	28
34	C	Angle Bay Pembrokeshire, U.K.	Hastarian	350	26
66	C	Boy Scout Camp Indiana U.S.A.	Osagian	354	28
76	C	Button Mold Knob,Kentucky U.S.A.	Osagian	354	26
77	C	Deam Lake,Borden, Indiana,U.S.A.	Osagian	354	26
26	L.m	Eifel, Germany	M. Devonian	385	26
30/31	C	Jasper National Park, Canada	Botomian	518	25

Since the glass slides were too large to fit inside the Teflon mold, they were cut using a Buehler® IsoMet slow speed circular saw and then embedded in epoxy. In some instances, the areas of interest would be small enough that multiple samples could be incorporated into one epoxy mold. The samples were prepared in a similar way to the cultured sea urchin spines. Two

standards, NIST-SRM 610 and 612 silicate glasses and MEX-calcite, were also embedded with the samples. The samples and standards were cast into epoxy and left to cure overnight.

After solidifying, the epoxy was removed from the mold and polished to ensure that the samples were flat and free of debris. Little polishing was necessary since the samples were thinly sectioned. Polishing the thin sectioned samples with coarse-grit SiC paper could have resulted in damage and consequently, polishing was done only with 3 μm diamond suspension. This caused some of the samples to have areas that were not completely exposed at the surface. Once polishing was complete, images were taken of the polished areas that would be analyzed by SIMS (Fig. 12).

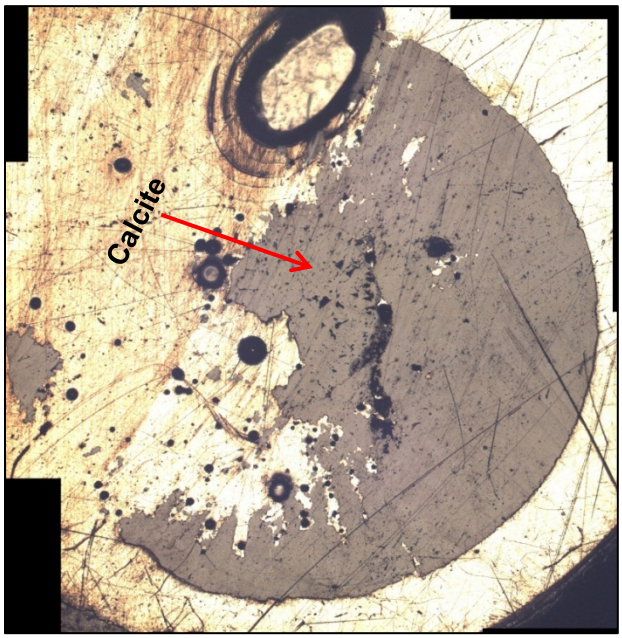

Figure 12: Optical microscope image of the paleo-echinoderm Sample 98 (crinoid) at a magnification of 2x. The dark grey area represents the calcite area of sample and the gold-colored portion is the epoxy.

The paleo-echinoderms were also analyzed using the SEM to assess where calcite was present on the sample. The elemental map was used to determine that calcium was evenly distributed throughout the sample and that Mg 'hotspots' were absent (Fig. 13). These 'hotspots' indicate areas of secondary dolomitization which have to be avoided during the analysis. The

secondary dolomitization would represent a later age at which the fossil was mineralized and would not be represented of the actual time the paleo-echinoderm was living. Some areas of the paleo-echinoderm fossils also contained high-iron (Fe) cement. In order to identify these cements, a mass/charge station corresponding to Fe^{3+} was added to the SIMS analysis definition. Spots were excluded from further consideration if $^{54}Fe/^{42}Ca$ intensities exceeded one count per second (cps) (Appendix C).

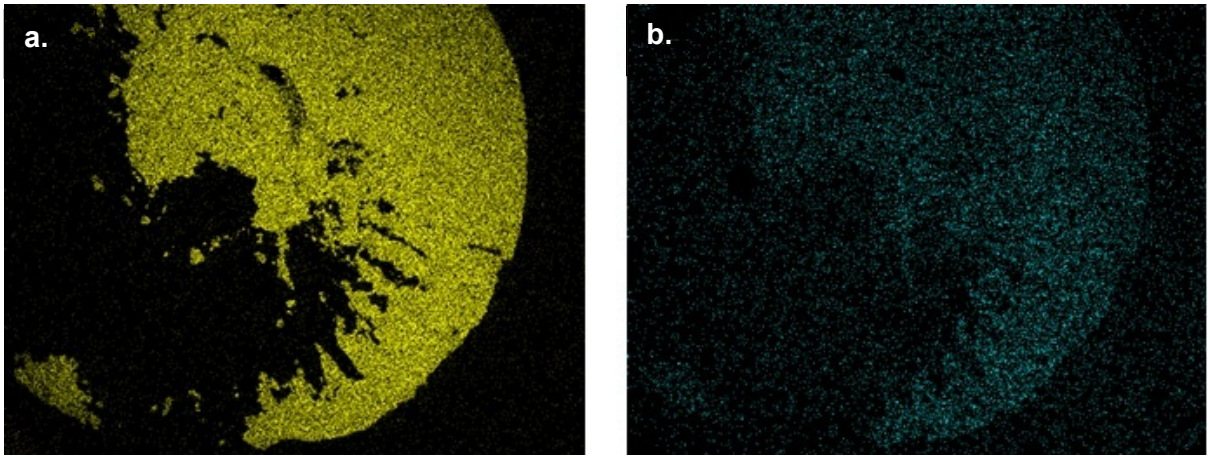

Figure 13: SEM elemental mapping of peleo-echinoderm Sample 98 (crinoid) showing the distribution of Ca (yellow) and Mg (blue).

Analytical Conditions

Cultured urchin spines were prepared and analyzed at the University of California Los Angeles (UCLA) National Science Foundation (NSF) Ion Microprobe Facility hosted by the Department of Earth System Sciences. Analysis of the urchin spines was done on the CAMECA SIMS *ims*-1270 using a duoplasmatron ion source and a mass-filtered $^{16}O^-$ primary ion beam at 43-46 nA. In all analyses, the lateral spot dimensions were between 30-40 μm in diameter. Instead of using energy filtering to obtain an interference-free mass spectrum, a high mass resolving power of 5000 (m/Δm) was applied to resolve isobaric interferences which offered superior sensitivity to energy filtering.

Individual spot analyses started with a 10 second pre-sputtering to remove the gold (Au) coat and mitigate the effects of possible surface contamination. Following the automated centering of the secondary ions in the field aperture, a magnet calibration was performed. Subsequently, intensities were integrated using and electron multiplier in 10 cycles with a total integration time of 10 minutes. Each of the cultured sea urchin spines was sampled with 5-20 individual analysis spots. The mass/charge stations analyzed were ^{6}Li+, ^{11}B+, ^{26}Mg+, ^{42}Ca+, ^{54}Fe+, and ^{55}Mn+. An offset of -70 eV for ^{26}Mg+ and ^{42}Ca+ was applied during the analysis because of their high ion intensities, which would otherwise saturate the electron multiplier. The data file records intensities as counts per second (cps). The in-house data reduction program ZIPS v3.0.4 was used to obtain dead-time (25 nsec) and drift-corrected ion intensity ratios and uncertainties.

In order to translate measured ion intensity ratios (Li/Ca, B/Ca, and Mg/Ca), ratios were normalized to calcites (CAL-HTP and UCI) for Li and Mg and a reference coral (*Porites spp*: M93-TB-FC-1) for B. These standards were prepared previously and analyzed in the SIMS before and after analysis on the echinoderms.

Standards

The standards used to normalize the intensity ratios of Li/Ca (CAL-HTP), B/Ca (M93), and Mg/Ca (UCI-CC) were calcite (CAL-HTP and UCI-CC) and coral (M93) (Table 5). These standards were previously prepared on separate epoxy mounts. Reference materials CAL-HTP (Li), UCI (Mg), LAS-20 (Mg), and NBS-19 (Mg) were cast together in one epoxy mount and reference coral M93-TB-FC-1 was cast in a separate epoxy mount. Both of these epoxy mounts containing the standards were analyzed under the same instrumental conditions before and after the analysis of the sea urchin samples (Appendix D). Two silicate glasses (NIST-SRM 610

and 612) were added to the each epoxy mount that contained samples and were used to monitor the drift of intensity ratios.

The bulk Li content in reference calcite, CAL-HTP, was determined by ICP-MS as ~2 ppm (Vigier et al., 2007). The standard deviation for SIMS spot analysis of lithium in reference calcite CAL-HTP was 3.5 % (1σ). Boron content in reference coral, M93-TB-FC-1, was determined by LA-ICP-MS as 39.3 ±2 ppm (Kasemann et al., 2009). The standard deviation of SIMS spots analyses of coral reference material M93-TB-FC-1 was 9.5 % (1σ). Magnesium content in reference calcite UCI was determined by LA-ICP-MS as 344.6 ppm (Gabitov et al., In Review). The standard deviation for the SIMS spot analysis of magnesium in the reference calcite UCI was 1% (1σ). Two other reference materials for Mg were also analyzed (NBS-19 and LAS-20), but UCI was chosen as the reference material to normalize the data.

Table 5: Reference materials used to normalize intensity ratios of cultured sea urchin spines and paleo-echinoderm samples. The material used and the actual concentrations are shown. Entire dataset for intensity ratios from the SIMS analysis on the standards is listed in Appendix D. Actual concentrations were found through different mass spectrometery methods.

Standard	Source	Material	Li/Ca (mmol/mol)	B/Ca (mmol/mol)	Mg/Ca (mmol/mol)
NIST SRM 610	(Hinton, 1999)	Silicate Glass	32.627	15.406	N/A
NIST SRM 612	(Hinton, 1999)	Silicate Glass	2.797	1.501	N/A
CAL-HTP	(Vigier et al., 2007)	Calcite	0.2887	N/A	N/A
M93-TB-FC-1	(Kasemann et al., 2009)	Coral	N/A	0.3642	N/A
UCI	(Gabitov et al., In Review)	Calcite	N/A	N/A	3.446

Normalizing Intensity Ratios

The normalized values for the urchin spines were calculated by dividing the intensity ratios from the sample to the standard and then multiplying by the actual value of the standard (mmol/mol) shown in Table 5, according to Equation 7 where X represents the element of interest. The actual value (mmol/mol) of the standards were determined using ICP-MS (UCI),

SIMS (CAL-HTP and M93), and electron probe (NIST-SRM 610 and 612 glasses) (Hinton, 1999; Kasemann et al., 2005; Vigier et al., 2007; Kasemann et al., 2009;).

$$\frac{\mathrm{X}}{\mathrm{Ca}}(\mathrm{mmol/mol}) = \frac{\left(\frac{\mathrm{X}}{42\mathrm{Ca}}\right)_{\text{SIMS sample}}}{\left(\frac{\mathrm{X}}{42\mathrm{Ca}}\right)_{\text{SIMS standard}}} \times \left(\frac{\mathrm{X}}{\mathrm{Ca}}\right)_{\text{actual standard value (Table 4)}} \quad (7)$$

The errors of each of standardized values were calculated according to Equation 8. These values represent the standardized errors (s.e) of each individual spot. The errors of the sample and standard are the errors that result from the reproducibility of the measured intensity ratios within each analysis when averaged over n cycles.

$$\text{Standardized Error} = \sqrt{\frac{\Delta\mathrm{A}^2}{\mathrm{B}^2} + \frac{\mathrm{A}^2\Delta\mathrm{B}^2}{\mathrm{B}^4}} \times \left(\frac{\mathrm{X}}{\mathrm{Ca}}\right)_{\text{actual standard value (Table 4)}} \quad (8)$$

- A = Measured X/Ca in the sample
- ∆A = 1 s.e. of measured X/Ca in the sample
- B = Measured X/Ca in the standard
- ∆B = 1 s.e. of measured X/Ca in the standard

The standard deviation of the standard mean $(SD_{\bar{X}})$ for the average of multiple spot analyses of an individual sample is determined from the standard deviation of the spot population (σ) and divided by the square-root of the number of spots that were averaged (n) (Equation 9).

$$SD_{\bar{X}} = \frac{\sigma}{\sqrt{n}} \quad (9)$$

Analysis of Sea Urchin Spines

The sea urchin spines were analyzed over the course of three days. Samples with large calcite areas were run overnight by setting up an automated chain analysis by programing preset locations. However, in some instances where target areas were too small to be reliably

assessed in the pre-programmed analysis mode (<5 μm), the analyses were set-up done by hand to ensure that the ion beam would be analyzing calcite and not epoxy. The list of the samples that were analyzed by SIMS is shown in Table 6. Due to time constraints, samples 1212 (1000 ppmv and 30°C), 1313 (1000 ppmv and 30°C), 4232 (400 ppmv and 20°C), and 4331 (400 ppmv and 30°C) were not analyzed.

Images After SIMS Analysis

After SIMS analysis was complete, images (after removing the Au coating by gently re-polishing) of the sea urchin spines were taken. These images were taken to record the exact position of the analysis spot to ensure that the ion beam was analyzing the calcite areas (Fig. 14). Intensities of Ca for each analysis spot were also checked to ensure that areas analyzed were calcite.

Figure 14: Image of *E. viridis* spine 1211 (1000 ppmv and 20°C) after SIMS analysis. There are 11 craters (black ellipses) on this sample and all SIMS analysis occurred within the calcite areas of the spine.

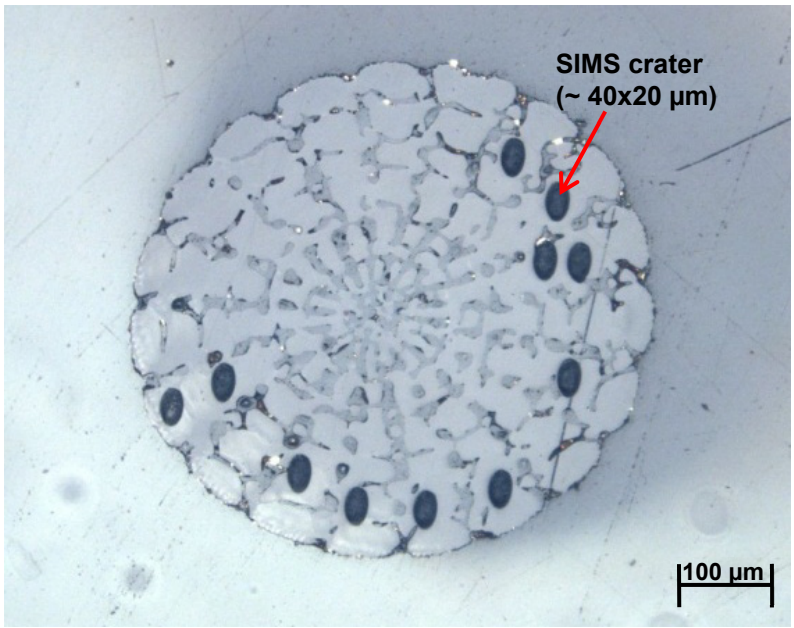

Table 6: Details from the SIMS analysis of *A. punctulata* and *E. viridis* spines.

ID	Species	Taxa	Mount	pCO_2 (ppmv)	T (°C)	# of ion spots (n)	Chain Analysis ?
JR-64	*Arbacia punctulata*	Temperate	3	400	25	9	Yes
JR-205	*Arbacia punctulata*	Temperate	3	600	25	8	Yes
JR-215	*Arbacia punctulata*	Temperate	3	900	25	8	Yes
JR-65	*Arbacia punctulata*	Temperate	3	400	25	6	Yes
JR-204	*Arbacia punctulata*	Temperate	3	600	25	7	Yes
JR-69	*Arbacia punctulata*	Temperate	3	900	25	8	Yes
JR-71	*Arbacia punctulata*	Temperate	3	2850	25	8	No
4213	*Echinometra viridis*	Tropical	9	400	20	10	Yes
1211	*Echinometra viridis*	Tropical	9	1000	30	10	Yes
4311	*Echinometra viridis*	Tropical	9	400	30	10	Yes
1311	*Echinometra viridis*	Tropical	9	1000	30	11	Yes
4233	*Echinometra viridis*	Tropical	9	400	20	8	Yes
1333	*Echinometra viridis*	Tropical	9	1000	30	8	Yes
4332	*Echinometra viridis*	Tropical	9	400	30	8	Yes
1233	*Echinometra viridis*	Tropical	9	1000	20	8	Yes
4221	*Echinometra viridis*	Tropical	10	400	20	11	Yes
4312	*Echinometra viridis*	Tropical	10	400	30	10	Yes
1312	*Echinometra viridis*	Tropical	10	1000	30	10	Yes
4222	*Echinometra viridis*	Tropical	10	400	20	10	Yes
1213	*Echinometra viridis*	Tropical	10	1000	20	10	Yes
4321	*Echinometra viridis*	Tropical	10	400	20	10	Yes
1221	*Echinometra viridis*	Tropical	10	1000	20	11	Yes
1333	*Echinometra viridis*	Tropical	10	1000	30	10	Yes

Analysis of Paleo-Echinoderms

The priority of which samples to analyze was based on age and the amount of samples present in the epoxy mount (Table 11). The epoxy mount with multiple paleo-echinoderm samples was analyzed first because it was deemed to be more efficient than changing the sample out of the SIMS holder (Table 12).

Table 7: Paleo-echinoderm sample list showing the samples that were analyzed (black) and samples that were not analyzed (red) in the SIMS. Sea surface temperature that the samples were collected from was estimated from Dickson (2004).

Sample No.	Species	# of spots (n)	Age (Ma)	SST (°C)	Analyzed?
62	Crinoid	3	53	13	Yes
39	Isocrinus	3	130	20	Yes
17	*Encrinurus cassianus*	-	152	26	No
29	*Balanocrinus pentagonalus*	3	156	22	Yes
61	Crinoid	-	164	20	No
32/33	Crinoid	-	166	22	No
47	*Balanocrinus soletois*	-	184	22	No
38	Crinoid	3	190	22	Yes
94	Echinoid	-	200	22	No
90	*Encrinurus cassianus*	3	220	24	Yes
97	Crinoid	4	253	27	97
83	Crinoid	-	260	18	No
99	Crinoid	-	297	27	No
98	Crinoid	-	291	28	No
93	Crinoid	-	292	28	No
70	*Agassizocrinus*	3	326	28	Yes
40/41	Crinoid	6	330	28	Yes
68	Crinoid	3	330	28	Yes
34	Crinoid	-	350	26	No
66	Crinoid	3	354	28	Yes
76	Crinoid	3	354	26	Yes
77	Crinoid	4	354	26	Yes
26	*Lepidocantrotus mulleri*	3	385	26	Yes
30/31	Crinoid	-	518	25	No

Results

Individual Spines of *A. punctulata*

The average normalized element/calcium ratio was taken for each *A. punctulata* spine analyzed (Table 7). *A. punctulata* spines from four different culturing conditions were examined, with two spines analyzed per culturing condition. The averages were taken from the complete dataset (Appendix A). Each individual spine revealed the variability of element-to-calcium ratio in spines from that culturing condition. For example, under pCO_2 of 600 ppmv, Mg/Ca for the two spines varied from76.4 (±2.0) mmol/mol to 88.0 (±1.5) mmol/mol (Fig. 17). Other element-to-calcium ratios varied but the difference was not significant. The element/calcium ratios for the eight *A. punctulata* spines analyzed were plotted (Fig. 15-17).

Table 8: Results from the SIMS analysis of *A. punctulata* spines. The elemental/calcium ratios were normalized to their respective standards. Each condition represents an average of the 10-11 SIMS analysis spots on an *A. punctulata* spine. All measured data can be found in Appendix A.

pCO_2 ppmv	T (°C)	Li/Ca (µmol/mol)	1 s.e	B/Ca (mmol/mol)	1 s.e	Mg/Ca (mmol/mol)	1 s.e
400	25	46.4	0.55	0.217	0.003	82.4	2.0
400	25	43.4	1.2	0.230	0.005	83.3	1.3
600	25	45.8	1.1	0.277	0.007	76.4	1.9
600	25	43.6	1.2	0.258	0.007	88.0	1.5
900	25	41.1	0.63	0.304	0.008	65.2	1.8
900	25	38.5	2.0	0.296	0.02	71.3	3.0
2850	25	36.0	2.5	0.292	0.011	77.6	3.0
2850	25	35.8	0.75	0.292	0.014	76.6	1.8

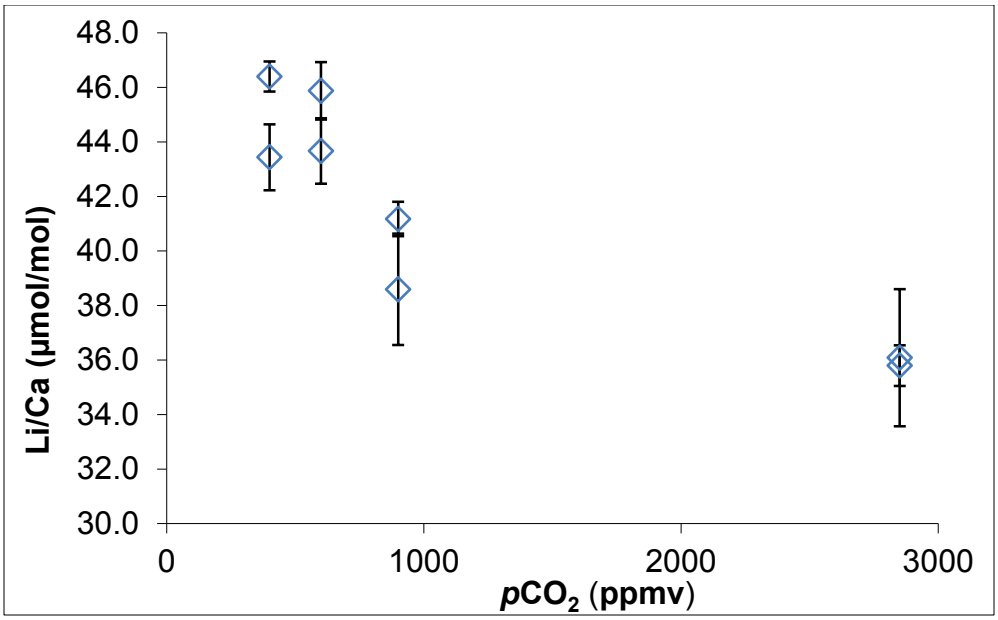

Figure 15: Normalized Li/Ca (µmol/mol) values for each *A. punctulata* spine cultured under varying pCO_2 (400, 600, 900, and 2850 ppmv) and constant temperature of 25°C. Each blue diamond represents the average of 10-11 SIMS spots in one *A. punctulata* spine for each culturing condition.

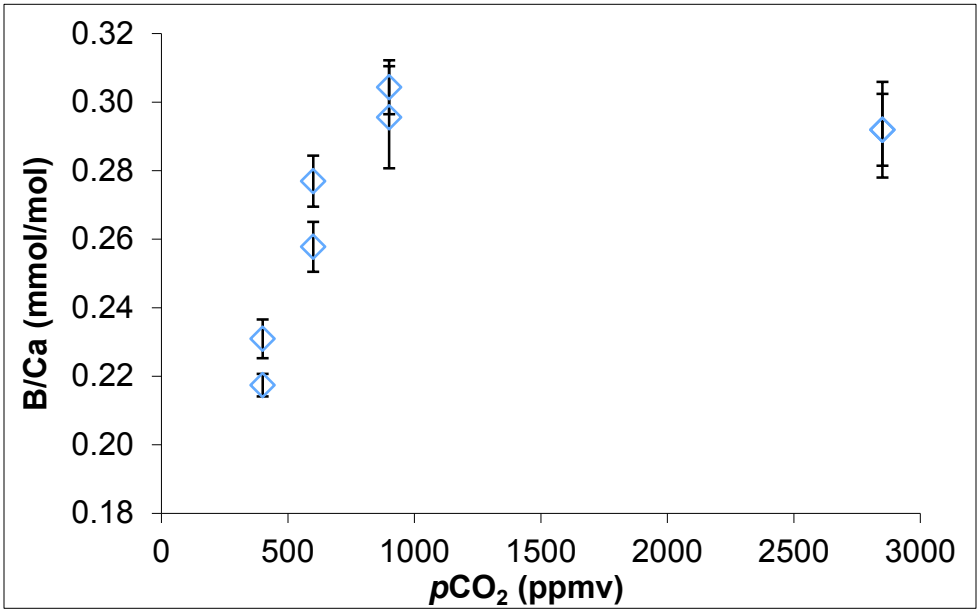

Figure 16: Normalized B/Ca (mmol/mol) values for each *A. punctulata* spine cultured under varying pCO_2 (400, 600, 900, and 2850 ppmv) and constant temperature of 25°C. Each blue diamond represents the average of 10-11 SIMS spots in one *A. punctulata* spine for each culturing condition.

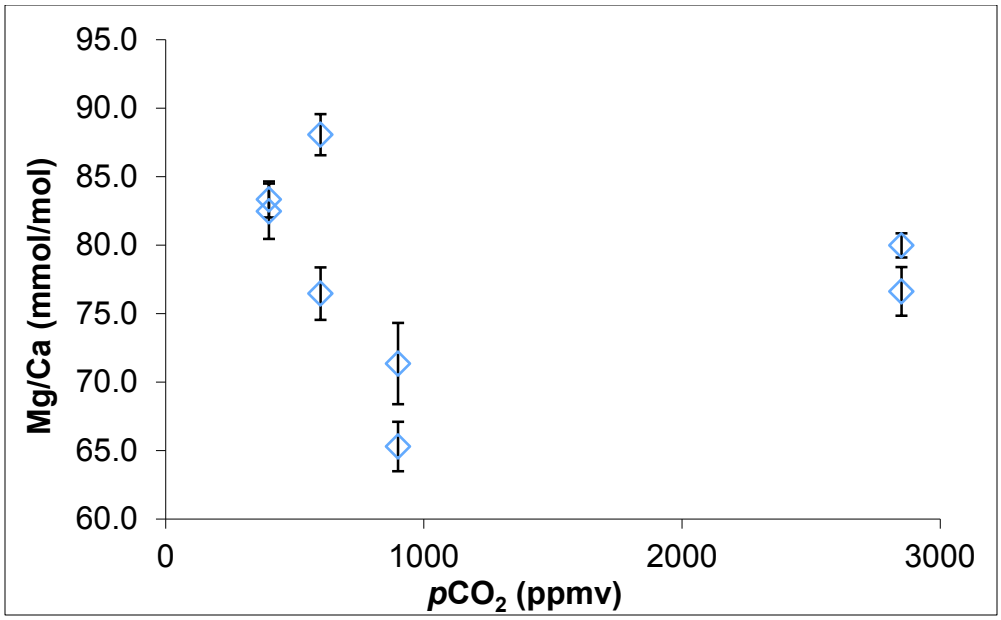

Figure 17: Normalized Mg/Ca (mmol/mol) values for each *A. punctulata* spine cultured under varying pCO_2 (400, 600, 900, and 2850 ppmv) and constant temperature of 25°C. Each blue diamond represents the average of 10-11 SIMS spots in one *A. punctulata* spine for each culturing condition.

Averaged Culturing Conditions of *A. punctulata*

Plotting the average of all SIMS analysis spots for each of the culturing conditions in *A. punctulata* shows how changing pCO_2 affected element/calcium ratios (Table 8). *A. punctulata*, which was grown under variable pCO_2 and constant temperature, showed an increase in B/Ca ratios from 0.222 (±0.003) mmol/mol to 0.300 (±0.008) mmol/mol in the intermediate pCO_2 value (400 ppmv to 900 ppmv). Li/Ca decreased from 45.2 (±0.1) µmol/mol to 35.8 (±0.6) µmol/mol with increasing pCO_2 (400 to 2850 ppmv).Mg/Ca had a maximum value of 82.8 (±1.3) mmol/mol at 400 ppmv and a minimum value of 68.3 (±1.9) mmol/mol in intermediate pCO_2 value (900 ppmv). The normalized values of each individual SIMS analysis spot on the sea urchin spine can be found in Appendix A. Values that had intensity counts of $^{42}Ca+$ (<15,000 cps) during the analysis were omitted.

Table 9: Average normalized element/calcium ratios in *A. punctulata* for each of the culturing condition. All measured data can be found in Appendix A.

Taxa	pCO_2 (ppmv)	T (°C)	# of Ion Spots	Li/Ca (µmol/mol)	1 s.e	B/Ca (mmol/mol)	1 s.e	Mg/Ca (mmol/mol)	1 s.e
Temperate	400	25	15	45.2	0.68	0.223	0.003	82.8	1.3
Temperate	600	25	14	44.7	0.83	0.267	0.006	82.2	2.0
Temperate	900	25	16	39.8	1.1	0.300	0.008	68.3	1.9
Temperate	2850	25	16	35.8	0.60	0.290	0.007	76.2	1.2

Individual Spines of *E. viridis*

An average of 10-12 SIMS analysis spots were taken for an individual *E. viridis* spine with culturing conditions of 400 or 1000 ppmv and 20°C or 30°C (Table 9). Similar to the variability seen in the *A. punctulata* spines, there is also variability between each individual *E. viridis* spine of the same culturing condition. Element-to-calcium values were plotted to either temperature (Fig 18-20) or pCO_2 (Fig 21-23).Each individual *E. viridis* element/calcium analysis spot can be found in Appendix B.

Table 10: Normalized element/calcium ratios for all *E. viridis* spines that were analyzed. All measured data can be found in Appendix B.

ID	pCO2 (ppmv)	T °C	Li/Ca (µmol/mol)	1 s.e	B/Ca (mmol/mol)	1 s.e	Mg/Ca (mmol/mol)	1 s.e
4222	**400**	**20**	45.4	1.42	0.314	0.011	95.9	1.6
4221	**400**	**20**	45.2	0.90	0.337	0.007	97.5	1.2
4312	**400**	**30**	84.9	0.75	0.426	0.008	104.4	0.6
4321	**400**	**30**	86.0	0.60	0.487	0.010	111.2	1.1
4213	**400**	**20**	20.4	0.41	0.297	0.008	87.6	1.5
4233	**400**	**20**	20.2	0.54	0.327	0.006	89.6	1.1
4332	**400**	**30**	31.7	1.54	0.321	0.011	95.2	3.7
4311	**400**	**30**	33.5	0.74	0.407	0.009	114.7	2.7
1233	**1000**	**20**	46.9	0.92	0.344	0.013	100.8	4.1
1211	**1000**	**20**	26.1	1.06	0.269	0.010	86.7	0.5
1311	**1000**	**30**	40.5	0.52	0.381	0.003	112.4	0.7
1333	**1000**	**30**	34.7	0.54	0.397	0.007	101.8	0.8
1221	**1000**	**20**	51.1	1.71	0.372	0.009	101.5	1.1
1213	**1000**	**20**	44.6	1.11	0.333	0.006	89.4	0.7
1312	**1000**	**30**	86.6	1.32	0.369	0.004	109.3	1.1
1332	**1000**	**30**	44.6	1.18	0.299	0.005	99.9	1.3

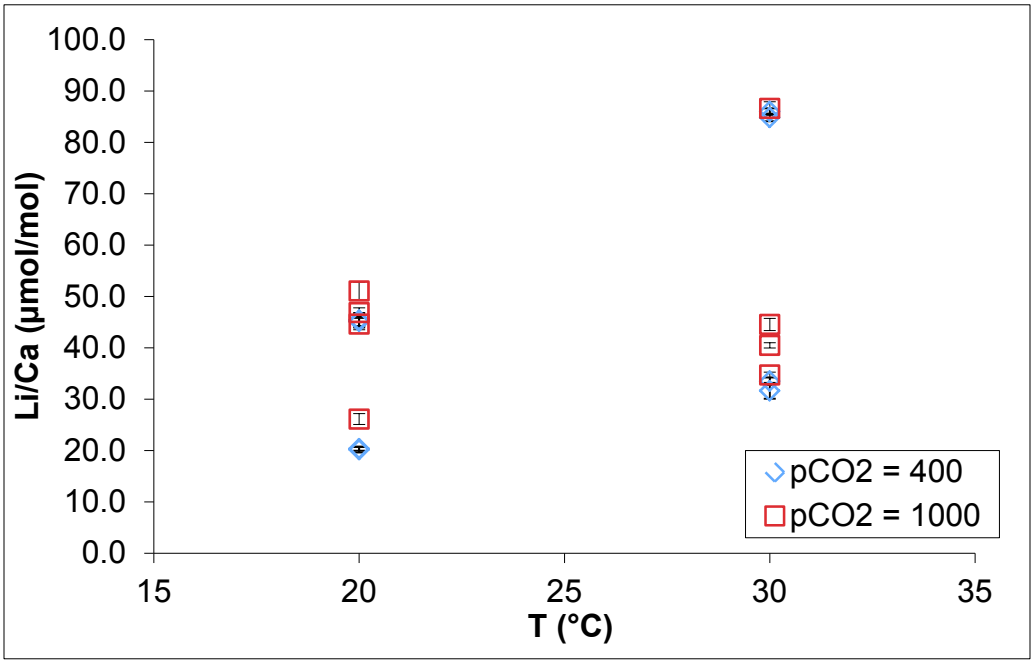

Figure 18: Normalized Li/Ca (µmol/mol) ratios for *E. viridis* spines cultured under varying pCO_2 (400 and 1000 ppmv) and temperature (20°C and 30°C). Each point represents the average of 10-12 SIMS analysis points for one spine with a single culturing condition. Blue diamonds and red squares represent spines grown under 400 ppmv and 1000 ppmv, respectively. Error bars represent 1σ.

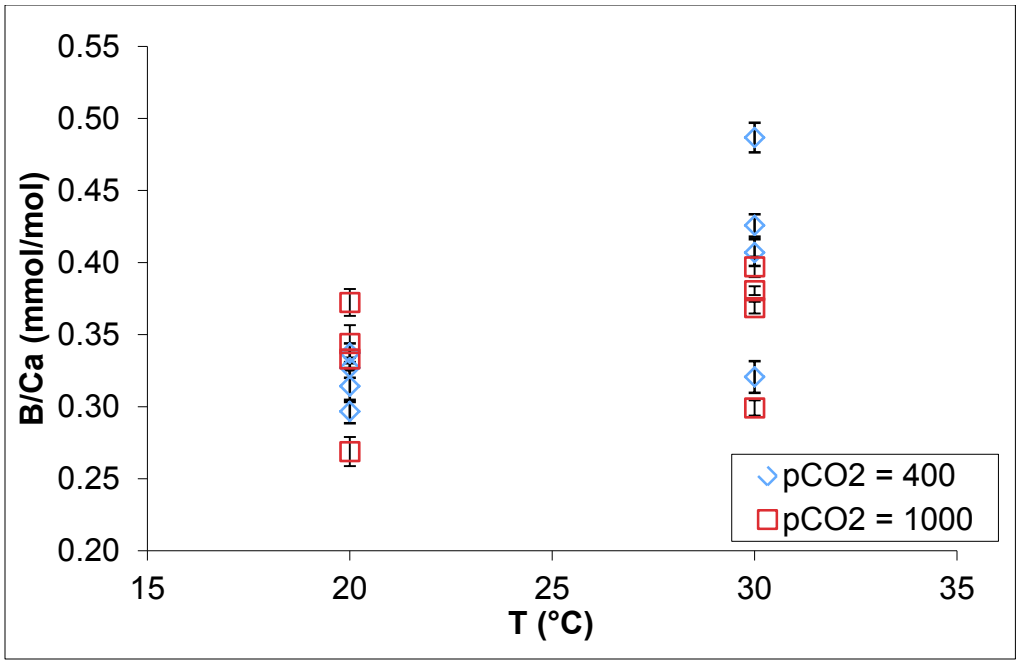

Figure 19: Normalized B/Ca (mmol/mol) ratios for *E. viridis* spines cultured under varying pCO_2 (400 and 1000 ppmv) and varying (20°C and 30°C). Each point represents the average of 10-12 SIMS analysis points for one *E. viridis* spine cultured under 1000 or 400 ppmv and 20°C or 30°C. Blue diamonds and red squares represent spines grown under 400 ppmv and 1000 ppmv, respectively. Error bars represent 1σ.

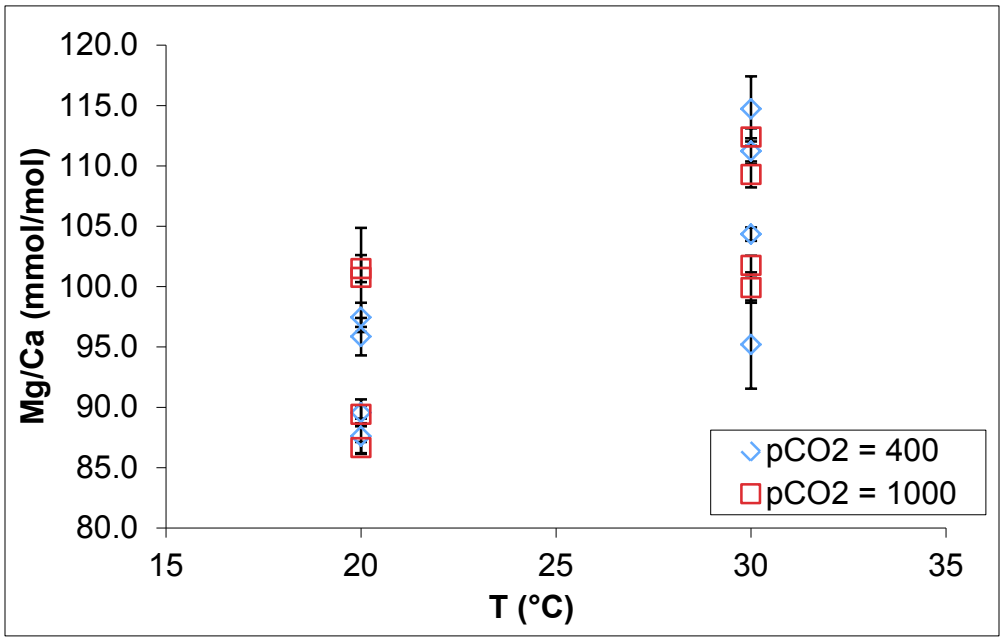

Figure 20: Normalized Mg/Ca (mmol/mol) ratios for *E. viridis* spines cultured under varying pCO_2 (400 and 1000 ppmv) and varying temperature (20°C and 30°C). Each point represents the average of 10-12 SIMS analysis points for one *E. viridis* spine cultured under 1000 or 400 ppmv and 20°C or 30°C. Blue diamonds and red squares represent spines grown under 400 ppmv and 1000 ppmv, respectively. Error bars represent 1σ.

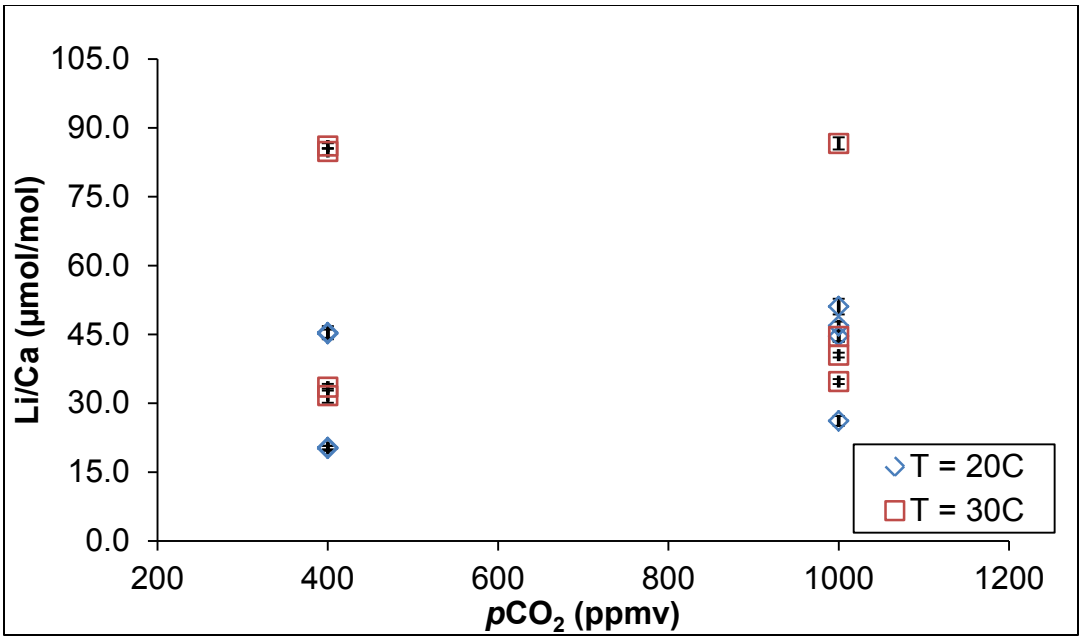

Figure 21: Normalized Li/Ca (µmol/mol) ratios for *E. viridis* spines cultured under varying pCO_2 (400 and 1000 ppmv) and varying temperature (20°C and 30°C). Each point represents an average of 10-12 SIMS analysis points of one *E. viridis* spine cultured under 1000 or 400 ppmv and 20°C or 30°C. Blue diamonds and red squares represent spines grown under 20°C and 30°C, respectively. Error bars represent 1σ.

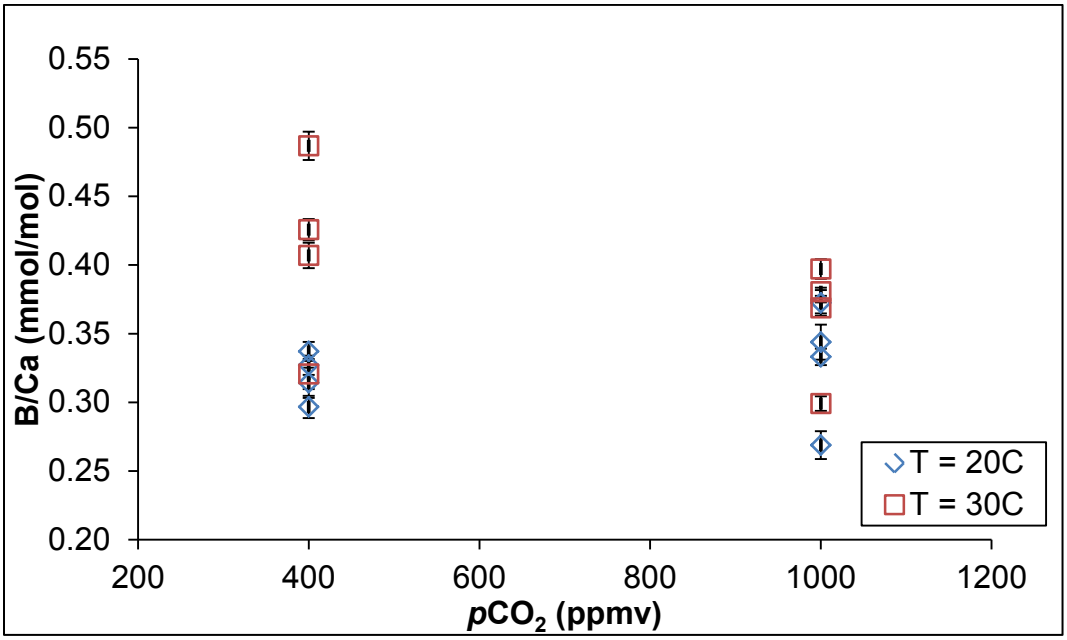

Figure 22: Normalized B/Ca (mmol/mol) ratios for *E. viridis* spines cultured under varying pCO_2 (400 and 1000 ppmv) and varying temperature (20°C and 30°C). Each point represents an average of 10-12 SIMS analysis points of one *E. viridis* spine cultured under 1000 or 400 ppmv and 20°C or 30°C. Blue diamonds and red squares represent spines grown under 20°C and 30°C, respectively. Error bars represent 1σ.

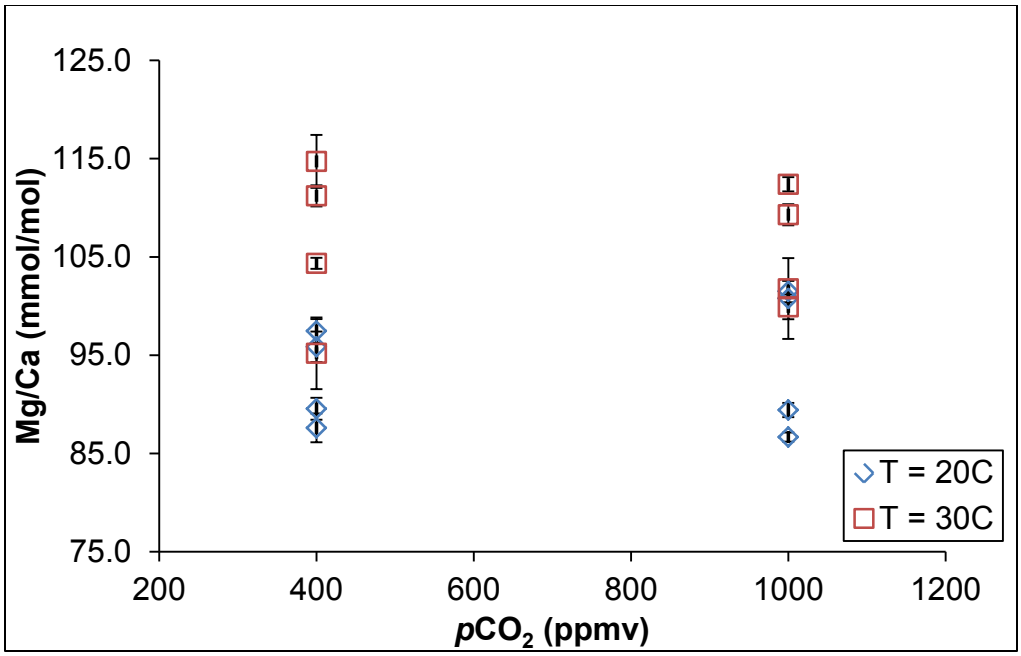

Figure 23: Normalized Mg/Ca (mmol/mol) ratios for *E. viridis* spines cultured under varying pCO_2 (400 and 1000 ppmv) and varying temperature (20°C and 30°C). Each point represents an average of 10-12 SIMS analysis points of one *E. viridis* spine cultured under 1000 or 400 ppmv and 20°C or 30°C. Blue diamonds and red squares represent spines grown under 20°C and 30°C, respectively. Error bars represent 1σ.

Averaged Culturing Conditions of *E. viridis*

Averages for all SIMS analyses were calculated for the four different treatments (400 & 1000 ppmv, 20°C & 30°C) in *E. viridis* spines (Table 10). This helped to reduce the variability that was found for the individual *E. viridis* spines. Generally, *E. viridis* spines grown at higher temperature seawater (30°C) had higher element-to-calcium values than spines grown at the lower temperature (20°C). There wasn't any significant pattern observed when pCO_2 increased from 400 to 1000 ppmv. The error bars represent the standard error of the mean for each spot.

Table 11: Normalized element/calcium ratios of the average for all SIMS analysis spots for each culturing condition *E. viridis*. All measured data is listed in Appendix B.

Taxa	T (°C)	pCO_2 (ppmv)	# of SIMS craters	Li/Ca (µmol/mol)	1 s.e.	B/Ca (mmol/mol)	1 s.e.	Mg/Ca (mmol/mol)	1 s.e.
Tropical	20	400	39	33.7	2.1	0.319	0.005	92.9	1.0
Tropical	30	400	38	60.7	2.5	0.413	0.011	106.0	1.7
Tropical	20	1000	39	42.2	3.4	0.330	0.007	94.5	1.2
Tropical	30	1000	39	52.2	3.8	0.360	0.006	106.2	1.0

Paleo-Echinoderms

During analysis, it was observed that within some of the paleo-echinoderm samples, the element/calcium ratios were heterogeneous. Samples with very little drift were samples that had homogenous elemental/calcium ratios throughout the analysis. Some samples were not fully polished because they were already thinly sectioned, and any additional polishing would damage the structure or cause the sample to be completely lost. A few spots were excluded from the data because they had anomalously high $^{54}Fe/^{42}Ca$ ratios. The Fe content could imply that the area analyzed was an iron rich cement that was embedded in the sample and this would not be part of the sample.

Table 12: Normalized element/calcium ratios calculated from SIMS analysis done on the paleo-echinoderm samples. The data shown represents the average of 3-6 SIMS analysis spots on an individual sample. All measured data is listed in Appendix C.

Sample	Age (Ma)	SST (°C)	n	Li/Ca µmmol/mol	1 s.e	B/Ca mmol/mol	1 s.e.	Mg/Ca mmol/mol	1 s.e.
62	53	13	3	102.7	25.9	0.891	0.089	77.5	1.6
40/41	330	28	6	58.5	26.1	0.452	0.080	69.1	5.0
39	156	20	3	44.8	22.7	1.561	0.299	58.4	9.7
68	330	28	3	2.53	0.77	0.474	0.076	89.4	4.3
70	326	28	3	33.6	1.72	0.507	0.002	57.5	0.9
77	354	26	4	8.8	3.33	0.137	0.038	25.4	6.2
76	354	26	3	25.4	4.17	0.384	0.035	32.7	2.3
66	354	28	3	9.13	0.16	0.255	0.028	28.1	2.6
29	156	22	3	89.2	5.73	0.731	0.009	38.0	4.7
38	190	22	3	6.70	0.72	0.072	0.019	25.9	0.9
26	385	26	3	9.24	2.51	0.039	0.013	38.4	6.0
90	220	24	3	4.43	0.20	0.279	0.002	102.1	2.2
97	253	27	4	12.3	3.11	0.247	0.070	73.4	8.6

Discussion

Is X/Ca in Sea Urchin Calcite Sensitive to Carbonate Chemistry, Temperature, or Both?

Lithium/Calcium

There is a positive correlation between Li/Ca ratios and seawater pCO_2 in *A. punctulata* spines (Fig. 24). Increased acidity in the ocean increases the dissolution rate of calcium carbonate shells and can cause calcification rates to be reduced (Shirayama and Thornton, 2005). The incorporation of minor elements in the ocean, such as Li, into the calcite matrix is passive and occurs because Li can be subsituted as Ca in the calcite matrix (Onuma et al., 1979; Okumura and Kitano, 1986). Therefore, under lower seawater pH, the endoskeleton of *A. punctulata* would not form as easily as it would under the modern ocean-pH (8.2), and thus result in reduced Li incorporation and skeletal Li/Ca ratios.

In *E. viridis* spines, when pCO_2 increased from 400 to 1000 ppmv, no significant correlation between pCO_2 and Li/Ca ratios was observed. Under 20°C seawater culturing condition, Li/Ca ratios increased with higher pCO_2 (from 400 to 1000 ppmv). However, under 30°C seawater culturing condition, Li/Ca ratios decreased by 13% with increasing pCO_2 increased (from 400 to 1000 ppmv) (Fig. 25). *E. viridis* may be experiencing more physiological stress under higher seawater pCO_2 (1000 ppmv), resulting in lower calcification rates (Courtney et al., 2013); this could cause the observed drop in Li/Ca. Overall, it appears that Li/Ca in *E. viridis* are higher under elevated seawater temperature (30°C). *E. viridis* produced variable responses in this study, however, temperature seems to have a stronger effect on the lithium-to-calcium ratio than seawater pH does.

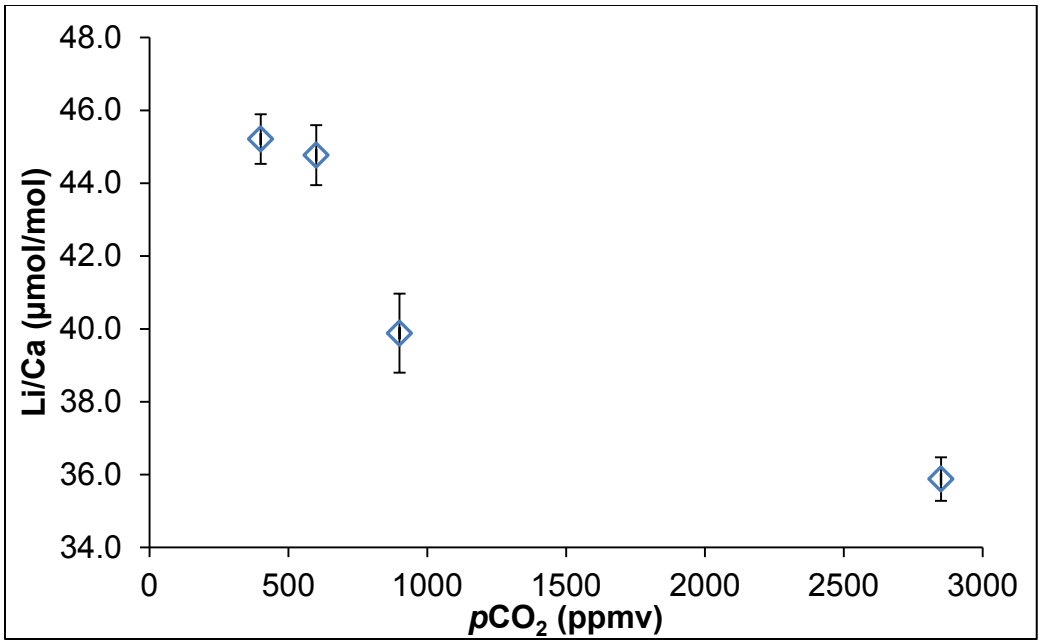

Figure 24: Normalized Li/Ca (µmol/mol) values of *A. punctulata* spines. Each blue diamond represents the average of two sea urchin spines with a total of 10-12 SIMS analysis spots (Appendix A) for a single culturing condition. The error bars represent the standard mean deviation for the average of the ion spots (1σ).

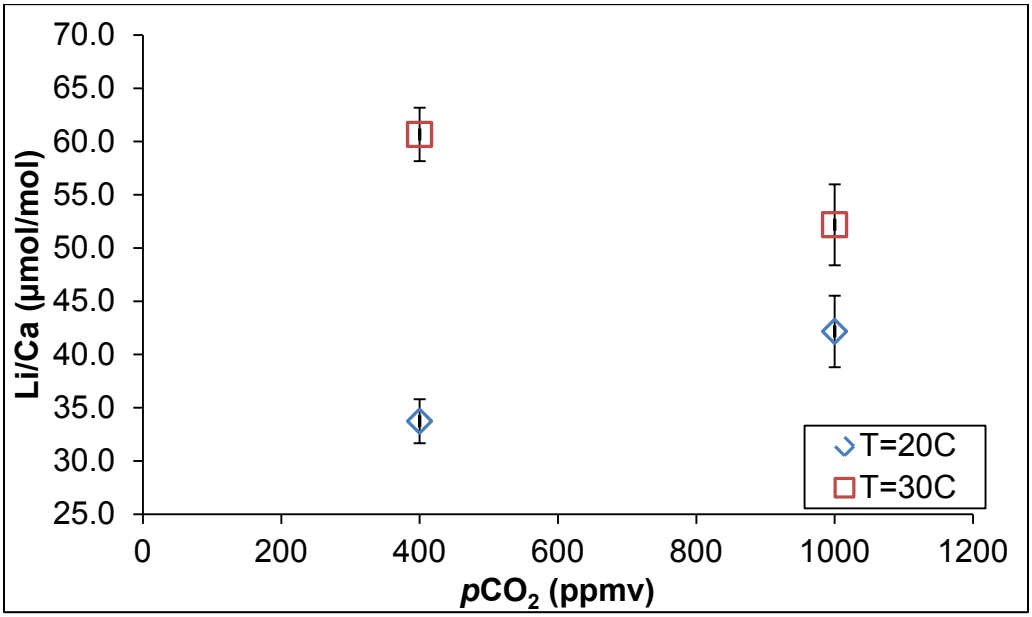

Figure 25: Normalized Li/Ca (µmol/mol) values for *E. viridis* spines grown at varying pCO_2 and temperature. Open blue diamonds and open red squares represent the spines that were cultured in seawater temperatures of 20°C and 30°C respectively. Each point represents the average of four sea urchin spines grown under the same condition (n=18-22) (Appendix B). Error bars represent the standard mean deviation for the average of the ion spots (1σ).

Previous studies on the effect of temperature on Li/Ca in foraminifera did not find any clear relationships (Delaney et al., 1985; Marriott et al., 2004b; Hall and Chan, 2004). Multiple species were extracted from core top samples (96-1796 m) from around the world and were compared to the same species cultured. Responses of Li/Ca in the foraminfera differed between the same species in the culturing and core top samples. Some species (*G. menardii*, *G. sacculifer*, *G. ruber*, and *O. universa*) displayed an increase in Li/Ca as temperature increased, whereas others (*G. truncatulinoid, G. menardii, G. sacculifer, G. ruber,* and *O. universa)* showed a drecease in Li/Ca as temperature increased (Delaney et al., 1985) (Fig. 2). There were some instances where an individual species did not show much change (*G. menardii*). Because the relationship between Li/Ca and temperature varied in culturing experiments on the same type of foraminifera species (such as *G. sacculifer* and *G, menardii*) (Fig. 2) and inorganic calcite, this sheds light on the difficulties of using Li/Ca in calcite as a temperature proxy. There may be other factors (abiotic or biotic) that affect the incorporation of Li into the calcite strcuture of the calcifying organisms.

Li/Ca in *E. viridis* spines*,* underwent an increase as seawater temperature increased from 20°C to 30°C (Fig. 26). This trend exists in spines from both of the 400 and 1000 ppmv pCO_2 culturing experiments.Temperature is a strong factor on the incorporation of Li^+ ions into the calcite structure. The correlation between temperature and Li/Ca detected here is much more pronounced than in other culturing studies done on foraminifera by Delaney et al. (1985) and an opposite reponse to what was found in inorganic precipitation experiments by Marriott et al. (2004b). Due to the size difference between sea urchins and foraminifera, it is postulated that sea urchins would require more resources for growth. Under elevated seawater temperature (30°C) this would mean increased calcification rates (higher metabolic rates) and more Li^+ incorporation (Hall and Chan, 2004).

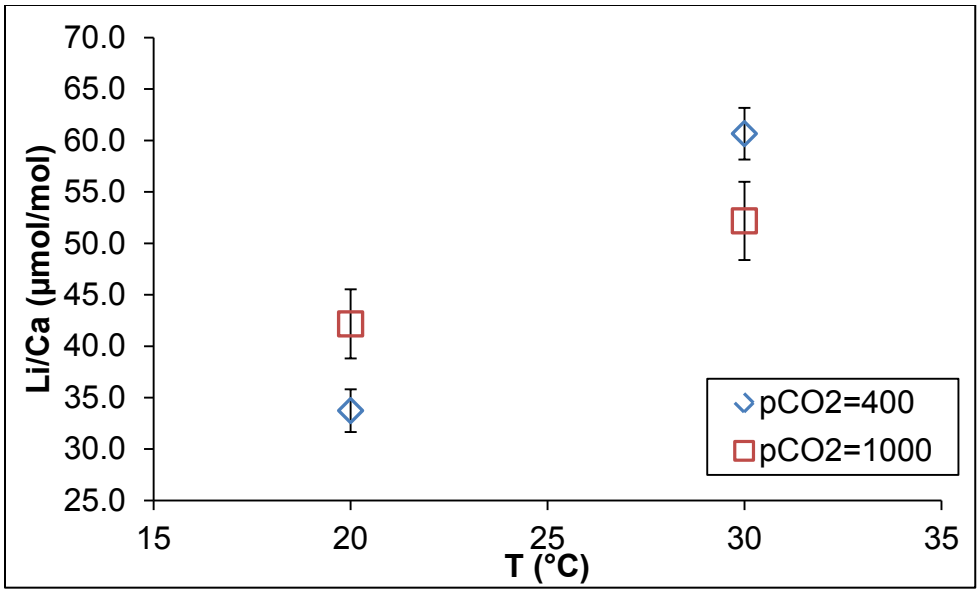

Figure 26: Normalized Li/Ca (µmol/mol) values for *E. viridis* spines grown at varying pCO_2 and temperature. Open blue diamonds represent the spines that were grown under 400 ppmv and the open red squares represent the spines that were grown under 1000 ppmv. Each point represents the average of four sea urchin spines grown under the same culturing condition (n=18-22) (Appendix B). Error bars represent the standard mean deviation for the average of the ion spots (1σ).

Boron/Calcium

B/Ca vs. pH trends in the temperate sea urchin spines are opposite to those expected based on experiments done on foraminifera and corals. B/Ca in temperate sea urchin spines, however, changes similarly with pH as observed for some species of cocolithophores (calcium carbonate forming phytoplankton) (Fig 29). Data for cultured specimens in this thesis support the hypothesis of Schneider and Erez (2006), Fabry et al. (2008), and Ries et al. (2009) that some species of marine calcifiers are able to modify the pH at the site of calcification, as the patterns in B/Ca in both species were similar to calcification rate (Fig. 27-28). Since B/Ca normally decreases with pH (higher pCO_2), then the relationship between B/Ca and pH was seen in *E. viridis* spines cultured under seawater temperatures of 30°C (Fig 28). The opposite was seen for *E. viridis* spines cultured under seawater temperatures of 20°C (Fig 28).The varied responses observed in *E. viridis* spines meant that there was no clear relationship between B/Ca and pCO_2 (Fig. 28).

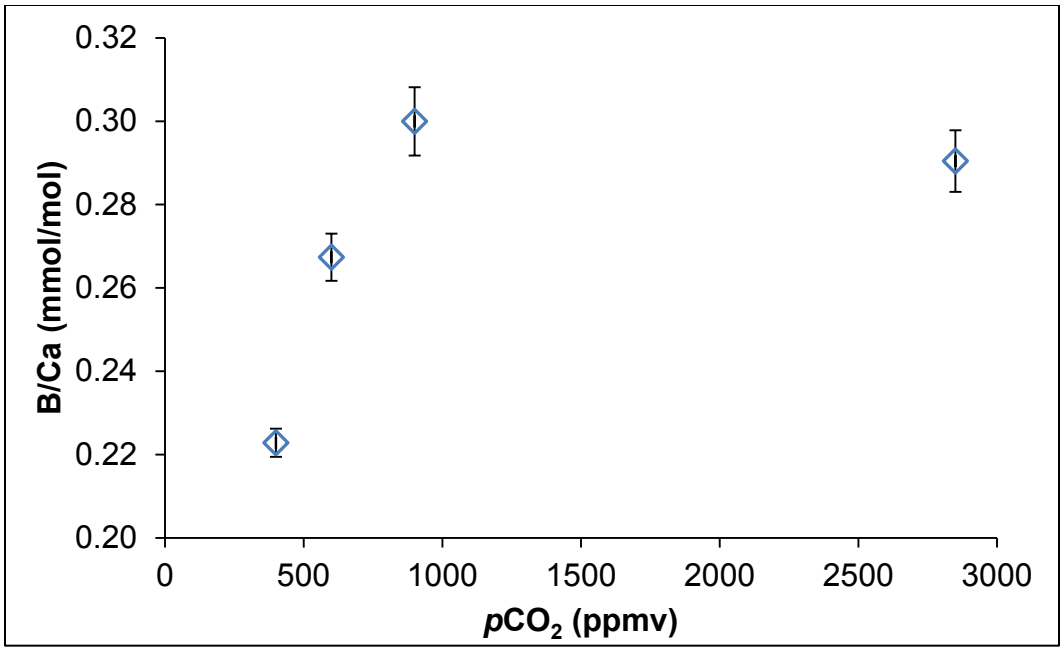

Figure 27: Normalized B/Ca (mmol/mol) values of *A. punctulata* spines. Each blue diamond represents the average of two sea urchin spines with a total of 10-12 SIMS analysis spots (Appendix A) for a single culturing condition. The error bars represent the standard mean deviation for the average of the ion spots (1σ).

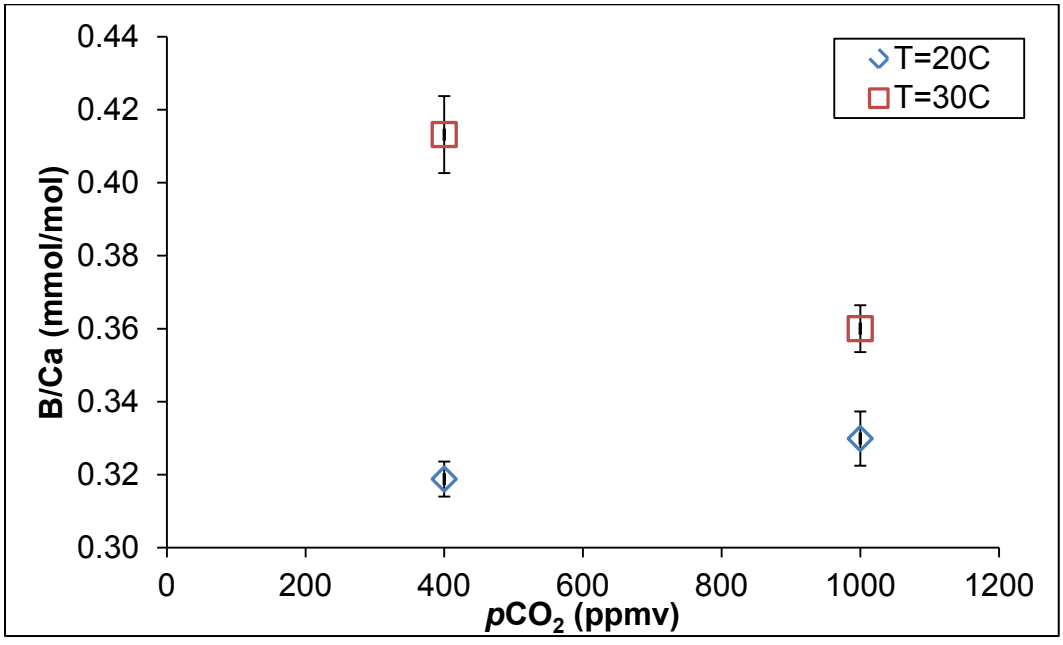

Figure 28: Normalized B/Ca (mmol/mol) values for *E. viridis* spines grown at varying pCO_2 and temperature. Open blue diamonds and open red squares represent the that were cultured in seawater temperatures of 20°C and 30°C respectively. Each point represents the average of four sea urchin spines grown under the same culturing condition (n=18-22) (Appendix B). Error bars represent the standard mean deviation for the average of the ion spots (1σ).

There have been several studies investigating B/Ca in planktonic foraminifera as a proxy for seawater pH that have found that B/Ca values tend to increase with increasing seawater pH (Yu et al., 2007; Foster 2008). A recent study examining B/Ca in several different species of cocolithophores found that the B/Ca varied from species to species (Stoll et al., 2012). There were two different responses found in *C. braarudii* and *E. huxleyii* under increased seawater pH (Fig 29). The study hypothesized that the two different responses were due to the individual species being able to regulate pH at the site of calcification (Stoll et al., 2012). This may be the same reason why *A. punctulata* had an opposite response compared to other studies. *A. punctulata* could be secreting a fluid layer around the site of calcification with a distinct pH and this may be causing the skeletal B/Ca ratios to be different than the surrounding seawater.

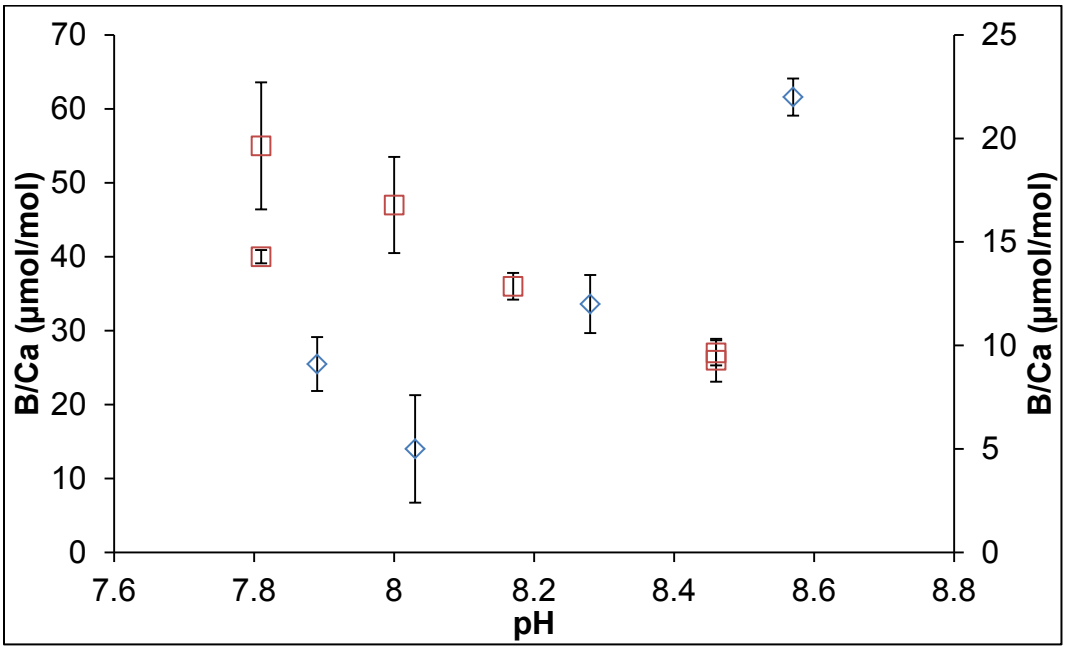

Figure 29: Reproduced figure of B/Ca ratios (µmol/mol) from SIMS analysis on cocolithophores, *C. braarudii* and *E. huxleyi* (Stoll et al., 2011). Both left and right y-axis represents B/Ca (mmol/mol) but at different levels because B/Ca was greater in *E. huxleyi*. Plot symbols are: □, *E. huxleyi* (RCC-1256) and ◊, *C. braarudii* (2009). Each point represents the average of 4-10 SIMS analysis.

As temperature increased from 20°C to 30°C, B/Ca ratios in E. *viridis* spines also increased (Fig. 30). The correlation with temperature suggests that temperature is a factor with

strong control on calcification rates, which affects how much boron gets incorporated into the calcite. However, pCO_2 also plays a role in the calcification rate of the *E. viridis*. Under elevated pCO_2 levels (1000 ppmv), the amount of B/Ca in the *E. viridis* spine is much lower than in an *E. viridis* spine that was grown in ambient pCO_2 levels (400 ppmv) (Fig. 30). *E. viridis* spines grown at 400 ppmv and in a seawater temperature of 30°C has a B/Ca ratio of 0.413 (±0.011) mmol/mol, whereas under 1000 ppmv the B/Ca ratio was 0.360 (±0.006) mmol/mol (Fig. 30). This simply can be explained without invoking differences in precipitation rates of sea urchins cultured under variable pCO_2. The lower B/Ca values reflects the fact that $B(OH)_4^-$ is less abundant at higher pCO_2 (lower pH) (Hemming et al., 1994).

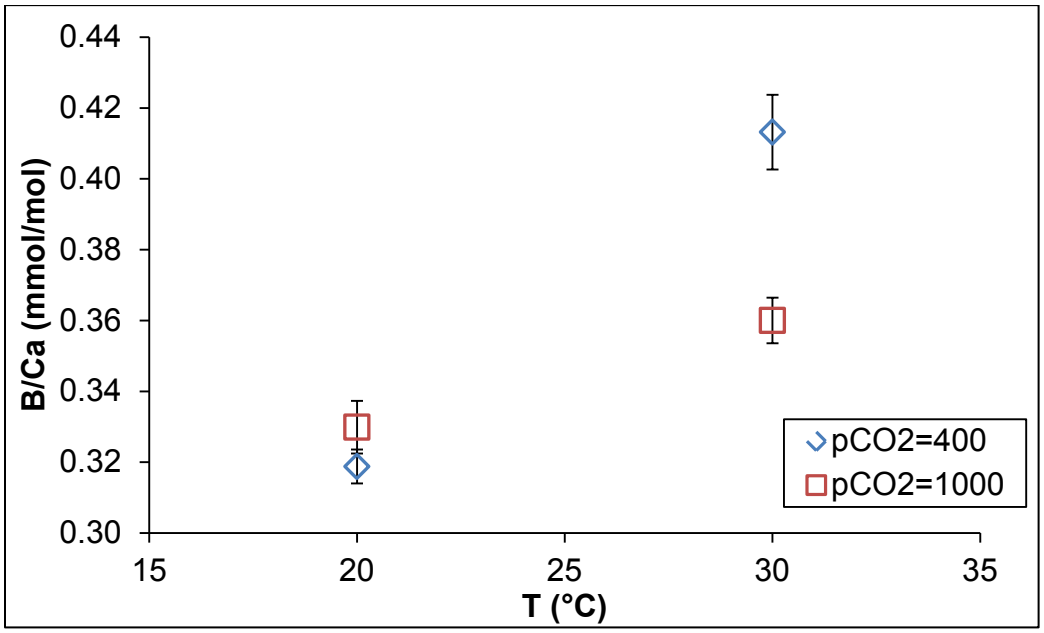

Figure 30: Normalized B/Ca (mmol/mol) values for *E. viridis* spines grown at varying pCO_2 and temperature. Open blue diamonds represent the spines that were grown under 400 ppmv and the open red squares represent the spines that were grown under 1000ppmv. Each point represents the average of four sea urchin spines grown under the same condition (n=18-22) (Appendix B). Error bars represent the standard mean deviation for the average of the ion spots (1σ).

Only B/Ca in *A. punctulata* spines had a similar trend to the calcification rates reported in the Ries et al. (2009) paper (Fig. 31). Other element ratios (Li/Ca and Mg/Ca) did not show this trend. B/Ca in the *A. punctulata* spines was plotted against the saturation state of calcite (Ω-

calcite). This was done instead of using pCO_2 so that it would be easier to compare it to the calcification rate found in Ries et al. (2009) study (Fig. 31). As Ω-calcite increases, B/Ca in the temperate sea urchin spine decreases because more dissolution than growth of the $CaCO_3$ shell is occurring and thus decreasing the amount of B/Ca that is incorporated. This implies that calcification rate as a function of seawater pCO_2 controls B/Ca. As seawater pH decreases the rate of calcification decreases because the seawater is more acidic due to the reduced carbonate ion concentrations. Another factor that may be important is possible increased dissolution of the sea urchin endoskeleton.

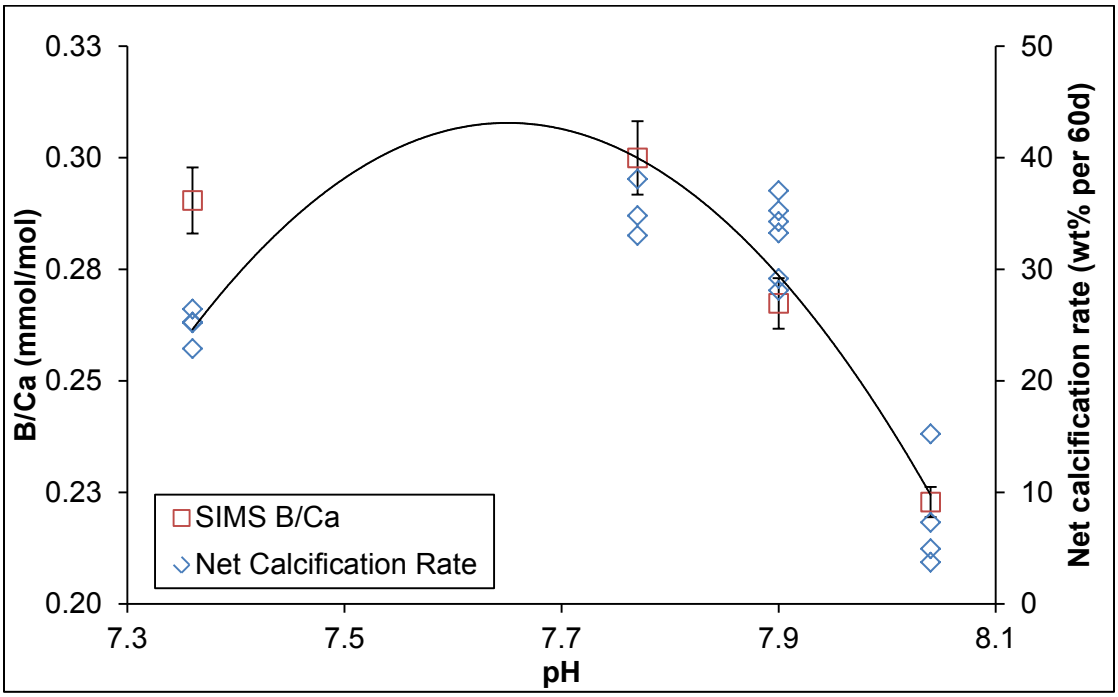

Figure 31: Data from SIMS analysis of B/Ca ratios (open red squares) in A. *punctulata* spines. The net calcification rate (wt % per 60d) of *A. punctulata* from the culturing experiment is shown (Ries et al., 2009). Net calcification rate (open blue diamonds) represents the percent weight difference between the initial and final buoyant weight of *A. punctulata*. Best fit line follows Ries et al. (2009) net calcification rate.

Magnesium/Calcium

The Mg/Ca in *A. punctulata* lacks a strong correlation with increasing seawater pCO_2 (Fig. 32). Seawater pH has a small effect on the Mg/Ca ratios: the values are higher (82.3 ±2.0 and 82.8 ±1.3 mmol/mol) under neutral seawater pCO_2 (400 and 600 ppmv). Mg/Ca values at

an intermediate pCO_2 (900 ppmv) were the lowest (68.3 ±1.9 mmol/mol) and then increase again (76.2 ±1.2) for the highest seawater pCO_2 (2850 ppmv) adjusted in the culturing experiments. An explanation to why Mg/Ca tends to be lower in seawater with high pCO_2 is that more acidic seawater affects the ability of *A. punctulata* to form its spines (Ries et al., 2009). The lower pH puts more stress on *A. punctulata* and negatively affects its growth. In both temperature treatments (20°C and 30°C) of the *E. viridis* spines, there was little change in Mg/Ca as pCO_2 increased from 400 to 1000 ppmv (Fig. 33). Generally, Mg/Ca ratios in *E. viridis* were higher under seawater temperatures of 30°C (106 ±1.7 and 106 ±1.0 mmol/mol) than seawater temperatures of 20°C (92.9 ±1.0 and 94.4 ±1.2 mmol/mol). This implies that temperature has a stronger control on Mg/Ca ratios in *E. viridis* spines than seawater pCO_2.

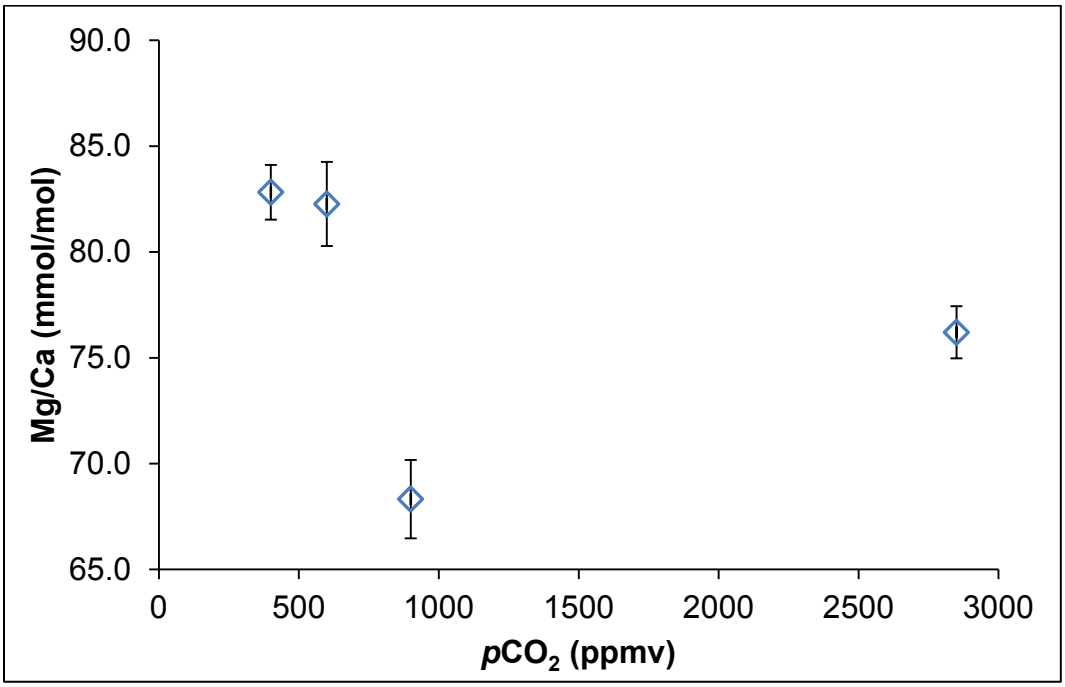

Figure 32: Normalized Mg/Ca (mmol/mol) values for the temperate sea urchin spines (*A.punctulata)*. Each blue diamond represents the average of two sea urchin spines with a total of 10-12 SIMS analysis spots (Appendix A) for a single culturing condition. Error bars represent the standard mean deviation for the average of the ion spots (1σ).

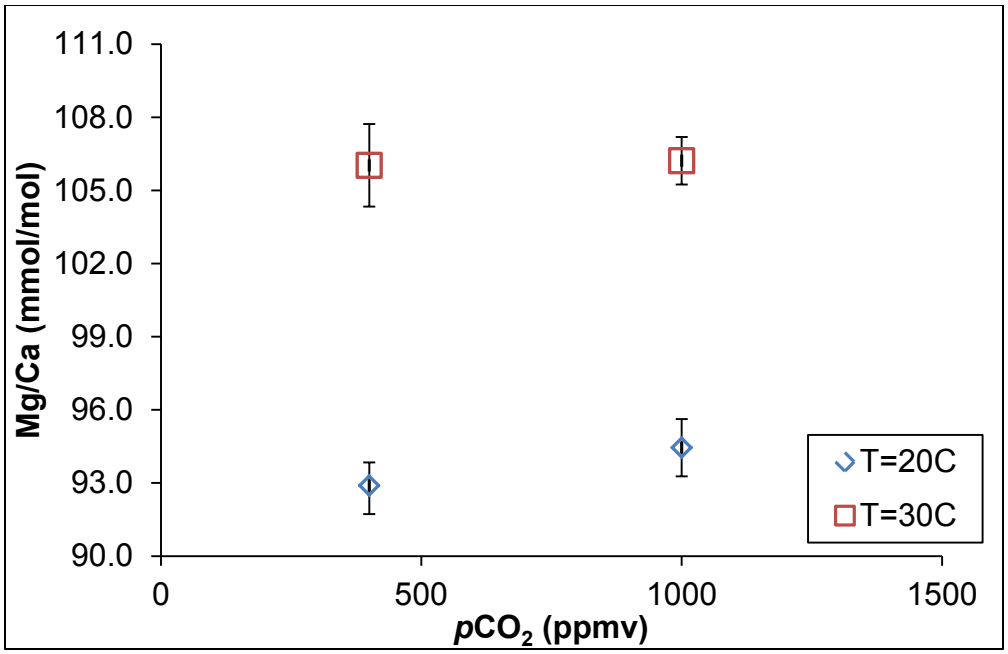

Figure 33: Normalized Mg/Ca (mmol/mol) values for tropical sea urchin (*E.viridis*) spines grown at varying pCO_2 and temperature. Open blue diamonds and open red squares represent the spines that were cultured in seawater temperatures of 20°C and 30°C respectively Each point represents the average of four sea urchin spines grown under the same condition (n=18-22) (Appendix B). Error bars represent the standard mean deviation for the average of the ion spots (1σ).

The relationship between Mg/Ca ratios and pH in this study was consistent with one other culturing study (Lea et al., 1999). Both sea urchins and planktonic foraminfera Mg/Ca were not affected by seawater pH. However, this result is contradictory with results of other recent studies; elevated Mg/Ca ratios in benthic and planktonic foraminfera under lower seawater pH were found by Russell et al. (2004) and Dissard et al. (2010). More experiements with seawater pH and sea urchins would have to be done before any conclusions can be assessed.

The relationship between Mg/Ca and temperature has been extensively studied (Rosenthal et al., 1997; Russell et al., 2004; Lea et al., 1999). These studies have found that as the temperature of seawater is increased, more Mg becomes incorporated into the calcite. This relationship was seen in the *E. viridis* spines under the different pCO_2 levels (Fig. 34). In 20°C seawater, there was an average Mg/Ca ratio of 93.67 ±1.3 mmol/mol and under a seawater

temperature of 30°C there was an average of 106.12 ±1.1 mmol/mol. This would equate to a 13% per °C increase. Similar results were found in Lea et al. (1999), there was a 10.2 % per °C increase in the species *G. bulloides* and a 8.5 % per °C increase in the species *O. universa* (Fig. 34). The result from *E. viridis* spines are similar to what was found in other species and this relationship could potentially be used as a proxy for seawater temperature.

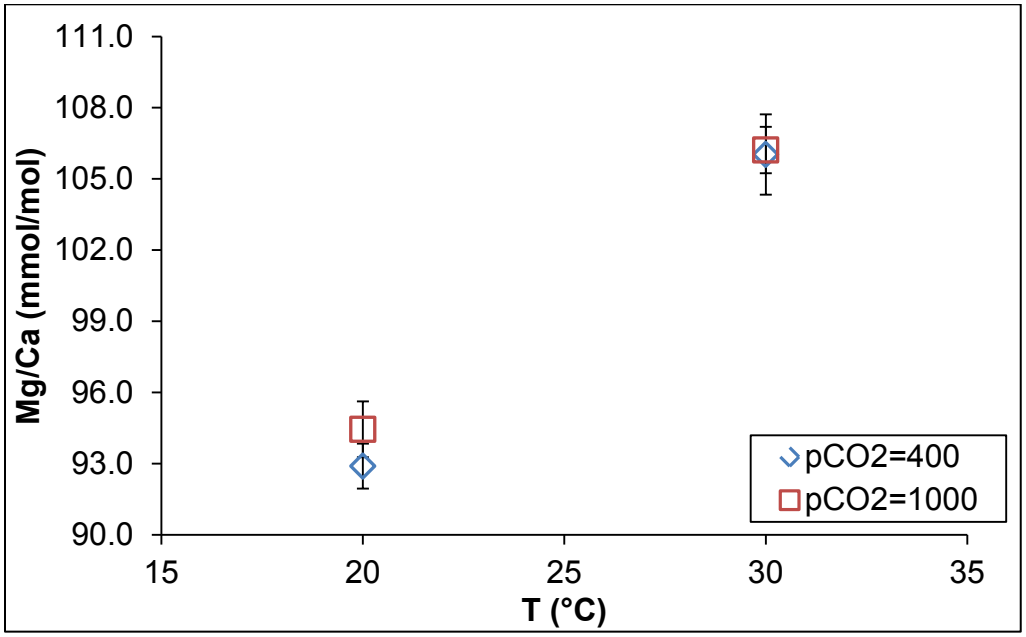

Figure 34: Normalized Mg/Ca (mmol/mol) values for tropical sea uruchin (*E. viridis*) spines grown at varying pCO_2 and temperature. Open blue diamonds represent the spines that were grown under 400 ppmv and the open red squares represent the spines that were grown under 1000ppmv. Each point represents the average of four sea urchin spines grown under the same condition (n=18-22) (Appendix A.2). Error bars represent the standard mean deviation for the average of the ion spots (1σ).

Summary of Cultured Sea Urchin Element-to-Calcium SIMS Analysis

The SIMS analysis on both *A. punctulata* and *E. viridis* spines revealed that the dominating control on elemental-to-calcium ratios in the sea urchin spines was temperature (Table 13). This was seen in the *E. viridis* spines where temperature was also manipulated, whereas the temperature was fixed for *A. punctulata*. These results support other studies that have postulated a temperature control on elemental partitioning between calcite and seawater as a function of calcification rate. Increased metabolism in sea urchins has been attributed to

increased seawater temperature and this would mean a higher calcification rate (Brockington and Clarke, 2000; Siikavuopio et al., 2006). Thus, the calcite would have a larger X/Ca value. Seawater pH is a secondary factor that affects the element/calcium ratios. This may be due to kinetic effects on net calcification rates or because the specimens were able to control pH at the site of calcification. Studies have found that some species of sea urchins were able to regulate their internal pH in order to compensate for the lower pH in the seawater, but the extent of control was limited (Spicer, 1995; Miles et al., 2007; Ries, 2011). This would minimize the effects that lower seawater pH would have on the spines, as was seen in the *E. viridis* spines. Only B/Ca in *A. punctulata* spines had a similar trend to what was found in the culturing experiment that grew these spines (Ries et al., 2009).

Table 13: Summary of responses from SIMS analysis on *A. punctulata* and *E. viridis* spines.

Taxa	T (°C)	pCO_2 (ppmv)	Element Ratio	Response	Response in Ries et al., 2009
Temperate	25	Increase 400 to 2850	Li/Ca	Decreased	Parabolic (positive under intermediate pCO_2,negative under highest pCO_2)
Temperate			B/Ca	Increased-Threshold	
Temperate			Mg/Ca	No response	
Tropical	20	Increase 400 to 1000	Li/Ca	Increased	
Tropical			B/Ca	Increased	
Tropical			Mg/Ca	Increased	
Tropical	30	Increase 400 to 1000	Li/Ca	Decreased	
Tropical			B/Ca	Decreased	
Tropical			Mg/Ca	Slightly Increased	
Tropical	Increase from 20 to 30	400	Li/Ca	Increased	
Tropical			B/Ca	Increased	
Tropical			Mg/Ca	Increased	
Tropical	Increase from 20 to 30	1000	Li/Ca	Increased	
Tropical			B/Ca	Increased	
Tropical			Mg/Ca	Increased	

Fossilized Paleo-Echinoderms

The data from the paleo-echinoderm analysis for the analyzed element-to-calcium ratios versus age are presented in the Fig. 35-37. Significant heterogeneity of X/Ca was determined on some of the samples, although in some cases this reflects only 2-3 spot analyses per sample. This may be caused by contamination with organic materials or mineral inclusions that

were encountered as the primary ion beam sputters through the sample surface. To monitor contamination, $^{54}Fe/^{42}Ca$ intensities were recorded which should be low in unaltered calcite. Because there are no suitable calcite standards to normalize Fe counts, the average intensity in counts per second (cps) was used (Appendix C). Analyses of calcite reference materials and NIST-SRM glasses yielded $^{54}Fe/^{42}Ca$ of 0.078 – 0.081 cps. Therefore, samples that had $^{54}Fe/^{42}Ca$ (cps) greater than 1 were excluded from the analysis, because this would indicate that the analysis volume included some high Fe cement material. For future analysis; a calcite standard with known Fe is desirable to quantity the abundance of Fe in unknown calcite.

Variations in X/Ca Over the Past 400 Million Years

The paleo-echinoderm samples show variable Li/Ca and B/Ca over the past 400 Ma and it appears that both Li/Ca and B/Ca has been increasing to present (Fig. 35-37). Li/Ca and B/Ca start out comparatively low 400 Ma ago, with values of 9.24 ±2.51 µmol/mol and 0.039 ±0.013 mmol/mol, respectively. Both Li/Ca and B/Ca slowly increase to 102.68 µmol/mol and 0.891 mmol/mol, respectively, in the last 50 Ma. The peak of both Li/Ca and B/Ca content in the paleo-echinoderm samples occurred in the species *B. pentagonalus* at 156 Ma. At 156 Ma, the Li/Ca and B/Ca values were 89.2 ±5.7 µmol/mol and 1.56 ±0.29 mmol/mol, respectively. For B/Ca greather than 300 Ma, the values overlap within uncertainty (Fig. 40). A maximum Mg/Ca ratio was found 220 Ma in the species *E. cassianus* (Fig. 41). The trend for Mg/Ca data was dissimilar to Li/Ca and B/Ca, and the trend appears to be following a cycle, with each cycle lasting roughly 100 Ma. This variability may be linked to the Wilson cycle, as the tectonic processes which influence the formation and destruction of continents influence the chemistry of seawater. For example, the formation of oceanic crust at mid-ocean ridges results in the removal of magnesium and the addition of calcium to seawater, and therefore changes in

seafloor spreading rates and the area of the ocean covered by ridges can influence X/Ca ratios in seawater (Katz et al., 2004).

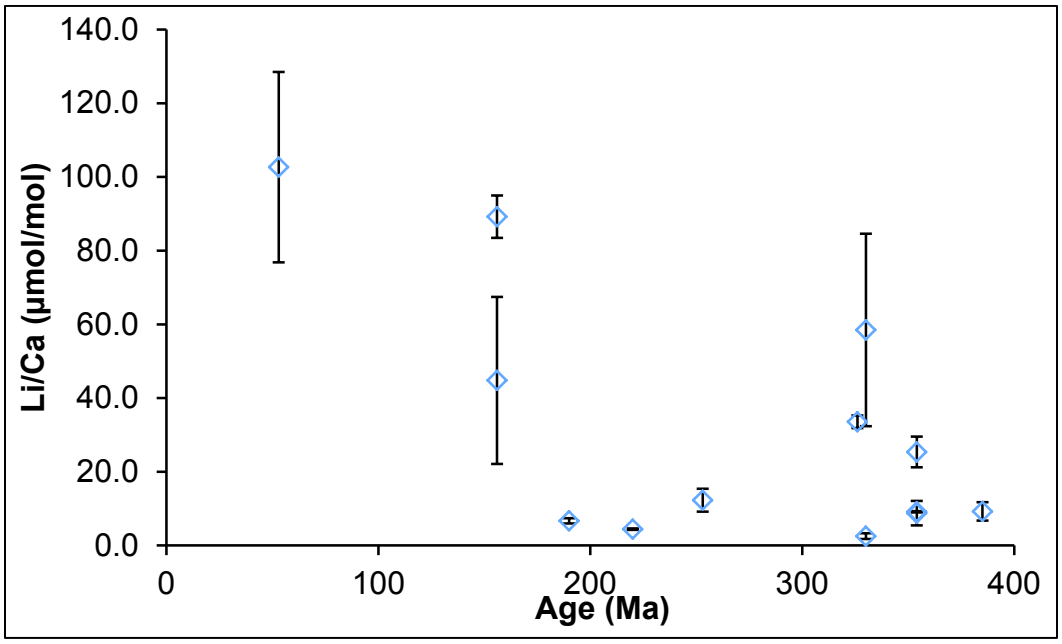

Figure 35: Normalized values for Li/Ca in the paleo-echinoderm samples vs. the age of the samples. Each point represents a paleo-echinoderm sample with the average of 3-5 SIMS analysis spots (Appendix C) per sample. Error bars represent the standard mean deviation for the average of the ion spots (1σ).

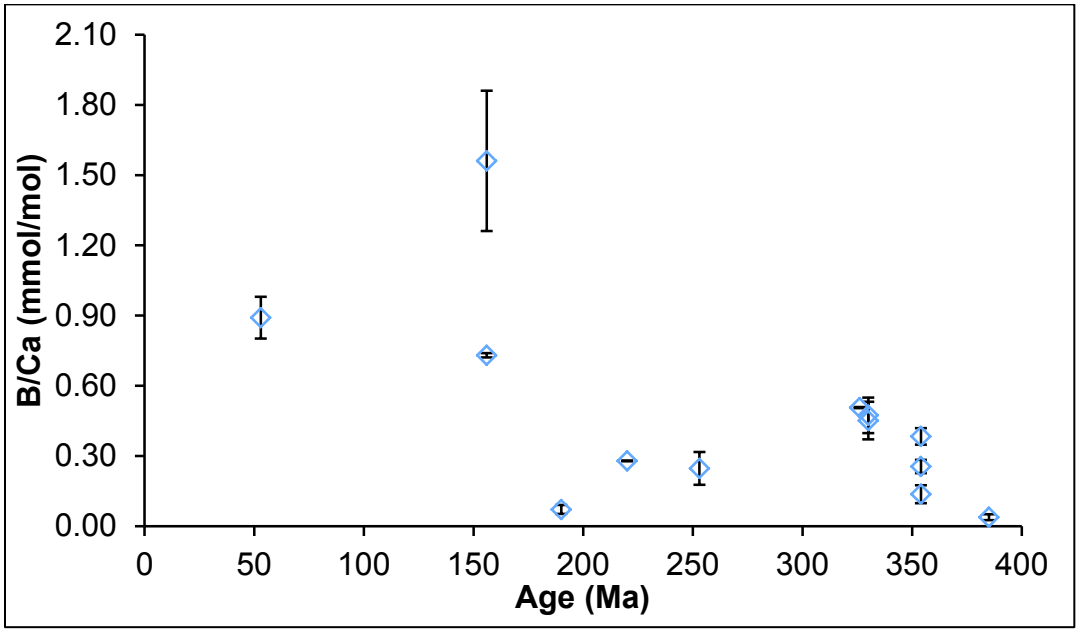

Figure 36 Normalized values for B/Ca in the paleo-echinoderm samples vs. the age of the samples. Each point represents the average of 3-5 SIMS spots (Appendix C) per paleo-echinoderm sample. Error bars represent the standard mean deviation for the average of the ion spots (1σ).

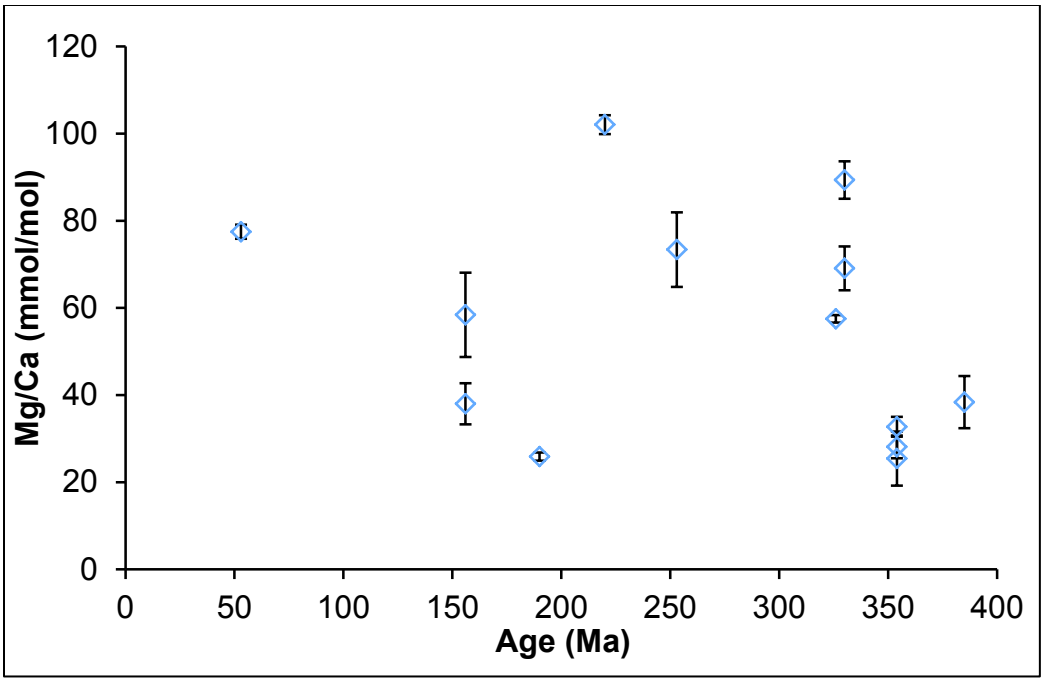

Figure 37: Normalized values for Mg/Ca in the paleo-echinoderm samples vs. the age of the samples. Each point represents a paleo-echinoderm sample with the average of 3-5 SIMS analysis spots (Appendix C) per sample. Error bars represent the standard mean deviation for the average of the ion spots (1σ).

Using Cultured Sea Urchins to Calculate Partition Coefficient

The modern sea urchin samples provided an insight into how elements were incorporated into the calcite structure. Using measured concentrations in calcite and seawater, a partition coefficient (D^c) was calculated for each of the element ratios. The partition coefficient (D^c) was defined as X/Ca in cultured sea urchin divided by X/Ca in the seawater (Equation 10).

$$D^c = \frac{\left(\frac{X}{Ca}\right)_{\text{cultured sea urchin}}}{\left(\frac{X}{Ca}\right)_{\text{seawater}}} \quad (10)$$

The X/Ca of the seawater was calculated using the current concentrations of the elements (Li, B, Ca, and Mg) in seawater (Turekian, 1968) (Table 14).

Table 14: The concentrations (ppm) of Li, B, Mg, and Ca found in the seawater and seawater X/Ca (Turekian, 1968).

	Concentration (ppm)	Seawater X/Ca
Li	0.194	0.000472
B	4.52	0.0110
Mg	1290	3.14
Ca	411	1.00

The partition coefficient (D^c) was calculated using the seawater X/Ca (Table 15).

Table 15: The partition coefficient values for sea urchins (temperate and tropical) under each of the culturing condition.

T (°C)	pCO_2 (ppmv)	D^cLi/Ca	D^cB/Ca	D^cMg/Ca
20	**400**	0.0715	0.0290	0.0296
20	**1000**	0.0893	0.0300	0.0301
25	**400**	0.0958	0.0203	0.0264
25	**600**	0.0948	0.0243	0.0262
25	**900**	0.0845	0.0273	0.0218
25	**2750**	0.0760	0.0264	0.0243
30	**400**	0.0129	0.0376	0.0338
30	**1000**	0.0111	0.0327	0.0338
Avg D^c		**0.0939**	**0.0284**	**0.0282**
Max D^c		**0.129**	**0.0376**	**0.0338**
Min D^c		**0.0715**	**0.0203**	**0.0218**

Using the calculated values of D^c, this can then be used to estimate the ratio of X/Ca of paleo-seawater. This was achieved by taking the SIMS X/Ca ratio found in the paleo-echinoderms and dividing it by the partition coefficient, D^c determined from culturing experiment (Equation 11).

$$\left(\frac{\mathrm{X}}{\mathrm{Ca}}\right)_{\mathrm{paleo-seawater}} = \frac{\left(\frac{\mathrm{X}}{\mathrm{Ca}}\right)_{\mathrm{paleo-echinoderm}}}{\mathrm{D^c}} \qquad (11)$$

Partition Coefficient Based on Corrected Temperature

The partition coefficient could be affected by the seawater temperature, but using the average D^c X/Ca may cause the calculated paleo-seawater to be unrealistic. Therefore, a comparison between the average and corrected D^c X/Ca based on temperature was made. The

temperature corrected D^c was extrapolated by taking the average D^c X/Ca for each culturing condition (Table 16). These values from Table 16 were plotted and a linear regression line was used to extrapolate D^c X/Ca over a range of temperatures (Fig. 38-40)

Table 16: Average D^c X/Ca for the seawater temperature that the sea urchins were cultured.

T (°C)	pCO_2 (ppmv)	D^c Li/Ca	D^c B/Ca	D^c Mg/Ca
20	**400**	0.0715	0.0290	0.02960
20	**1000**	0.0893	0.0300	0.03009
25	**400**	0.0958	0.00203	0.02639
25	**600**	0.0948	0.0243	0.02621
25	**900**	0.0845	0.0273	0.02177
25	**2750**	0.0760	0.0264	0.02428
30	**400**	0.0129	0.0376	0.03378
30	**1000**	0.0111	0.0327	0.03384

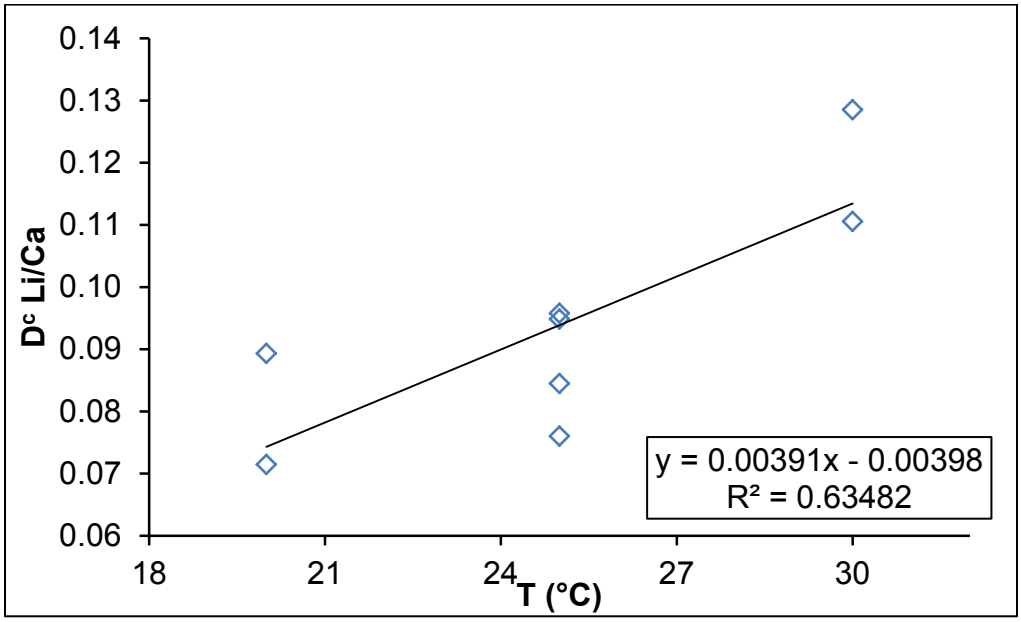

Figure 38: Scatterplot for D^c Li/Ca versus the temperature. Each point represents the average of a single culturing condition for temperate and tropical sea urchin. The linear trend line was plotted with the graph.

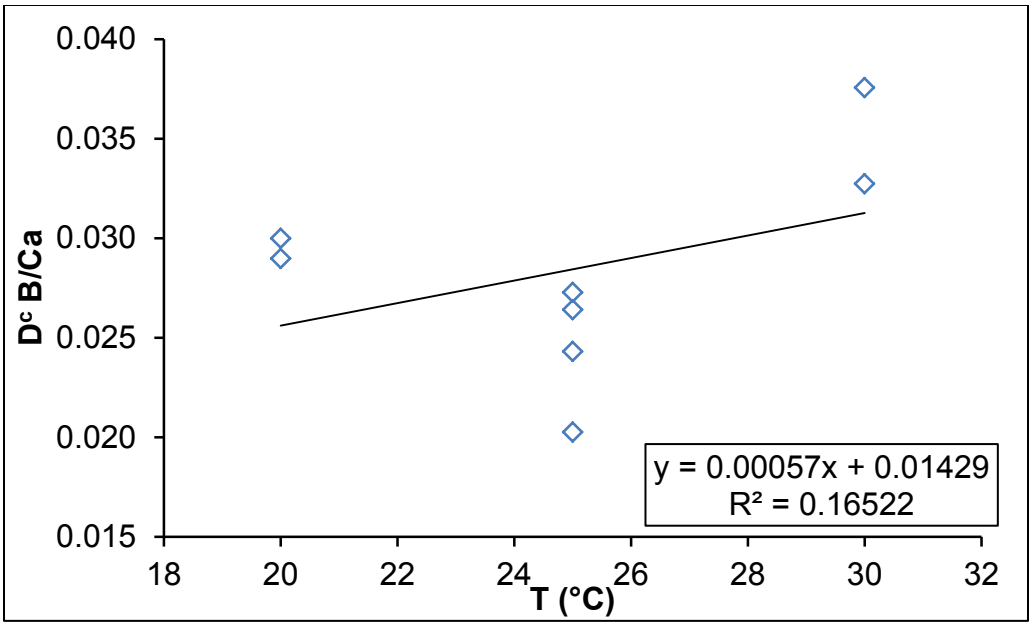

Figure 39: Scatterplot for D^c B/Ca versus the temperature. Each point represents the average of a single culturing condition for temperate and tropical sea urchin. The linear trend line was plotted with the graph.

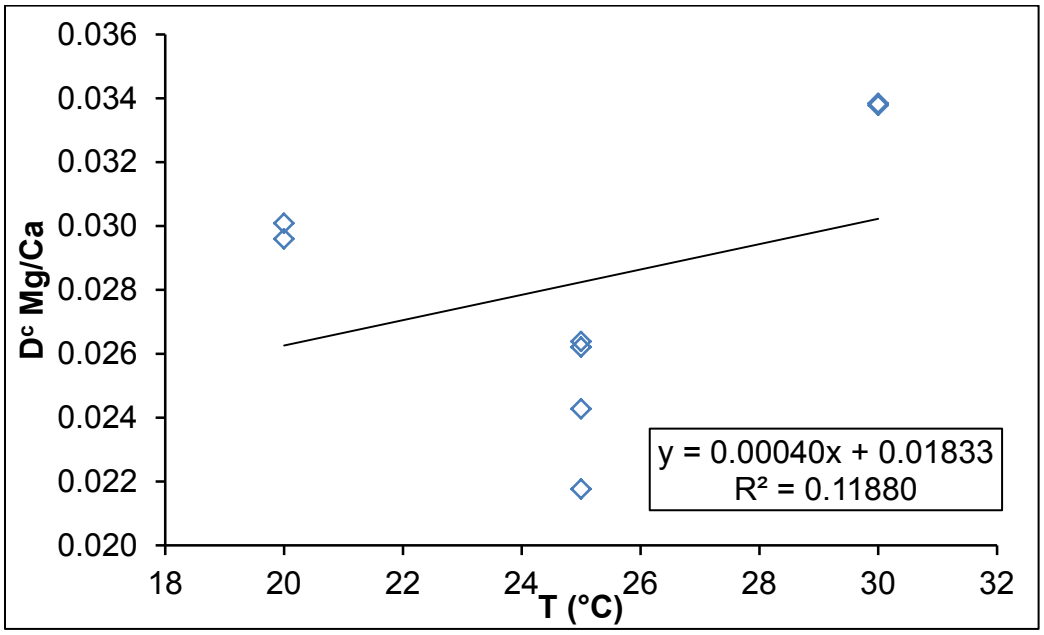

Figure 40: Scatterplot for D^c Mg/Ca versus the temperature. Each point represents the average of a single culturing condition for temperate and tropical sea urchin. The linear trend line was plotted with the graph.

Only the linear regression lines for D^c Li/Ca had a marginal fit (R^2=0.63), whereas the other two, B/Ca and Mg/Ca, resulted in poor fits (R^2=0.17 and R^2=0.12, respectively). This may

be due to averaging data from the two different species analyzed. These two species could have different metabolic rates, which would affect the partition coefficient. However, the values were still plotted together because the paleo-echinoderm samples contain multiple species within the echinoderm family. Therefore, since *A. punctulata* and *E. viridis* also fall under the echinoderm family, plotting together would give a rough estimate of the ocean's element-to-calcium ratios. The slope of the regression line was used to calculate the D^c X/Ca over a range of temperatures (10-35°C) that sea urchins can be found. The corrected D^c X/Ca based on of the seawater temperature along with the uncorrected D^c X/Ca are shown in Table 17.

Table 17: Corrected D^c values for all elements in the paleo-echinoderm samples. The corrected and uncorrected seawater Mg/Ca values and the percent difference between the numbers.

SST (°C)	Age (Ma)	D^c Li/Ca Corrected	Seawater Li/Ca	D^c B/Ca Corrected	Seawater B/Ca	D^c Mg/Ca Corrected	Seawater Mg/Ca
13	**53**	0.0469	0.002190	0.0217	0.0411	0.0235	3.3
28	**330**	0.1055	0.000554	0.0303	0.0149	0.0295	2.3
20	**156**	0.0742	0.000603	0.0257	0.0608	0.0263	2.2
28	**330**	0.1055	0.000024	0.0303	0.0157	0.0295	3.0
28	**326**	0.1055	0.000318	0.0303	0.0168	0.0295	2.0
26	**354**	0.0977	0.000090	0.0291	0.0047	0.0287	0.9
26	**354**	0.0977	0.000260	0.0291	0.0132	0.0287	1.1
28	**354**	0.1055	0.000087	0.0303	0.0084	0.0295	1.0
22	**156**	0.0820	0.001090	0.0268	0.0332	0.0271	1.4
22	**190**	0.0820	0.000082	0.0268	0.0027	0.0271	1.0
26	**385**	0.0977	0.000095	0.0291	0.0013	0.0287	1.3
24	**220**	0.0899	0.000049	0.0280	0.0010	0.0279	3.7
27	**253**	0.1016	0.000121	0.0297	0.0083	0.0291	2.5
Avg		**0.0917**	**0.000428**	**0.0282**	**0.0178**	**0.0281**	**1.97**

The corrected and uncorrected D^c X/Ca values were plotted together; it was found that there was not a significant difference between the corrected and uncorrected seawater element-to-calcium ratio, except for younger samples (Fig. 41-43).

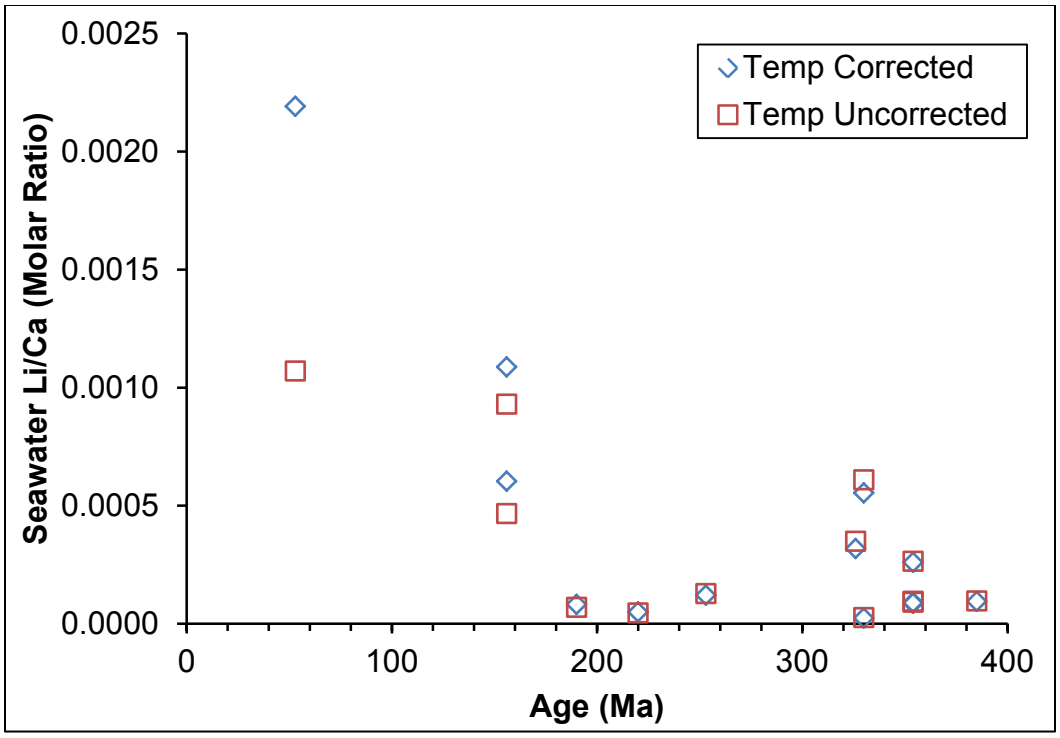

Figure 41: Comparing the corrected D^c Li/Ca based on the seawater temperature and the uncorrected D^c Li/Ca based off of the average of all of the culturing conditions.

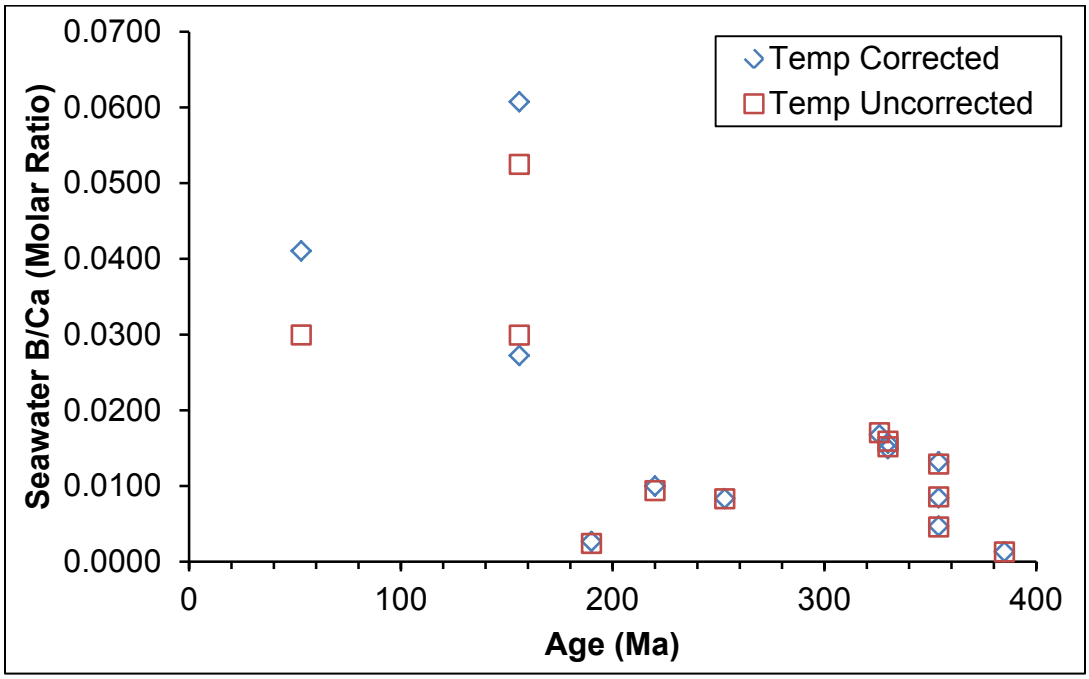

Figure 42: Comparing the corrected D^c B/Ca based on the seawater temperature and the uncorrected D^c B/Ca based off of the average of all of the culturing conditions.

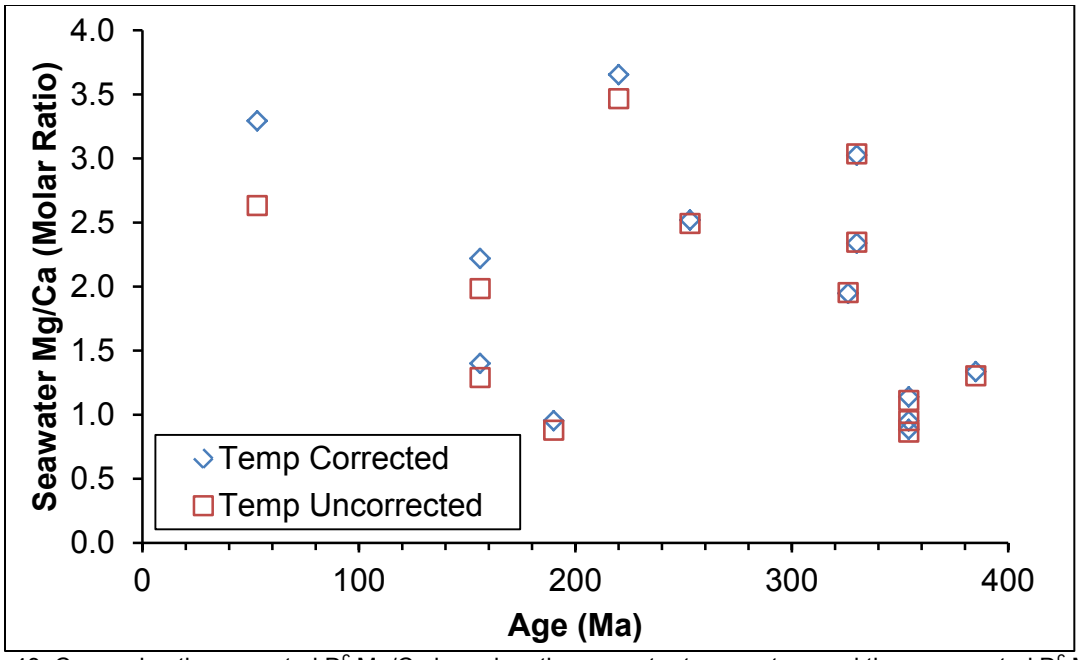

Figure 43: Comparing the corrected D^c Mg/Ca based on the seawater temperature and the uncorrected D^c Mg/Ca based off of the average of all of the culturing conditions.

Since the variability between the corrected (with temperature) and uncorrected (based on average) D^c X/Ca was small, the average D^c of all three elements can be used for calculating the paleo-seawater conditions (Table 18).The seawater temperatures for these fossilized samples were predicted and there can be some variability (Dickson 2004).

Table 18: Paleo-seawater Li, B, and Mg for each of the paleo-echinoderms using the partition coefficient found from the cultured sea urchin spines. Paleo-seawater was found using the average D^c of the cultured sea urchin spines.

Sample	Age (Ma)	SST (°C)	Seawater Li/Ca	Seawater B/Ca	Seawater Mg/Ca
62	**53**	**13**	0.0006830	0.02510	2.7
40/41	**330**	**28**	0.0006100	0.01520	2.4
39	**156**	**20**	0.0004670	0.05250	2.0
68	**330**	**28**	0.0000264	0.01590	3.0
70	**326**	**28**	0.0003500	0.0171	2.0
77	**354**	**26**	0.0000914	0.00460	0.9
76	**354**	**26**	0.0002650	0.01290	1.1
66	**354**	**28**	0.0000952	0.00858	1.0
29	**156**	**22**	0.0009300	0.02990	1.3
38	**190**	**22**	0.0000699	0.00242	0.9
26	**385**	**26**	0.0000964	0.00131	1.3
90	**220**	**24**	0.0000462	0.00940	3.5
97	**253**	**27**	0.0001280	0.00832	2.5

The ranges for paleo-seawater X/Ca were calculated using the maximum and minimum values of the partition coefficient for each element. Since the D^c X/Ca was determined from cultured sea urchins, this would demonstrate the range (max and min) of each paleo-seawater X/Ca with the use of cultured sea urchins partition coefficients (Fig. 44-46). For both Li/Ca and B/Ca reconstruction curves, there is a large range for the youngest samples. The reason for this is unclear but it may be caused by alteration or contamination of the paleo-echinoderm samples. The elemental concentration may not be uniform throughout the internal structure of samples, which would introduce uncertainties into the measurement. Because all three graphs represent the different elements analyzed in the 13 paleo-echinoderm samples, values from Mg/Ca do not show a large difference between points corrected and not corrected for temperature. However, this is not conclusive because each paleo-echinoderm only received between 3-5 analysis spots. More analyses need to be performed to obtain higher confidence in the Mg/Ca of paleo-echinoderms.

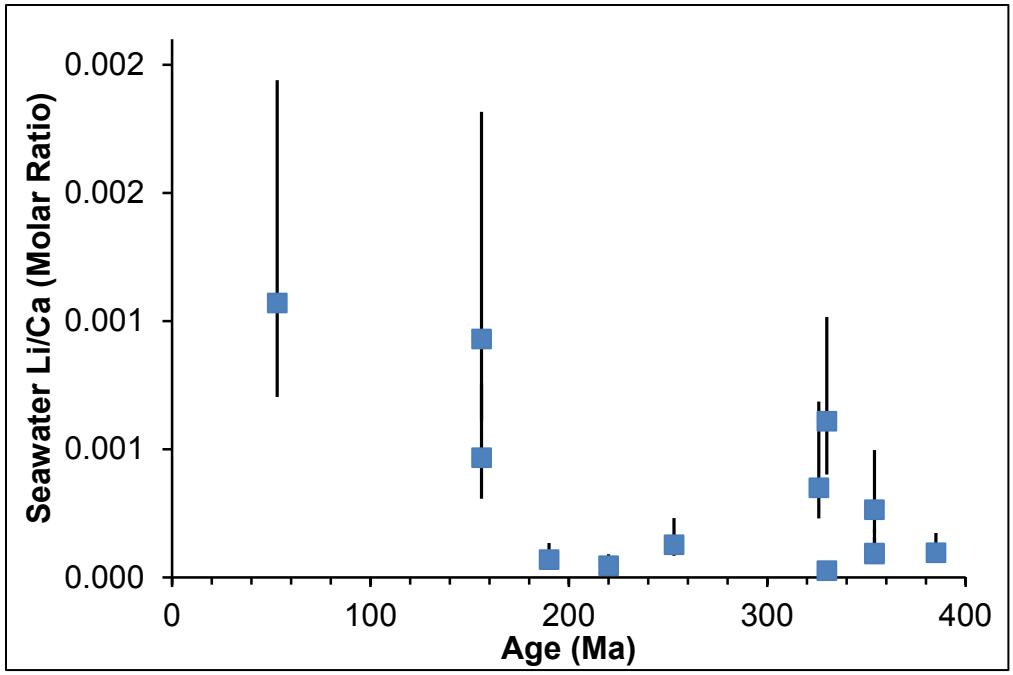

Figure 44: Paleo-seawater Li/Ca molar ratio from the SIMS analysis on 13 paleo-echinoderm samples using the partition coefficient found from the cultured sea urchins. Solid squares represent seawater Li/Ca using the average D^cLi/Ca and vertical lines are the range for values of Max and Min D^cLi/Ca

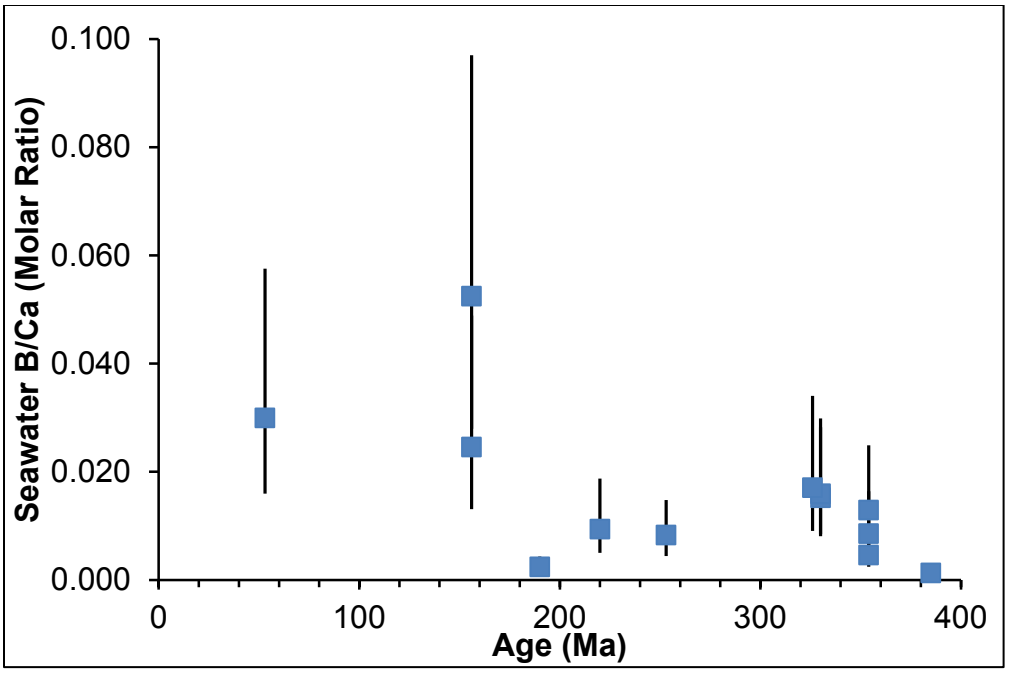

Figure 45: Paleo-seawater B/Ca molar ratio from the SIMS analysis on 13 paleo-echinoderm samples using the partition coefficient found from the cultured sea urchins. Solid squares represent seawater Li/Ca using the average $D^{c}B/Ca$ and vertical lines are the range for values of Max and Min $D^{c}B/Ca$

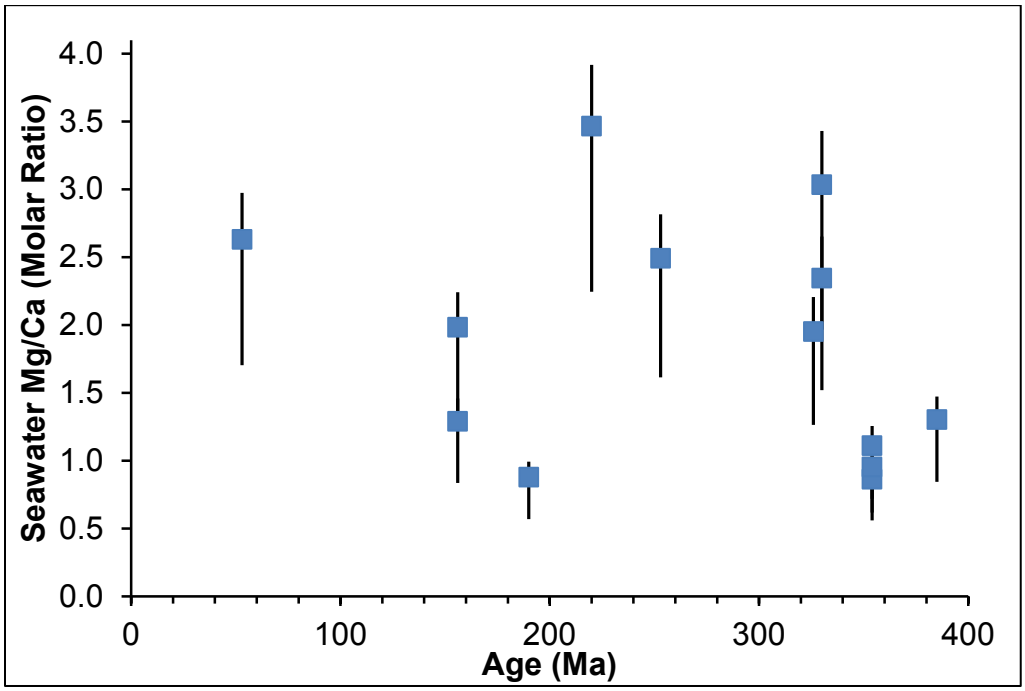

Figure 46: Paleo-seawater Mg/Ca molar ratio from the SIMS analysis on 13 paleo-echinoderm samples using the partition coefficient found from the cultured sea urchins. Solid squares represent seawater Li/Ca using the average $D^{c}Mg/Ca$ and vertical lines are the range for values of Max and Min $D^{c}Mg/Ca$

SIMS and Electron Ion Microprobe Analysis on Mg/Ca in Paleo-Echinoderm Samples

The paleo-seawater Mg/Ca ratio was determined using the partition coefficient from the cultured sea urchin spines. The range for the paleo-seawater Mg/Ca fell within the same range found in previous studies (Hardie et al., 1996; Stanley et al., 2002; Dickson, 2004). The Mg/Ca ratios from the SIMS analysis of the paleo-echinoderm spines were similar to Dickson (2004) (Fig. 47). There are several data points where Mg/Ca ratios from the two studies diverge, and this could be due to the heterogeneity or surface contamination within the paleo-samples. However, most of the points in between do fall close to each other and follow a similar trend.

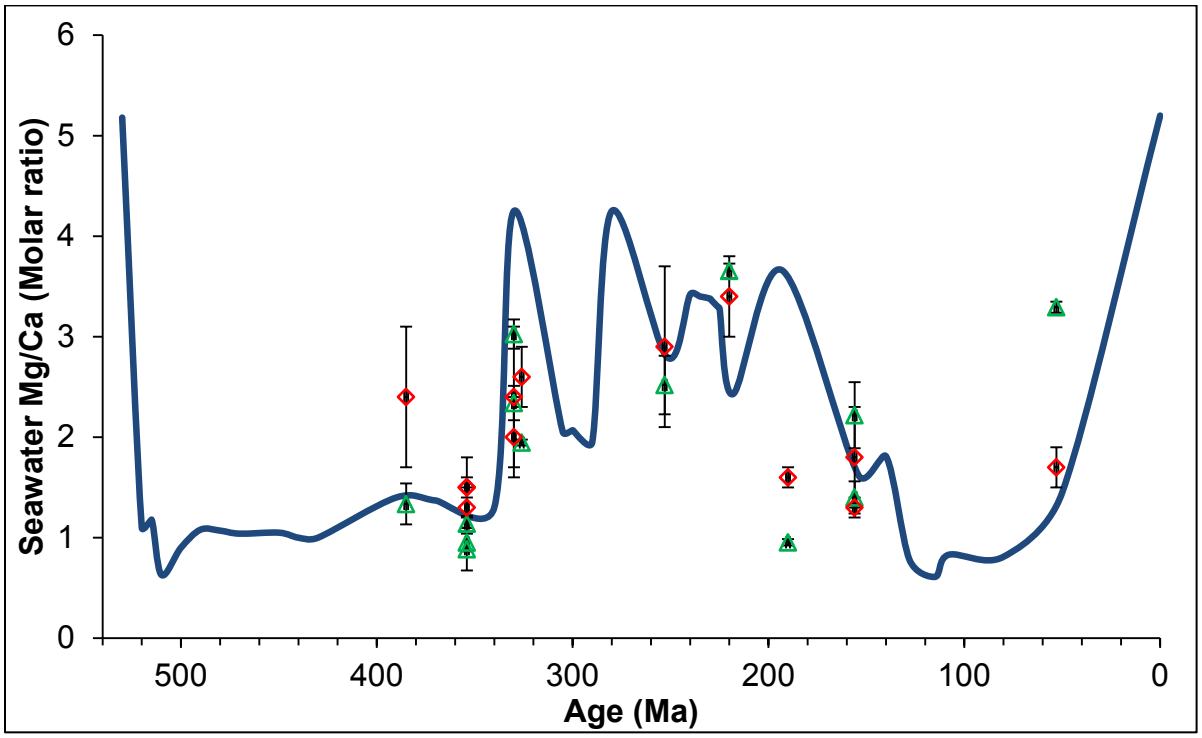

Figure 47: Seawater Mg/Ca content from the SIMS analysis of the paleo-echinoderm and the electron microprobe analysis of the same samples from Dickson (2004). The seawater Mg/Ca for the paleo-echinoderm was found by using the partition coefficient (D^c) that was calculated in the cultured sea urchins. Similarly, this was done in the Dickson (2004) study. Open red diamonds represent seawater Mg/Ca values from the Dickson (2004) electron microprobe analysis. Open green triangles represent the data found from SIMS analysis. Solid blue line represents seawater Mg/Ca estimation by Hardie et al. (1996)

Comparing the seawater Mg/Ca found in this study with Dickson (2004) gives the confidence for the results found in this study (Fig 48). The linear regression line had a marginal fit (R^2=0.50) and this could be a reflection on the low number of analysis spots (n=3-5) in the paleo-echinoderm samples. Thus, more analysis spots could increase the precision of Mg/Ca in this study. Moreover, the analysis of more paleo-echinoderm samples may also improve the correlation between the SIMS analysis in this thesis and Dickson (2004) study.

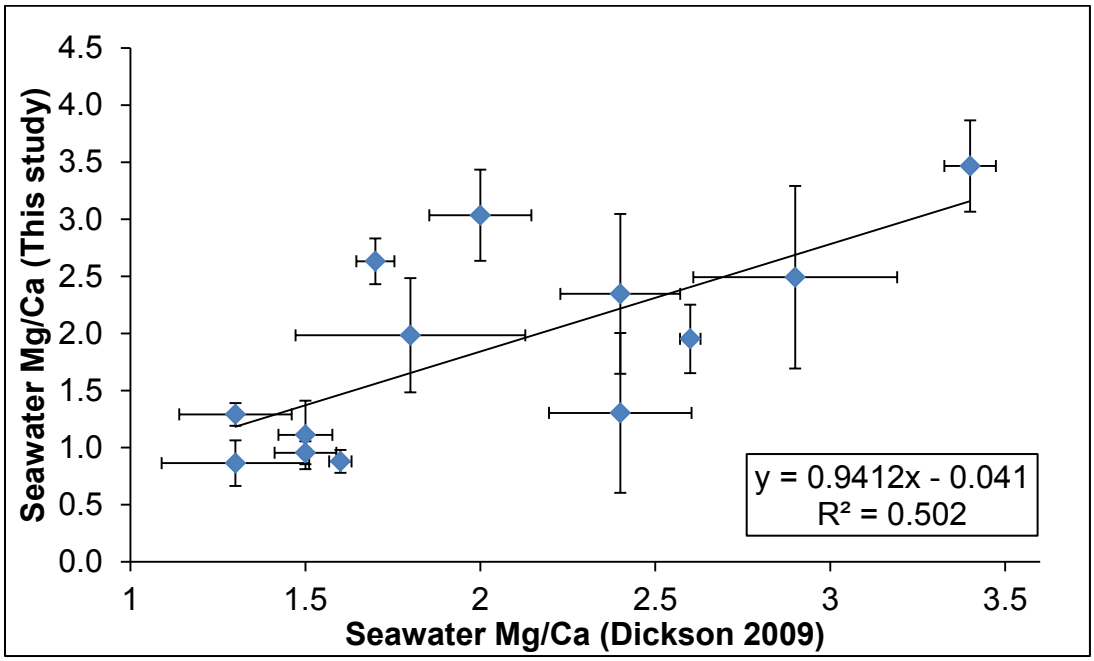

Figure 48: Cross plot of seawater Mg/Ca (molar ratio) from this study (y-axis) and Dickson (2004) study (x-axis).

The relative difference between this study and Dickson (2004) showed that, in most cases, seawater Mg/Ca values in this study were lower than Dickson (2004) (Table 19). The largest difference of 1.10 (±0.08) was found in *Lepidocantrotus mulleri* (Sample 26), which also was the oldest (385 Ma) paleo-echinoderm sampled in this study. Because there were a small number of analysis spots (n = 3-5), there could be multiple reasons why this difference was very large. One attribution to the large difference was because with a small number of analysis spots,

one outlier from the analysis could misrepresent the data. So increasing the number of analysis spots for the samples could help increase the confidence of the data.

Table 19: Paleo-seawater Mg/Ca values for the paleo-echinoderm samples. The average D^c was found by using the average partition coefficient

Sample	Age (Ma)	Seawater Mg/Ca Dickson (2004)	Seawater Mg/Ca This study	Difference between This study and Dickson (2004) (mmol/mol)	Relative Change (%)
62	53	1.7	2.6	0.9	35.4
40/41	330	2.4	2.3	-0.1	2.3
39	156	1.8	2.0	0.2	9.3
68	330	2.0	3.0	1.0	34.1
70	326	2.6	2.0	-0.6	33.2
77	354	1.3	0.9	-0.4	50.5
76	354	1.5	1.1	-0.4	35.0
66	354	1.5	1.0	-0.5	57.1
29	156	1.3	1.3	0.0	0.7
38	190	1.6	0.9	-0.7	82.1
26	385	2.4	1.3	-1.1	84.1
90	220	3.4	3.5	0.1	1.9
97	253	2.9	2.5	-0.4	16.3

The average difference between the seawater Mg/Ca in this study and the Dickson (2004) study equated to -0.16 mmol/mol (34% relative change). Some of the SIMS Mg/Ca values in this study were lower than what was found in Dickson (2004) electron microprobe study (1.1 mmol/mol and 84% relative change). This may be attributed to the heterogeneity in the paleo-echinoderm samples. There is a possibility that the analysis spot was placed on domains with low Mg or an unknown source of Mg contamination exists. This could affect the total amount of Mg in the sample, so more analysis is needed on the sample.

Implications from Paleo-Echinoderm Analysis

Partition coefficients were calculated using the information gathered from SIMS analysis of cultured sea urchin spines. The SIMS analysis was robust in that the values for seawater Mg/Ca was similar to those of the Dickson (2004) study using the electron microprobe. The data from this study shows that the SIMS could potentially be used as another way to measure

elemental composition in samples. Causes for the variability in Li/Ca and B/Ca for the paleo-echinoderm samples remain presently unresolved. Li and B could have been introduced to the surface of the sample due to the minimal polishing and cleaning of the thin-sections used here. One solution to resolve surface contamination would be prolonged depth profiling analysis by SIMS. By performing longer analyses for each analysis spot, the variability from the surface contaminants could be reduced and this would help decrease the uncertainty. As mentioned previously, increasing the number of analysis spots on the paleo-echinoderm samples could also help to reduce the variability in the data if the heterogeneity results from beam overlap onto the cement or impurities within the calcite.

One first-order implication of SIMS analysis presented here is that element-to-calcium ratios can be reliably determined in paleo-echinoderm samples because Mg/Ca from SIMS analysis matched those in the Dickson (2004) electron microprobe study (Fig. 47). Therefore, past ocean compositions may be reconstructed using fossilized echinoderms, which are found throughout the world. The worldwide distribution of these fossils would mean that samples are readily available and that a complete history of the past ocean composition can be determined.

Several questions need to be addressed before further analyzing the paleo-echinoderm samples. Since these samples are fossilized, there were some that were fossilized in rock that can contain different materials. Visually, these materials can be hard to distinguish from the echinoderm stereo (sponge-like porous structure) unless proper identification was done using methods such as backscatter SEM. Identifying where the stereom was in relation to the rock would help minimize contamination from dolomite or other artifacts in the fossil during analysis on the SIMS. This was done in Dickson (2004) using backscatter secondary electron (BSE) imaging, but due to time constraints it was not done in this study. Using BSE mapping to document where the location of the unaltered echinoderms in relation to the surrounding rock

would aid with the targeting for SIMS spot analyses. Although lack of BSE imaging is recognized as a limitation of the reconnaissance SIMS analyses presented here, this thesis demonstrates the potential of gathering element/calcium ratios from paleo-echinoderm samples.

Conclusion

SIMS analysis on cultured temperate (*A. punctulata)* and tropical (*E. viridis*) sea urchin spines revealed the amount of lithium, boron, and magnesium incorporated into the calcite structure of the spines under variable temperature and pCO_2. Seawater temperature had a stronger effect on elemental/calcium ratios than pCO_2. This was more apparent in the *E. viridis* because both variables (T and pCO_2) were manipulated. A positive response to temperature would indicate that there was an increased calcification rate in the sea urchins. Seawater pH did affect the amount of Li/Ca and B/Ca in sea urchin spines but this signal was overshadowed by temperature.

The B/Ca of the temperate species had a similar curve to the calcification rate found in Ries et al. (2009) for the same species. This would indicate that B/Ca content in the sea urchin spine was also affected by seawater pH. The lower pH of the seawater would mean less boron that was incorporated into the sea urchin endoskeleton. This reached a threshold at 900 ppmv and was subsequently lower at the highest pCO_2 treatment. It was hypothesized that because these are more complex organism they are able to have more control on the pH at the site of calcification (Schneider and Erez, (2006); Fabry et al., (2008); Ries et al., 2009).

For future research, more analyses of sea urchin spines along the longitudinal portion are required because it would show the precise location where the new growth under laboratory conditions began. The analyses done in this study were done on a width of the spine that was 2 mm from the tip. The sea urchins were collected as adults so new growth on the spine would be seen from at least 2 mm from the tip of the spine. However, this was an estimation as different spines on the same sea urchin were not always uniform in length. Therefore, a longitudinal analysis could show precisely where the change from amorphous calcite to calcite occurred. It would also be interesting to see how the spine growth was affected by the change in

environmental conditions. Documenting the change in element-to-calcium ratios over time would help to see how these organisms respond under environmental stress.

Applying partition coefficients determined from the cultured sea urchins, permitted the reconstruction of model paleo-seawater X/Ca. Model paleo-seawater Mg/Ca based on SIMS partition coefficients was similar to estimates by Dickson (2004) for the same samples based on electron microprobe analysis. Potential advantages of SIMS compared to electron microprobe analysis are higher sensitivity coupled with smaller analysis volumes required to measure Mg/Ca. Future work on the paleo-echinoderms should focus on using the backscatter electron imaging to identify where the stereoms are located within the fossilized medium. The pre-characterization using BSE (Dickson, 2001) revealed complex intergrowth between fossilized echinoderms and matrix which restricts some domains from being reliably analyzed. Careful BSE prior to SIMS analysis would reduce the time spent searching for the calcite and increase the number of spots that can be analyzed on the fossilized echinoderms.

The data gathered from the SIMS analysis provided useful information on the amount of element-to-calcium that was found in the cultured sea urchin spines. Understanding how certain elements are incorporated into the calcium carbonate structure would help develop proxies to understand past climates. Ultimately, this could help us understand how our oceans will respond to future increases in atmospheric CO_2.

Appendix A: *A. punctulata* SIMS Data

A.1: Intensity Ratios

Table A.1: Intensities ratios ($^{6}Li/^{42}Ca$, $B/^{42}Ca$, $Mg/^{42}Ca$, $^{54}Fe/^{42}Ca$, and $Mn/^{42}Ca$) of *A. punctulata* spines. Values highlighted in red were omitted from the analysis because the Ca intensities (cps) were low (< 1.5E5 cps).

	$^{6}Li/^{42}Ca$	1 s.e.	$B/^{42}Ca$	1 s.e.	$Mg/^{42}Ca$	1 s.e.	$^{54}Fe/^{42}Ca$	1 s.e.	$Mn/^{42}Ca$	1 s.e.
JR65, 400 ppmv, 25C										
JR65_400_25.ais	3.45E-02	7.36E-05	2.79E-02	6.55E-05	3.05	2.44E-02	6.94E-05	7.04E-06	5.75E-04	2.09E-05
JR65_400_25@1.ais	3.68E-02	2.12E-04	2.76E-02	9.45E-05	2.87	2.20E-02	1.35E-04	8.80E-06	7.57E-04	1.42E-05
JR65_400_25@2.ais	3.26E-02	1.20E-04	2.68E-02	1.17E-04	3.08	1.64E-02	3.79E-05	3.76E-06	8.20E-04	2.79E-05
JR65_400_25@3.ais	3.58E-02	1.55E-04	2.54E-02	1.58E-04	3.03	2.30E-02	1.18E-04	1.04E-05	8.75E-04	1.69E-05
JR65_400_25@4.ais	3.98E-02	1.38E-04	2.90E-02	1.05E-04	3.24	2.43E-02	3.43E-05	8.45E-06	5.22E-04	1.22E-05
JR65_400_25@5.ais	3.71E-02	1.82E-04	2.47E-02	8.38E-05	3.04	2.15E-02	8.75E-05	1.07E-05	5.54E-04	1.66E-05
Avg	**3.61E-02**		**2.69E-02**		**3.05**		**8.04E-05**		**6.84E-04**	
s.d.	**2.46E-03**		**1.61E-03**		**0.12**		**4.12E-05**		**1.52E-04**	
s.d.%	**6.83**		**5.98**		**3.86**		**51.28**		**22.19**	
JR64, 400 ppmv, 25C										
JR64_400_25.ais	3.77E-02	2.42E-04	2.56E-02	8.04E-05	3.36	2.20E-02	1.49E-05	4.82E-06	6.23E-04	2.53E-05
JR64_400_25@1.ais	3.74E-02	1.02E-04	2.69E-02	9.26E-05	3.22	2.31E-02	6.94E-05	5.62E-06	7.12E-04	1.95E-05
JR64_400_25@2.ais	3.72E-02	1.15E-04	2.37E-02	7.70E-05	2.91	1.97E-02	1.58E-05	3.16E-06	6.12E-04	2.06E-05
JR64_400_25@3.ais	3.76E-02	1.44E-04	2.37E-02	8.25E-05	2.76	2.00E-02	9.09E-06	2.38E-06	5.64E-04	2.61E-05
JR64_400_25@4.ais	3.80E-02	1.35E-04	2.52E-02	1.21E-04	3.20	2.19E-02	1.86E-05	3.77E-06	6.33E-04	2.06E-05
JR64_400_25@5.ais	3.85E-02	1.69E-04	2.66E-02	9.33E-05	3.17	2.59E-02	1.09E-05	2.65E-06	6.38E-04	1.67E-05
JR64_400_25@6.ais	4.01E-02	1.59E-04	2.62E-02	6.42E-05	2.98	1.98E-02	7.21E-06	1.49E-06	5.34E-04	1.98E-05
JR64_400_25@7.ais	4.12E-02	1.13E-04	2.46E-02	8.77E-05	2.86	2.04E-02	3.05E-06	9.32E-07	5.02E-04	1.93E-05
JR64_400_25@8.ais	3.93E-02	8.04E-05	2.53E-02	6.60E-05	2.73	1.69E-02	2.58E-05	6.89E-06	9.56E-04	3.89E-05
Avg	**3.86E-02**		**2.53E-02**		**3.02**		**1.94E-05**		**6.42E-04**	
s.d.	**1.37E-03**		**1.15E-03**		**0.22**		**1.99E-05**		**1.33E-04**	
s.d.%	**3.56**		**4.54**		**7.36**		**102.44**		**20.79**	

	$^{6}Li/^{42}Ca$	1 s.e.	$B/^{42}Ca$	1 s.e.	$Mg/^{42}Ca$	1 s.e.	$^{54}Fe/^{42}Ca$	1 s.e.	$Mn/^{42}Ca$	1 s.e.
JR204, 600 ppmv, 25C										
JR204_600_25.ais	3.70E-02	1.46E-04	2.94E-02	6.86E-05	2.58	2.08E-02	8.32E-06	2.24E-06	1.72E-04	9.15E-06
JR204_600_25@1.ais	3.46E-02	1.48E-04	2.90E-02	1.57E-04	2.63	2.41E-02	5.85E-06	1.87E-06	2.56E-04	1.86E-05
JR204_600_25@2.ais	3.84E-02	2.20E-04	3.52E-02	1.03E-04	2.61	1.96E-02	1.02E-05	3.87E-06	2.96E-04	1.50E-05
JR204_600_25@3.ais	3.89E-02	2.36E-04	3.39E-02	1.19E-04	2.95	1.73E-02	1.10E-05	3.50E-06	4.35E-04	2.18E-05
JR204_600_25@4.ais	4.19E-02	1.46E-04	3.22E-02	7.67E-05	3.02	2.29E-02	1.13E-05	3.06E-06	2.42E-04	1.30E-05
JR204_600_25@5.ais	3.67E-02	1.67E-04	3.28E-02	7.25E-05	2.92	2.38E-02	8.05E-06	2.24E-06	2.64E-04	1.24E-05
JR204_600_25@6.ais	3.95E-02	9.00E-05	3.33E-02	1.75E-04	2.90	1.94E-02	2.73E-05	8.44E-06	2.90E-04	2.00E-05
Avg	**3.81E-02**		**3.23E-02**		**2.80**		**1.17E-05**		**2.79E-04**	
s.d.	**2.31E-03**		**2.29E-03**		**0.19**		**7.14E-06**		**8.00E-05**	
s.d.%	**6.07**		**7.11**		**6.63**		**60.92**		**28.65**	
JR205, 600 ppmv, 25C										
JR205_600_25.ais	3.85E-02	2.26E-04	3.01E-02	2.10E-04	3.41	2.60E-02	1.67E-05	4.02E-06	1.76E-04	7.53E-06
JR205_600_25@1.ais	3.95E-02	1.71E-04	3.31E-02	1.24E-04	3.35	2.60E-02	1.01E-05	2.21E-06	2.30E-04	1.36E-05
JR205_600_25@2.ais	3.47E-02	1.53E-04	2.75E-02	1.50E-04	3.27	2.36E-02	1.35E-04	2.36E-05	3.53E-04	1.41E-05
JR205_600_25@3.ais	3.33E-02	2.37E-04	2.85E-02	1.91E-04	3.15	2.78E-02	1.88E-05	3.98E-06	2.31E-04	1.38E-05
JR205_600_25@4.ais	3.92E-02	1.25E-04	3.09E-02	1.34E-04	3.18	3.21E-02	3.79E-04	4.13E-05	2.27E-04	1.23E-05
JR205_600_25@5.ais	3.49E-02	1.03E-04	2.76E-02	6.45E-05	3.25	3.05E-02	2.09E-05	3.67E-06	2.30E-04	2.17E-05
JR205_600_25@6.ais	*2.61E-02*	*4.74E-04*	*1.98E-02*	*2.42E-04*	*2.38*	*1.77E-02*	*2.30E-04*	*2.84E-05*	*1.32E-03*	*3.45E-05*
JR205_600_25@7.ais	3.41E-02	9.49E-05	3.24E-02	9.04E-05	2.97	3.08E-02	6.25E-05	8.80E-06	2.69E-04	1.04E-05
Avg	**3.50E-02**		**2.87E-02**		**3.12**		**1.09E-04**		**3.80E-04**	
s.d.	**4.35E-03**		**4.18E-03**		**0.33**		**1.33E-04**		**3.85E-04**	
s.d.%	**12.42**		**14.55**		**10.49**		**122.22**		**101.29**	

	$^{6}Li/^{42}Ca$	1 s.e.	$B/^{42}Ca$	1 s.e.	$Mg/^{42}Ca$	1 s.e.	$^{54}Fe/^{42}Ca$	1 s.e.	$Mn/^{42}Ca$	1 s.e.
JR69, 900 ppmv, 25C										
JR69_900_25.ais	3.25E-02	1.47E-04	3.91E-02	1.87E-04	2.41	1.58E-02	8.78E-06	2.59E-06	7.25E-04	1.40E-05
JR69_900_25@1.ais	3.42E-02	1.81E-04	3.40E-02	1.68E-04	2.51	1.80E-02	1.71E-05	1.23E-05	8.32E-04	2.12E-05
JR69_900_25@2.ais	3.58E-02	7.50E-05	3.64E-02	8.90E-05	2.53	1.88E-02	8.68E-06	3.43E-06	8.02E-04	2.14E-05
JR69_900_25@3.ais	3.34E-02	1.03E-04	3.79E-02	1.35E-04	2.17	1.61E-02	2.21E-05	4.41E-06	7.89E-04	2.64E-05
JR69_900_25@4.ais	3.65E-02	1.13E-04	3.65E-02	1.47E-04	2.71	2.07E-02	2.61E-05	4.15E-06	1.00E-03	3.09E-05
JR69_900_25@5.ais	3.48E-02	9.11E-05	3.43E-02	1.07E-04	2.22	1.80E-02	1.50E-05	3.36E-06	6.77E-04	1.37E-05
JR69_900_25@6.ais	3.22E-02	1.33E-04	3.08E-02	1.32E-04	2.22	1.48E-02	7.51E-06	2.51E-06	7.51E-04	1.46E-05
JR69_900_25@7.ais	3.43E-02	3.26E-04	3.46E-02	2.39E-04	2.38	1.92E-02	3.56E-05	3.96E-06	6.28E-04	2.23E-05
Avg	**3.42E-02**		**3.54E-02**		**2.39**		**1.76E-05**		**7.76E-04**	
s.d.	**1.48E-03**		**2.59E-03**		**0.19**		**9.88E-06**		**1.14E-04**	
s.d.%	**4.34**		**7.32**		**7.83**		**56.10**		**14.67**	
JR215, 900ppmv, 25C										
JR215_900_25.ais	3.44E-02	2.22E-04	3.46E-02	1.55E-04	2.85	2.46E-02	1.98E-05	3.26E-06	2.51E-04	1.82E-05
JR215_900_25@1.ais	3.81E-02	1.10E-04	4.00E-02	8.04E-05	3.05	2.12E-02	4.55E-05	5.43E-06	1.66E-04	9.49E-06
JR215_900_25@2.ais	3.47E-02	1.20E-04	3.77E-02	1.08E-04	2.65	2.63E-02	1.61E-04	5.97E-05	2.46E-04	2.60E-05
JR215_900_25@3.ais	2.97E-02	2.09E-04	3.88E-02	6.35E-04	2.32	2.47E-02	2.44E-04	1.92E-05	1.44E-03	7.35E-05
JR215_900_25@4.ais	2.67E-02	6.35E-05	2.84E-02	2.13E-04	2.43	1.80E-02	1.53E-04	1.32E-05	6.69E-04	1.99E-05
JR215_900_25@5.ais	3.70E-02	1.02E-04	2.64E-02	1.27E-04	2.88	1.99E-02	5.23E-05	7.03E-06	9.11E-03	8.65E-05
JR215_900_25@6.ais	2.47E-02	1.79E-04	3.66E-02	2.14E-04	2.14	1.21E-02	7.35E-05	6.91E-06	8.37E-04	2.57E-05
JR215_900_25@7.ais	3.13E-02	1.88E-04	3.30E-02	1.72E-04	2.59	1.40E-02	3.25E-04	9.27E-05	3.05E-04	1.60E-05
Avg	**3.21E-02**		**3.44E-02**		**2.61**		**1.34E-04**		**1.63E-03**	
s.d.	**4.80E-03**		**4.90E-03**		**0.31**		**1.07E-04**		**3.05E-03**	
s.d.%	**14.98**		**14.25**		**11.75**		**80.03**		**187.54**	

	$^{6}Li/^{42}Ca$	1 s.e.	$B/^{42}Ca$	1 s.e.	$Mg/^{42}Ca$	1 s.e.	$^{54}Fe/^{42}Ca$	1 s.e.	$Mn/^{42}Ca$	1 s.e.
JR224, 2850 ppmv, 25C										
JR224_2850_25@8.ais	3.23E-02	6.29E-04	3.36E-02	4.27E-04	2.96	2.71E-02	3.19E-04	1.81E-05	6.50E-04	2.90E-05
JR224_2850_25@9.ais	2.91E-02	2.24E-04	3.93E-02	6.23E-04	2.85	1.88E-02	1.38E-04	2.07E-05	7.98E-04	1.09E-04
JR224_2850_25@10.ais	*2.86E-02*	*6.00E-04*	*3.73E-02*	*9.20E-04*	*2.84*	*3.10E-02*	*5.39E-04*	*1.20E-04*	*1.20E-03*	*3.99E-05*
JR224_2850_25@11.ais	3.18E-02	1.38E-04	2.85E-02	2.40E-04	2.98	2.45E-02	1.09E-04	1.56E-05	3.28E-04	2.62E-05
JR224_2850_25@12.ais	*2.68E-02*	*3.28E-04*	*4.09E-02*	*2.84E-03*	*2.45*	*1.04E-02*	*8.74E-04*	*8.63E-05*	*2.89E-03*	*3.50E-04*
JR224_2850_25@13.ais	2.82E-02	1.14E-04	2.82E-02	2.70E-04	2.75	1.37E-02	1.15E-04	1.38E-05	6.49E-04	5.65E-05
JR224_2850_25@14.ais	2.96E-02	2.02E-04	3.97E-02	6.68E-04	3.00	2.10E-02	4.04E-04	1.89E-05	9.26E-04	4.06E-05
JR224_2850_25@15.ais	2.79E-02	6.89E-05	3.82E-02	2.77E-04	2.57	1.76E-02	3.09E-04	2.17E-05	1.51E-03	8.35E-05
JR224_2850_25@16.ais	2.80E-02	1.45E-04	3.17E-02	1.97E-04	2.84	1.81E-02	1.98E-04	1.01E-05	8.06E-04	3.74E-05
JR224_2850_25@17.ais	3.11E-02	1.01E-04	3.28E-02	3.23E-04	2.52	1.81E-02	7.24E-04	1.09E-04	2.73E-03	1.89E-04
Avg	**2.93E-02**		**3.50E-02**		**2.78**		**3.73E-04**		**1.25E-03**	
s.d.	**1.82E-03**		**4.67E-03**		**0.20**		**2.65E-04**		**8.84E-04**	
s.d.%	**6.21**		**13.33**		**7.17**		**71.04**		**70.83**	
JR71, 2850 ppmv, 25C										
JR71_2850_25@18.ais	3.04E-02	2.84E-04	3.49E-02	2.43E-03	2.58	1.14E-02	2.25E-04	2.16E-05	9.92E-04	1.67E-04
JR71_2850_25@19.ais	2.76E-02	1.43E-04	3.22E-02	9.34E-04	2.74	1.37E-02	3.39E-04	2.52E-05	1.08E-03	5.04E-05
JR71_2850_25@20.ais	2.85E-02	2.53E-04	3.43E-02	4.29E-04	2.74	1.79E-02	2.54E-04	1.20E-05	9.81E-04	5.01E-05
JR71_2850_25@21.ais	3.14E-02	1.60E-04	2.99E-02	1.61E-04	2.76	2.06E-02	8.52E-05	4.90E-06	2.00E-04	1.72E-05
JR71_2850_25@22.ais	3.13E-02	1.67E-04	3.30E-02	1.46E-03	2.54	1.57E-02	1.91E-04	1.86E-05	9.20E-04	9.52E-05
JR71_2850_25@23.ais	2.95E-02	9.63E-05	3.55E-02	6.72E-04	2.90	2.11E-02	2.40E-04	3.64E-05	6.47E-04	2.53E-05
JR71_2850_25@4.ais	3.37E-02	4.00E-04	3.63E-02	3.93E-04	3.15	3.17E-02	2.66E-05	5.19E-06	1.02E-04	9.04E-06
JR71_2850_25@5.ais	*2.66E-02*	*2.11E-04*	*3.31E-02*	*6.24E-04*	*2.81*	*1.84E-02*	*1.01E-03*	*2.84E-04*	*1.15E-03*	*5.67E-05*
Avg	**3.03E-02**		**3.37E-02**		**2.77**		**1.94E-04**		**7.04E-04**	
s.d.	**2.06E-03**		**2.19E-03**		**0.20**		**1.06E-04**		**4.02E-04**	
s.d.%	**6.80**		**6.50**		**7.33**		**54.63**		**57.14**	

A.2: Normalized Ratios

Table A.2: Normalized Li/Ca, B/Ca, and Mg/Ca ratios (mmol/mol) for *A. punctulata* spines. Li/Ca was normalized to HTP-CC standard, B/Ca was normalized to M93 standard, and Mg/Ca was normalized to NBS-19 standard (Appendix D).Values highlighted in red were omitted from the analysis because the Ca intensities (cps) were low (< 1.5E5 cps).

	Li/Ca mmol/mol	1 s.e	B/Ca mmol/mol	1 s.e	Mg/Ca mmol/mol	1 s.e
JR65, 400 ppmv, 25C						
JR65_400_25.ais	4.15E-02	9.09E-05	0.240	2.96E-03	83.4	0.296
JR65_400_25@1.ais	4.43E-02	2.56E-04	0.237	3.61E-03	78.4	0.278
JR65_400_25@2.ais	3.92E-02	1.46E-04	0.230	4.07E-03	84.1	0.295
JR65_400_25@3.ais	4.31E-02	1.88E-04	0.218	4.89E-03	82.6	0.293
JR65_400_25@4.ais	4.79E-02	1.67E-04	0.249	4.00E-03	88.5	0.313
JR65_400_25@5.ais	4.46E-02	2.21E-04	0.212	3.08E-03	83.0	0.293
Avg	**4.34E-02**		**0.231**		**83.3**	
s.d.	**1.21E-03**		**5.64E-03**		**1.31**	
s.d.%	**2.79**		**2.44**		**1.6**	
JR64, 400 ppmv, 25C						
JR64_400_25.ais	4.53E-02	2.92E-04	0.220	3.08E-03	91.7	0.323
JR64_400_25@1.ais	4.51E-02	1.25E-04	0.231	3.50E-03	87.9	0.311
JR64_400_25@2.ais	4.48E-02	1.39E-04	0.204	2.84E-03	79.6	0.281
JR64_400_25@3.ais	4.52E-02	1.74E-04	0.204	2.97E-03	75.4	0.267
JR64_400_25@4.ais	4.58E-02	1.64E-04	0.216	4.01E-03	87.3	0.308
JR64_400_25@5.ais	4.64E-02	2.05E-04	0.229	3.49E-03	86.5	0.308
JR64_400_25@6.ais	4.82E-02	1.93E-04	0.225	2.76E-03	81.3	0.287
JR64_400_25@7.ais	4.96E-02	1.38E-04	0.212	3.17E-03	78.1	0.276
JR64_400_25@8.ais	4.73E-02	9.89E-05	0.217	2.72E-03	74.6	0.262
Avg	**4.64E-02**		**0.217**		**82.5**	
s.d.	**5.51E-04**		**3.29E-03**		**2.02**	
s.d.%	**1.19**		**1.51**		**2.5**	
JR204, 600 ppmv, 25C						
JR204_600_25.ais	4.45E-02	1.77E-04	0.252	3.18E-03	70.3	0.250
JR204_600_25@1.ais	4.17E-02	1.79E-04	0.249	5.23E-03	71.9	0.258
JR204_600_25@2.ais	4.62E-02	2.66E-04	0.302	4.69E-03	71.3	0.253
JR204_600_25@3.ais	4.68E-02	2.85E-04	0.291	4.90E-03	80.5	0.283
JR204_600_25@4.ais	5.04E-02	1.77E-04	0.277	3.69E-03	82.4	0.292
JR204_600_25@5.ais	4.41E-02	2.02E-04	0.281	3.66E-03	79.7	0.283
JR204_600_25@6.ais	4.75E-02	1.10E-04	0.286	6.15E-03	79.1	0.279
Avg	**4.59E-02**		**0.277**		**76.5**	
s.d.	**1.05E-03**		**7.44E-03**		**1.92**	
s.d.%	**2.29**		**2.69**		**2.5**	

	Li/Ca mmol/mol	1 s.e	B/Ca mmol/mol	1 s.e	Mg/Ca mmol/mol	1 s.e
JR205, 600 ppmv, 25C						
JR205_600_25.ais	4.63E-02	2.73E-04	0.259	6.61E-03	93.1	0.330
JR205_600_25@1.ais	4.75E-02	2.07E-04	0.284	4.91E-03	91.5	0.325
JR205_600_25@2.ais	4.17E-02	1.85E-04	0.236	4.92E-03	89.2	0.316
JR205_600_25@3.ais	4.00E-02	2.86E-04	0.245	5.98E-03	85.9	0.307
JR205_600_25@4.ais	4.71E-02	1.52E-04	0.265	4.90E-03	86.9	0.314
JR205_600_25@5.ais	4.20E-02	1.26E-04	0.237	2.90E-03	88.7	0.319
JR205_600_25@6.ais	*3.14E-02*	*5.70E-04*	*0.170*	*6.40E-03*	*65.0*	*0.230*
JR205_600_25@7.ais	4.10E-02	1.16E-04	0.279	4.04E-03	81.1	0.293
Avg	**0.044**		**0.258**		**88.1**	
s.d.	**1.20E-03**		**7.28E-03**		**1.50**	
s.d.%	**2.75**		**2.82**		**1.7**	
JR69, 900 ppmv, 25C						
JR69_900_25.ais	3.91E-02	1.78E-04	0.336	7.18E-03	65.7	0.231
JR69_900_25@1.ais	4.11E-02	2.19E-04	0.292	6.05E-03	68.4	0.242
JR69_900_25@2.ais	4.30E-02	9.26E-05	0.312	4.50E-03	69.0	0.244
JR69_900_25@3.ais	4.02E-02	1.26E-04	0.326	5.79E-03	59.3	0.210
JR69_900_25@4.ais	4.39E-02	1.37E-04	0.313	5.88E-03	74.1	0.263
JR69_900_25@5.ais	4.19E-02	1.11E-04	0.294	4.67E-03	60.5	0.215
JR69_900_25@6.ais	3.88E-02	1.62E-04	0.265	4.84E-03	60.5	0.213
JR69_900_25@7.ais	4.13E-02	3.92E-04	0.297	7.81E-03	64.9	0.231
Avg	**4.12E-02**		**0.304**		**65.3**	
s.d.	**6.31E-04**		**7.87E-03**		**1.81**	
s.d.%	**1.53**		**2.59**		**2.8**	
JR215, 900ppmv, 25C						
JR215_900_25.ais	4.14E-02	2.67E-04	0.297	5.81E-03	77.9	0.278
JR215_900_25@1.ais	4.58E-02	1.34E-04	0.343	4.80E-03	83.1	0.294
JR215_900_25@2.ais	4.18E-02	1.46E-04	0.324	5.13E-03	72.3	0.261
JR215_900_25@3.ais	3.57E-02	2.52E-04	0.333	1.77E-02	63.3	0.230
JR215_900_25@4.ais	3.22E-02	7.90E-05	0.243	6.48E-03	66.4	0.235
JR215_900_25@5.ais	4.45E-02	1.24E-04	0.227	4.26E-03	78.7	0.278
JR215_900_25@6.ais	2.98E-02	2.16E-04	0.314	7.48E-03	58.4	0.205
JR215_900_25@7.ais	3.76E-02	2.28E-04	0.283	6.03E-03	70.7	0.248
Avg	**3.86E-02**		**0.296**		**71.4**	
s.d.	**2.04E-03**		**1.49E-02**		**2.96**	
s.d.%	**5.29**		**5.04**		**4.2**	

	Li/Ca mmol/mol	1 s.e	B/Ca mmol/mol	1 s.e	Mg/Ca mmol/mol	1 s.e
JR224, 2850 ppmv, 25C						
JR224_2850_25@8.ais	3.88E-02	7.58E-04	0.289	1.21E-02	80.8	0.290
JR224_2850_25@9.ais	3.50E-02	2.70E-04	0.337	1.75E-02	77.7	0.274
JR224_2850_25@10.ais	*3.44E-02*	*7.23E-04*	*0.320*	*2.42E-02*	*77.7*	*0.282*
JR224_2850_25@11.ais	3.83E-02	1.67E-04	0.245	7.13E-03	81.3	0.290
JR224_2850_25@12.ais	*3.22E-02*	*3.96E-04*	*0.351*	*6.99E-02*	*66.9*	*0.233*
JR224_2850_25@13.ais	3.40E-02	1.39E-04	0.242	7.80E-03	75.0	0.262
JR224_2850_25@14.ais	3.56E-02	2.44E-04	0.341	1.86E-02	81.8	0.289
JR224_2850_25@15.ais	3.35E-02	8.54E-05	0.328	9.17E-03	70.0	0.247
JR224_2850_25@16.ais	3.37E-02	1.76E-04	0.272	6.46E-03	77.6	0.273
JR224_2850_25@17.ais	3.74E-02	1.23E-04	0.281	9.56E-03	68.8	0.243
Avg	**3.58E-02**		**0.292**		**76.6**	
s.d.	**7.46E-04**		**1.40E-02**		**1.78**	
s.d.%	**2.08**		**4.79**		**2.3**	
JR71, 2850 ppmv, 25C						
JR71_2850_25@18.ais	3.66E-02	3.43E-04	0.299	5.95E-02	70.5	0.246
JR71_2850_25@19.ais	3.32E-02	1.73E-04	0.276	2.39E-02	74.8	0.262
JR71_2850_25@20.ais	3.43E-02	3.06E-04	0.294	1.22E-02	74.9	0.264
JR71_2850_25@21.ais	3.78E-02	1.94E-04	0.257	5.43E-03	75.4	0.267
JR71_2850_25@22.ais	3.77E-02	2.01E-04	0.283	3.63E-02	69.4	0.244
JR71_2850_25@23.ais	3.55E-02	1.18E-04	0.305	1.81E-02	79.1	0.280
JR71_2850_25@4.ais	4.06E-02	4.82E-04	0.312	1.17E-02	86.0	0.310
JR71_2850_25@5.ais	*3.21E-02*	*2.55E-04*	*0.284*	*1.67E-02*	*76.7*	*0.270*
Avg	**3.65E-02**		**0.290**		**75.7**	
s.d.	**2.48E-03**		**1.88E-02**		**5.55**	
s.d.%	**6.80**		**6.50**		**7.3**	

Appendix B: *E. viridis* SIMS Data

B.1: Intensity Ratios

Table B.1: Intensity ratios ($^{6}Li/^{42}Ca$, $B/^{42}Ca$, $Mg/^{42}Ca$, $^{54}Fe/^{42}Ca$, and $Mn/^{42}Ca$) of *E. viridis* spines. Values highlighted in red were omitted from the analysis because the Ca intensities (cps) were low (< 1.50E5 cps).

	$^{6}Li/^{42}Ca$	1 s.e.	$B/^{42}Ca$	1 s.e.	$Mg/^{42}Ca$	1 s.e.	$^{54}Fe/^{42}Ca$	1 s.e.	$Mn/^{42}Ca$	1 s.e.
4222, 400 ppmv, 20C										
4222_400_20.ais	3.19E-02	9.71E-05	3.09E-02	1.61E-04	3.12	2.47E-02	1.57E-04	5.84E-05	2.82E-04	2.50E-05
4222_400_20@1.ais	4.10E-02	1.85E-04	3.86E-02	1.29E-04	3.54	2.39E-02	1.15E-05	2.85E-06	1.33E-04	8.61E-06
4222_400_20@2.ais	3.28E-02	2.43E-04	3.36E-02	3.26E-04	3.46	1.93E-02	7.68E-05	9.12E-06	3.62E-04	3.35E-05
4222_400_20@3.ais	4.11E-02	1.64E-04	4.04E-02	1.85E-04	3.68	2.69E-02	1.27E-05	2.11E-06	1.20E-04	8.01E-06
4222_400_20@4.ais	3.97E-02	1.29E-04	3.73E-02	9.34E-05	3.54	2.46E-02	6.59E-06	2.60E-06	9.98E-05	9.32E-06
4222_400_20@5.ais	3.80E-02	1.39E-04	3.70E-02	1.15E-04	3.53	2.55E-02	1.08E-05	2.96E-06	1.05E-04	8.13E-06
4222_400_20@6.ais	3.48E-02	2.55E-04	3.07E-02	1.45E-04	3.35	2.40E-02	2.40E-05	3.60E-06	1.66E-04	1.18E-05
4222_400_20@7.ais	3.66E-02	7.68E-05	3.75E-02	9.83E-05	3.63	1.90E-02	4.63E-05	6.48E-06	2.83E-04	1.89E-05
4222_400_20@8.ais	3.78E-02	2.04E-04	3.63E-02	2.30E-04	3.50	2.17E-02	1.51E-05	3.93E-06	1.28E-04	1.02E-05
4222_400_20@9.ais	4.34E-02	1.73E-04	4.38E-02	1.61E-04	3.76	2.32E-02	2.60E-05	4.44E-06	1.17E-04	9.24E-06
Avg	**3.77E-02**		**3.66E-02**		**3.51**		**3.87E-05**		**1.80E-04**	
s.d.	**3.74E-03**		**4.05E-03**		**0.18**		**4.67E-05**		**9.37E-05**	
s.d.%	**9.92**		**11.07**		**5.10**		**120.85**		**52.17**	
4213, 400ppm 20C										
4213_400_20.ais	3.59E-02	3.01E-04	3.20E-02	4.61E-04	3.31	3.49E-02	5.23E-05	5.00E-06	2.81E-04	2.04E-05
4213_400_20@1.ais	3.75E-02	1.20E-04	3.24E-02	2.30E-04	3.32	2.82E-02	4.30E-05	6.23E-06	1.87E-04	1.46E-05
4213_400_20@2.ais	4.00E-02	3.20E-04	3.25E-02	3.28E-04	3.04	2.87E-02	2.13E-04	6.56E-05	6.00E-04	6.06E-05
4213_400_20@3.ais	3.76E-02	2.31E-04	3.14E-02	3.26E-04	3.14	2.71E-02	6.31E-05	9.69E-06	2.92E-04	1.66E-05
4213_400_20@4.ais	4.24E-02	9.79E-05	3.65E-02	1.33E-04	3.37	2.34E-02	1.20E-05	2.94E-06	1.19E-04	8.49E-06
4213_400_20@5.ais	3.78E-02	8.46E-05	3.32E-02	1.16E-04	3.07	2.26E-02	5.97E-05	1.12E-05	2.52E-04	2.96E-05
4213_400_20@6.ais	3.58E-02	5.36E-04	3.61E-02	5.40E-04	3.13	3.34E-02	4.75E-05	4.91E-06	2.41E-04	1.22E-05
4213_400_20@7.ais	3.59E-02	2.66E-04	3.54E-02	2.61E-04	3.09	2.41E-02	2.06E-05	4.99E-06	2.00E-04	1.12E-05
4213_400_20@8.ais	3.40E-02	3.01E-04	4.14E-02	3.24E-04	3.56	2.20E-02	3.64E-05	5.35E-06	2.23E-04	1.35E-05
4213_400_20@9.ais	3.80E-02	1.73E-04	3.47E-02	2.00E-04	3.08	2.78E-02	2.68E-05	5.64E-06	1.24E-04	5.77E-06
Avg	**3.75E-02**		**3.46E-02**		**3.21**		**5.74E-05**		**2.52E-04**	
s.d.	**2.38E-03**		**2.99E-03**		**0.17**		**5.72E-05**		**1.36E-04**	
s.d.%	**6.34**		**8.66**		**5.28**		**99.53**		**53.85**	

	$^{6}Li/^{42}Ca$	1 s.e.	$B/^{42}Ca$	1 s.e.	$Mg/^{42}Ca$	1 s.e.	$^{54}Fe/^{42}Ca$	1 s.e.	$Mn/^{42}Ca$	1 s.e.
4221, 400 ppmv, 20C										
4221_400_20.ais	4.01E-02	1.63E-04	3.97E-02	1.81E-04	3.65	2.37E-02	1.25E-05	3.10E-06	1.62E-04	1.14E-05
4221_400_20@1.ais	3.33E-02	1.58E-04	3.49E-02	3.67E-04	3.62	2.49E-02	4.37E-05	7.05E-06	2.83E-04	2.00E-05
4221_400_20@2.ais	3.46E-02	2.58E-04	3.84E-02	1.94E-04	3.69	3.13E-02	7.50E-06	2.87E-06	1.54E-04	1.79E-05
4221_400_20@3.ais	3.97E-02	1.79E-04	4.33E-02	1.60E-04	3.57	2.24E-02	6.38E-06	2.09E-06	1.15E-04	1.38E-05
4221_400_20@4.ais	3.84E-02	7.86E-05	4.06E-02	1.17E-04	3.52	2.27E-02	2.27E-05	2.52E-06	1.63E-04	9.00E-06
4221_400_20@5.ais	3.92E-02	2.06E-04	4.22E-02	2.27E-04	3.51	2.58E-02	7.93E-06	3.05E-06	1.36E-04	6.36E-06
4221_400_20@6.ais	4.00E-02	1.38E-04	4.24E-02	1.96E-04	3.67	2.64E-02	3.17E-05	3.86E-06	1.30E-04	6.59E-06
4221_400_20@7.ais	3.45E-02	2.10E-04	3.65E-02	1.81E-04	3.18	2.77E-02	1.11E-04	1.11E-05	3.16E-04	1.49E-05
4221_400_20@8.ais	3.95E-02	1.57E-04	3.89E-02	1.42E-04	3.71	3.10E-02	1.13E-05	1.78E-06	1.27E-04	8.45E-06
4221_400_20@9.ais	3.63E-02	4.17E-04	3.70E-02	3.26E-04	3.56	2.83E-02	3.83E-05	4.61E-06	2.75E-04	1.68E-05
4221_400_20@10.ais	3.70E-02	3.12E-04	3.80E-02	3.34E-04	3.59	3.42E-02	2.69E-05	7.13E-06	1.81E-04	1.04E-05
Avg	**3.75E-02**		**3.93E-02**		**3.57**		**2.91E-05**		**1.86E-04**	
s.d.	**2.49E-03**		**2.66E-03**		**0.15**		**3.01E-05**		**7.10E-05**	
s.d.%	**6.63**		**6.78**		**4.13**		**103.62**		**38.22**	
4233, 400ppmv, 20C										
4233_400_20.ais	3.98E-02	1.22E-04	4.13E-02	8.23E-05	3.33	2.18E-02	7.59E-06	1.58E-06	1.20E-04	9.30E-06
4233_400_20@1.ais	4.06E-02	1.49E-04	3.67E-02	1.46E-04	3.22	2.40E-02	3.64E-05	7.07E-06	1.08E-04	9.39E-06
4233_400_20@2.ais	3.81E-02	1.77E-04	3.99E-02	1.59E-04	3.36	2.42E-02	1.38E-05	2.54E-06	1.25E-04	1.04E-05
4233_400_20@3.ais	3.75E-02	7.76E-05	3.98E-02	1.26E-04	3.35	2.26E-02	7.96E-06	1.72E-06	1.06E-04	8.62E-06
4233_400_20@4.ais	3.83E-02	9.56E-05	3.66E-02	1.16E-04	3.28	2.59E-02	6.09E-06	1.57E-06	7.91E-05	5.80E-06
4233_400_20@5.ais	3.38E-02	1.69E-04	3.49E-02	1.64E-04	3.03	2.61E-02	9.86E-06	2.39E-06	1.12E-04	7.34E-06
4233_400_20@6.ais	3.25E-02	2.14E-04	3.62E-02	2.62E-04	3.27	2.69E-02	1.35E-05	2.99E-06	1.19E-04	8.19E-06
4233_400_20@7.ais	3.62E-02	2.47E-04	3.94E-02	1.60E-04	3.40	2.68E-02	8.49E-06	2.66E-06	1.16E-04	5.68E-06
Avg	**3.71E-02**		**3.81E-02**		**3.28**		**1.29E-05**		**1.10E-04**	
s.d.	**2.81E-03**		**2.29E-03**		**0.12**		**9.85E-06**		**1.42E-05**	
s.d.%	**7.57**		**6.00**		**3.52**		**76.06**		**12.83**	

	$^{6}Li/^{42}Ca$	1 s.e.	$B/^{42}Ca$	1 s.e.	$Mg/^{42}Ca$	1 s.e.	$^{54}Fe/^{42}Ca$	1 s.e.	$Mn/^{42}Ca$	1 s.e.
4312, 400 ppmv, 30C										
4312_400_30.ais	6.99E-02	1.84E-04	5.31E-02	1.86E-04	3.80	2.49E-02	5.82E-06	1.92E-06	3.73E-05	5.24E-06
4312_400_30@1.ais	6.91E-02	1.42E-04	5.24E-02	1.32E-04	3.90	2.47E-02	7.59E-06	1.62E-06	3.39E-05	5.65E-06
4312_400_30@2.ais	6.69E-02	3.61E-04	4.64E-02	4.83E-04	3.80	4.62E-02	3.74E-04	1.02E-04	5.02E-04	9.34E-05
4312_400_30@3.ais	7.04E-02	1.35E-04	4.94E-02	1.42E-04	3.72	2.12E-02	1.92E-05	4.41E-06	5.23E-05	4.78E-06
4312_400_30@4.ais	7.30E-02	2.00E-04	5.09E-02	2.57E-04	3.81	2.67E-02	3.28E-06	1.17E-06	3.09E-05	5.39E-06
4312_400_30@5.ais	6.86E-02	1.64E-04	4.61E-02	2.01E-04	3.78	2.15E-02	3.15E-05	4.71E-06	1.24E-04	1.65E-05
4312_400_30@6.ais	7.09E-02	4.23E-04	4.89E-02	9.18E-05	3.82	2.58E-02	1.10E-05	3.21E-06	3.42E-05	5.16E-06
4312_400_30@7.ais	7.15E-02	7.99E-04	4.57E-02	3.85E-04	3.80	3.23E-02	4.20E-05	1.42E-05	9.61E-05	8.20E-06
4312_400_30@8.ais	7.18E-02	1.87E-04	4.97E-02	2.28E-04	3.95	2.83E-02	2.30E-05	3.06E-06	8.29E-05	1.23E-05
4312_400_30@9.ais	7.31E-02	2.28E-04	5.32E-02	9.69E-05	3.85	2.86E-02	4.60E-06	1.50E-06	4.54E-05	7.08E-06
Avg	**7.05E-02**		**4.96E-02**		**3.82**		**5.22E-05**		**1.04E-04**	
s.d.	**1.96E-03**		**2.86E-03**		**6.48E-02**		**1.14E-04**		**1.43E-04**	
s.d.%	**2.78**		**5.76**		**1.70**		**217.99**		**138.08**	
4321, 400 ppmv, 30C										
4321_400_30.ais	6.97E-02	1.91E-04	5.80E-02	3.44E-04	4.10	2.43E-02	1.46E-05	2.30E-06	5.01E-05	6.23E-06
4321_400_30@1.ais	7.13E-02	2.04E-04	6.14E-02	1.62E-04	3.93	2.90E-02	1.05E-05	2.08E-06	4.00E-05	5.98E-06
4321_400_30@2.ais	7.27E-02	2.24E-04	6.00E-02	1.84E-04	3.84	2.38E-02	1.09E-05	3.59E-06	3.68E-05	6.14E-06
4321_400_30@3.ais	7.38E-02	1.36E-04	6.19E-02	2.10E-04	4.03	2.76E-02	6.41E-06	2.25E-06	2.17E-05	4.05E-06
4321_400_30@4.ais	7.15E-02	2.33E-04	5.06E-02	2.83E-04	4.21	3.18E-02	1.74E-04	1.38E-05	4.39E-04	2.13E-05
4321_400_30@5.ais	6.86E-02	4.15E-04	5.79E-02	2.14E-04	4.03	2.95E-02	3.25E-05	3.83E-06	9.89E-05	9.75E-06
4321_400_30@6.ais	7.04E-02	3.71E-04	5.52E-02	2.24E-04	4.06	2.73E-02	1.08E-05	2.44E-06	3.60E-05	8.01E-06
4321_400_30@7.ais	7.22E-02	2.26E-04	5.58E-02	2.49E-04	4.15	2.72E-02	1.19E-05	2.60E-06	3.97E-05	4.91E-06
4321_400_30@8.ais	7.16E-02	1.88E-04	5.26E-02	2.05E-04	4.23	3.11E-02	1.63E-05	2.99E-06	8.95E-05	1.24E-05
4321_400_30@9.ais	7.30E-02	1.58E-04	5.35E-02	1.42E-04	4.17	2.78E-02	1.52E-05	2.86E-06	3.79E-05	5.51E-06
Avg	**7.15E-02**		**5.67E-02**		**4.07**		**3.03E-05**		**8.89E-05**	
s.d.	**1.58E-03**		**3.79E-03**		**0.12**		**5.10E-05**		**1.25E-04**	
s.d.%	**2.21**		**6.69**		**3.06**		**168.16**		**141.00**	

	$^{6}Li/^{42}Ca$	1 s.e.	$B/^{42}Ca$	1 s.e.	$Mg/^{42}Ca$	1 s.e.	$^{54}Fe/^{42}Ca$	1 s.e.	$Mn/^{42}Ca$	1 s.e.
4311, 400 ppmv 30C										
4311_400_30.ais	6.85E-02	1.90E-04	5.18E-02	2.14E-04	4.38	2.95E-02	5.39E-05	8.22E-06	9.75E-05	9.78E-06
4311_400_30@1.ais	6.10E-02	3.41E-04	4.62E-02	3.52E-04	4.33	2.59E-02	2.61E-04	2.40E-05	6.35E-04	3.63E-05
4311_400_30@2.ais	6.73E-02	1.19E-04	4.98E-02	1.33E-04	4.39	2.92E-02	2.19E-04	3.27E-05	1.39E-04	1.42E-05
4311_400_30@3.ais	*7.68E-02*	*7.08E-04*	*4.06E-02*	*3.00E-04*	*2.91*	*2.34E-02*	*2.17E-05*	*4.44E-06*	*1.06E-04*	*7.04E-06*
4311_400_30@4.ais	5.67E-02	2.20E-04	4.77E-02	3.38E-04	3.97	2.52E-02	5.76E-05	8.71E-06	1.31E-04	1.11E-05
4311_400_30@5.ais	5.88E-02	2.14E-04	4.87E-02	3.79E-04	3.92	3.13E-02	5.66E-05	1.97E-05	1.42E-04	2.06E-05
4311_400_30@6.ais	6.07E-02	3.24E-04	4.06E-02	1.50E-04	3.62	1.31E-02	4.47E-05	8.51E-06	1.60E-04	8.47E-06
4311_400_30@7.ais	6.17E-02	2.36E-04	4.90E-02	2.27E-04	4.30	2.17E-02	1.41E-05	5.57E-06	3.98E-05	3.71E-06
4311_400_30@8.ais	5.75E-02	2.33E-04	4.49E-02	1.17E-04	4.46	3.18E-02	6.34E-05	6.36E-06	1.58E-04	8.79E-06
4311_400_30@9.ais	6.26E-02	4.40E-04	4.80E-02	1.99E-04	4.47	3.01E-02	2.58E-05	4.33E-06	4.76E-05	5.34E-06
Avg	**6.32E-02**		**4.67E-02**		**4.07**		**8.17E-05**		**1.72E-04**	
s.d.	**6.12E-03**		**3.73E-03**		**0.50**		**8.55E-05**		**1.79E-04**	
s.d.%	**9.69**		**7.98**		**12.16**		**104.61**		**104.10**	
4332, 400ppmv, 30C										
4332_400_30.ais	5.19E-02	1.25E-04	3.00E-02	1.24E-04	2.97	2.06E-02	2.76E-05	5.38E-06	2.38E-04	1.46E-05
4332_400_30@1.ais	5.06E-02	1.68E-04	3.48E-02	1.53E-04	3.18	2.18E-02	2.49E-05	5.39E-06	1.62E-04	1.17E-05
4332_400_30@2.ais	5.79E-02	1.45E-04	3.78E-02	1.91E-04	3.74	2.74E-02	3.14E-05	9.77E-06	6.98E-05	7.65E-06
4332_400_30@3.ais	4.59E-02	1.73E-04	3.80E-02	2.50E-04	2.97	3.49E-02	3.26E-05	5.48E-06	3.08E-04	1.79E-05
4332_400_30@4.ais	6.24E-02	4.95E-04	3.97E-02	1.80E-04	3.86	2.62E-02	3.31E-05	5.79E-06	9.81E-05	8.04E-06
4332_400_30@5.ais	6.50E-02	2.52E-04	4.15E-02	2.42E-04	3.73	2.50E-02	2.30E-05	4.93E-06	6.33E-05	5.30E-06
4332_400_30@6.ais	6.42E-02	2.07E-04	3.70E-02	7.99E-05	3.68	2.76E-02	8.58E-06	3.87E-06	3.58E-05	6.32E-06
4332_400_30@7.ais	6.82E-02	3.01E-04	4.01E-02	2.03E-04	3.77	2.44E-02	7.89E-06	1.78E-06	3.54E-05	4.69E-06
Avg	**5.83E-02**		**3.73E-02**		**3.49**		**2.36E-05**		**1.26E-04**	
s.d.	**8.02E-03**		**3.61E-03**		**0.38**		**1.02E-05**		**1.01E-04**	
s.d.%	**13.77**		**9.67**		**10.84**		**42.99**		**79.87**	

	$^{6}Li/^{42}Ca$	1 s.e.	$B/^{42}Ca$	1 s.e.	$Mg/^{42}Ca$	1 s.e.	$^{54}Fe/^{42}Ca$	1 s.e.	$Mn/^{42}Ca$	1 s.e.
1211, 1000ppmv, 20C										
1211_1000_20.ais	4.71E-02	2.57E-04	2.78E-02	1.45E-04	3.15	2.23E-02	1.41E-04	1.52E-05	4.15E-04	2.08E-05
1211_1000_20@1.ais	5.43E-02	1.70E-04	3.12E-02	1.37E-04	3.19	2.32E-02	2.00E-05	3.81E-06	1.16E-04	9.29E-06
1211_1000_20@2.ais	5.04E-02	3.39E-04	2.91E-02	2.42E-04	3.16	2.17E-02	2.17E-05	3.21E-06	1.59E-04	1.20E-05
1211_1000_20@3.ais	5.54E-02	1.49E-04	3.26E-02	1.11E-04	3.21	2.21E-02	2.91E-05	4.27E-06	1.26E-04	1.24E-05
1211_1000_20@4.ais	4.41E-02	1.74E-04	2.57E-02	1.86E-04	3.12	1.90E-02	2.12E-04	2.84E-05	3.33E-04	1.53E-05
1211_1000_20@5.ais	5.31E-02	3.30E-04	3.04E-02	8.46E-05	3.13	1.83E-02	3.58E-05	1.03E-05	1.33E-04	6.07E-06
1211_1000_20@6.ais	5.31E-02	1.17E-04	3.27E-02	1.51E-04	3.22	2.68E-02	3.59E-05	4.51E-06	1.57E-04	1.05E-05
1211_1000_20@7.ais	3.67E-02	4.06E-04	3.53E-02	3.19E-04	3.19	3.38E-02	1.63E-05	3.52E-06	1.14E-04	1.35E-05
1211_1000_20@8.ais	4.20E-02	8.28E-05	3.87E-02	1.58E-04	3.28	2.68E-02	7.54E-06	2.65E-06	1.12E-04	8.22E-06
1211_1000_20@9.ais	4.50E-02	5.08E-04	2.96E-02	2.35E-04	3.11	2.28E-02	2.45E-05	3.70E-06	1.38E-04	1.00E-05
Avg	**0.0481**		**0.0313**		**3.17**		**5.44E-05**		**1.80E-04**	
s.d.	**6.18E-03**		**3.74E-03**		**0.05**		**6.71E-05**		**1.05E-04**	
s.d.%	**12.83**		**11.93**		**1.68**		**123.36**		**58.46**	
1213, 1000 ppmv, 20C										
1213_1000_20.ais	3.77E-02	1.47E-04	3.88E-02	9.64E-05	3.35	2.21E-02	4.90E-05	7.06E-06	2.39E-04	1.26E-05
1213_1000_20@1.ais	3.90E-02	1.62E-04	4.21E-02	1.02E-04	3.32	2.78E-02	5.79E-06	1.28E-06	1.89E-04	1.10E-05
1213_1000_20@2.ais	4.10E-02	1.30E-04	3.98E-02	8.27E-05	3.45	2.09E-02	6.19E-06	1.31E-06	9.92E-05	1.04E-05
1213_1000_20@3.ais	3.96E-02	2.31E-04	4.09E-02	1.19E-04	3.21	2.66E-02	3.67E-06	1.72E-06	1.23E-04	8.42E-06
1213_1000_20@4.ais	3.66E-02	4.02E-04	3.91E-02	2.88E-04	3.30	2.75E-02	6.55E-06	1.82E-06	1.19E-04	7.51E-06
1213_1000_20@5.ais	3.86E-02	8.38E-05	3.88E-02	1.36E-04	3.26	2.33E-02	5.17E-06	1.73E-06	1.81E-04	1.61E-05
1213_1000_20@6.ais	3.59E-02	1.12E-04	3.50E-02	2.03E-04	3.19	2.32E-02	9.35E-06	2.95E-06	1.76E-04	1.42E-05
1213_1000_20@7.ais	3.10E-02	1.37E-04	4.03E-02	1.08E-04	3.19	2.40E-02	9.93E-06	2.65E-06	2.17E-04	1.76E-05
1213_1000_20@8.ais	3.40E-02	7.39E-05	3.66E-02	1.38E-04	3.21	2.13E-02	5.57E-06	1.59E-06	2.15E-04	1.16E-05
1213_1000_20@9.ais	3.73E-02	2.27E-04	3.63E-02	1.25E-04	3.28	2.30E-02	7.64E-06	2.40E-06	1.53E-04	1.37E-05
Avg	**3.71E-02**		**3.88E-02**		**3.28**		**1.09E-05**		**1.71E-04**	
s.d.	**2.91E-03**		**2.21E-03**		**0.08**		**1.352E-05**		**4.67E-05**	
s.d.%	**7.84**		**5.69**		**2.58**		**124.24**		**27.27**	

	$^{6}Li/^{42}Ca$	1 s.e.	$B/^{42}Ca$	1 s.e.	$Mg/^{42}Ca$	1 s.e.	$^{54}Fe/^{42}Ca$	1 s.e.	$Mn/^{42}Ca$	1 s.e.
1221, 1000 ppmv, 20C										
1221_1000_20.ais	4.28E-02	2.14E-04	4.35E-02	2.56E-04	3.69	2.61E-02	5.15E-06	1.55E-06	1.08E-04	5.87E-06
1221_1000_20@1.ais	3.53E-02	1.07E-04	4.26E-02	2.09E-04	3.61	2.55E-02	1.42E-05	3.97E-06	2.04E-04	1.83E-05
1221_1000_20@2.ais	4.19E-02	3.31E-04	4.62E-02	2.46E-04	3.76	2.29E-02	1.14E-05	2.18E-06	1.73E-04	1.71E-05
1221_1000_20@3.ais	4.22E-02	2.04E-04	4.10E-02	9.51E-05	3.55	2.63E-02	3.87E-06	1.04E-06	1.14E-04	8.81E-06
1221_1000_20@4.ais	4.32E-02	1.46E-04	4.19E-02	1.13E-04	3.61	2.65E-02	6.62E-06	2.19E-06	1.04E-04	5.44E-06
1221_1000_20@5.ais	3.86E-02	1.85E-04	4.27E-02	3.07E-04	3.61	2.44E-02	1.45E-05	3.81E-06	2.05E-04	1.27E-05
1221_1000_20@6.ais	4.65E-02	8.87E-05	4.91E-02	9.96E-05	3.82	2.89E-02	6.16E-06	1.81E-06	9.72E-05	9.19E-06
1221_1000_20@7.ais	4.62E-02	2.50E-04	4.74E-02	2.74E-04	3.85	3.16E-02	3.19E-05	4.05E-06	1.88E-04	1.51E-05
1221_1000_20@8.ais	3.44E-02	3.38E-04	3.53E-02	8.50E-05	3.60	2.01E-02	2.55E-05	4.96E-06	2.16E-04	9.73E-06
1221_1000_20@9.ais	4.82E-02	1.95E-04	4.45E-02	1.13E-04	3.88	2.75E-02	2.83E-06	1.62E-06	9.02E-05	5.13E-06
1221_1000_20@10.ais	4.75E-02	2.46E-04	4.29E-02	1.93E-04	3.93	2.85E-02	5.53E-06	2.19E-06	9.52E-05	6.33E-06
Avg	**4.24E-02**		**4.34E-02**		**3.72**		**1.16E-05**		**1.45E-04**	
s.d.	**4.71E-03**		**3.62E-03**		**0.14**		**9.434E-06**		**5.15E-05**	
s.d.%	**11.09**		**8.34**		**3.66**		**81.29**		**35.51**	
1233, 1000ppmv, 20C										
1233_1000_20.ais	8.69E-02	3.12E-04	3.86E-02	7.95E-05	3.56	2.12E-02	1.18E-05	2.24E-06	5.38E-05	7.56E-06
1233_1000_20@1.ais	8.64E-02	4.39E-04	3.85E-02	1.53E-04	3.49	2.75E-02	1.10E-05	2.76E-06	6.13E-05	9.62E-06
1233_1000_20@2.ais	8.99E-02	4.12E-04	4.04E-02	1.44E-04	3.76	2.09E-02	1.06E-05	2.84E-06	6.47E-05	6.64E-06
1233_1000_20@3.ais	8.88E-02	2.93E-04	4.00E-02	9.98E-05	3.62	2.64E-02	7.66E-06	2.48E-06	5.93E-05	6.07E-06
1233_1000_20@4.ais	8.78E-02	4.67E-04	3.91E-02	2.03E-04	3.75	2.15E-02	9.09E-06	1.69E-06	5.30E-05	5.10E-06
1233_1000_20@5.ais	9.16E-02	2.21E-04	4.28E-02	9.33E-05	3.71	2.71E-02	9.44E-06	2.03E-06	7.15E-05	6.59E-06
1233_1000_20@6.ais	7.67E-02	3.57E-04	3.96E-02	1.14E-04	3.65	3.11E-02	2.18E-04	1.97E-05	8.12E-04	6.92E-05
1233_1000_20@7.ais	8.21E-02	2.48E-04	4.15E-02	1.21E-04	3.98	3.44E-02	3.06E-05	8.08E-06	1.28E-04	7.32E-06
Avg	**8.63E-02**		**4.00E-02**		**3.69**		**3.85E-05**		**1.63E-04**	
s.d.	**4.77E-03**		**1.48E-03**		**0.15**		**7.29E-05**		**2.63E-04**	
s.d.%	**5.53**		**3.70**		**4.08**		**189.19**		**161.69**	

	$^{6}Li/^{42}Ca$	1 s.e.	$B/^{42}Ca$	1 s.e.	$Mg/^{42}Ca$	1 s.e.	$^{54}Fe/^{42}Ca$	1 s.e.	$Mn/^{42}Ca$	1 s.e.
1311, 1000ppmv, 30C										
1311_1000_30.ais	7.67E-02	2.79E-04	4.35E-02	1.40E-04	4.13	2.89E-02	1.13E-05	2.39E-06	3.76E-05	3.65E-06
1311_1000_30@1.ais	7.43E-02	2.28E-04	4.52E-02	1.33E-04	4.18	2.84E-02	1.68E-05	3.81E-06	6.00E-05	7.27E-06
1311_1000_30@2.ais	7.63E-02	2.76E-04	4.40E-02	1.16E-04	4.17	2.89E-02	1.51E-05	3.10E-06	3.89E-05	5.34E-06
1311_1000_30@3.ais	7.66E-02	2.11E-04	4.51E-02	1.83E-04	4.23	3.35E-02	1.93E-05	4.42E-06	3.49E-05	4.33E-06
1311_1000_30@4.ais	7.71E-02	2.41E-04	4.52E-02	1.46E-04	3.96	2.63E-02	1.66E-05	4.20E-06	4.65E-05	6.20E-06
1311_1000_30@5.ais	7.93E-02	2.44E-04	4.48E-02	1.59E-04	4.10	2.61E-02	1.23E-05	3.31E-06	3.87E-05	4.01E-06
1311_1000_30@6.ais	7.49E-02	1.67E-04	4.34E-02	1.36E-04	4.02	2.96E-02	9.17E-06	3.26E-06	4.45E-05	3.54E-06
1311_1000_30@7.ais	7.25E-02	2.80E-04	4.26E-02	2.26E-04	4.09	3.88E-02	3.48E-05	5.31E-06	6.65E-05	7.30E-06
1311_1000_30@8.ais	7.32E-02	2.42E-04	4.62E-02	1.57E-04	4.03	2.72E-02	1.03E-05	2.39E-06	4.22E-05	4.53E-06
1311_1000_30@9.ais	7.03E-02	3.19E-04	4.27E-02	1.81E-04	4.13	2.82E-02	4.26E-05	6.20E-06	1.14E-04	8.59E-06
1311_1000_30@10.ais	6.87E-02	6.79E-04	4.50E-02	1.92E-04	4.24	3.15E-02	1.31E-05	3.96E-06	4.39E-05	6.90E-06
Avg	**7.43E-02**		**4.44E-02**		**4.12**		**1.90E-05**		**5.16E-05**	
s.d.	**3.24E-03**		**1.19E-03**		**0.09**		**1.10E-05**		**2.27E-05**	
s.d.%	**4.36**		**2.68**		**2.25**		**57.84**		**44.04**	
1333, 1000 ppmv, 30C										
1333_1000_30.ais	6.37E-02	4.08E-04	4.58E-02	3.48E-04	3.78	3.44E-02	1.91E-05	5.14E-06	4.01E-04	1.04E-05
1333_1000_30@1.ais	6.67E-02	2.95E-04	5.02E-02	3.53E-04	3.68	2.44E-02	2.23E-05	2.88E-06	3.08E-04	1.65E-05
1333_1000_30@2.ais	5.97E-02	3.38E-04	4.62E-02	1.94E-04	3.54	2.20E-02	2.62E-05	3.35E-06	2.75E-04	1.49E-05
1333_1000_30@3.ais	6.18E-02	4.01E-04	4.30E-02	1.59E-04	3.75	2.55E-02	2.98E-04	8.82E-05	8.42E-04	2.77E-05
1333_1000_30@4.ais	6.22E-02	6.90E-04	4.32E-02	4.72E-04	3.77	2.57E-02	4.56E-05	8.42E-06	9.53E-04	2.95E-05
1333_1000_30@5.ais	6.40E-02	3.05E-04	4.78E-02	1.99E-04	3.73	2.64E-02	9.07E-06	1.72E-06	2.86E-04	1.28E-05
1333_1000_30@6.ais	6.49E-02	2.68E-04	4.66E-02	2.50E-04	3.82	2.15E-02	2.80E-05	4.38E-06	3.07E-04	1.67E-05
1333_1000_30@7.ais	6.85E-02	2.52E-04	4.72E-02	1.07E-04	3.75	2.79E-02	1.60E-04	1.69E-05	6.15E-04	3.12E-05
Avg	**6.39E-02**		**4.62E-02**		**3.73**		**7.60E-05**		**4.98E-04**	
s.d.	**2.82E-03**		**2.37E-03**		**0.08**		**1.02E-04**		**2.71E-04**	
s.d.%	**4.41**		**5.12**		**2.26**		**133.92**		**54.45**	

	$^{6}Li/^{42}Ca$	1 s.e.	$B/^{42}Ca$	1 s.e.	$Mg/^{42}Ca$	1 s.e.	$^{54}Fe/^{42}Ca$	1 s.e.	$Mn/^{42}Ca$	1 s.e.
1312, 1000 ppmv, 30C										
1312_1000_30.ais	7.15E-02	2.04E-04	4.24E-02	1.70E-04	3.75	2.80E-02	9.43E-06	3.08E-06	5.80E-05	7.20E-06
1312_1000_30@1.ais	7.20E-02	2.69E-04	4.31E-02	1.17E-04	3.98	2.74E-02	5.64E-06	2.29E-06	4.62E-05	6.56E-06
1312_1000_30@2.ais	7.45E-02	1.94E-04	4.20E-02	1.84E-04	4.05	3.21E-02	8.08E-06	1.53E-06	4.78E-05	6.36E-06
1312_1000_30@3.ais	6.98E-02	3.22E-04	4.09E-02	1.73E-04	4.08	2.89E-02	6.63E-06	1.70E-06	5.78E-05	4.61E-06
1312_1000_30@4.ais	7.00E-02	1.48E-04	4.16E-02	1.33E-04	3.95	3.04E-02	9.90E-06	2.66E-06	5.16E-05	9.38E-06
1312_1000_30@5.ais	7.29E-02	2.87E-04	4.33E-02	3.13E-04	4.00	3.36E-02	8.70E-06	2.48E-06	6.19E-05	7.84E-06
1312_1000_30@6.ais	7.24E-02	2.60E-04	4.31E-02	1.73E-04	4.05	3.12E-02	6.02E-06	1.66E-06	4.51E-05	5.14E-06
1312_1000_30@7.ais	7.81E-02	1.98E-04	4.53E-02	9.82E-05	4.08	3.13E-02	1.14E-05	3.64E-06	7.54E-05	9.38E-06
1312_1000_30@8.ais	6.48E-02	2.25E-04	4.22E-02	1.35E-04	3.90	2.46E-02	1.41E-04	1.18E-05	3.64E-04	2.92E-05
1312_1000_30@9.ais	7.37E-02	4.26E-04	4.56E-02	2.98E-04	4.21	3.26E-02	5.21E-06	2.39E-06	3.58E-05	6.50E-06
Avg	**7.20E-02**		**4.30E-02**		**4.00**		**2.12E-05**		**8.44E-05**	
s.d.	**3.46E-03**		**1.49E-03**		**0.12**		**4.214E-05**		**9.89E-05**	
s.d.%	**4.81**		**3.47**		**3.12**		**198.77**		**117.22**	
1332, 1000 ppmv, 30C										
1332_1000_30.ais	3.68E-02	1.51E-04	3.45E-02	2.59E-04	3.67	2.72E-02	7.39E-05	1.02E-05	4.31E-04	1.78E-05
1332_1000_30@1.ais	3.50E-02	1.04E-04	3.30E-02	1.92E-04	3.81	4.91E-02	1.13E-05	2.24E-06	2.09E-04	1.17E-05
1332_1000_30@2.ais	4.26E-02	1.96E-04	3.81E-02	1.13E-04	3.84	2.44E-02	6.28E-06	1.84E-06	1.46E-04	1.16E-05
1332_1000_30@3.ais	4.04E-02	2.88E-04	3.73E-02	1.04E-04	3.61	2.57E-02	2.95E-05	3.97E-06	1.95E-04	8.93E-06
1332_1000_30@4.ais	4.01E-02	3.84E-04	3.68E-02	2.46E-04	3.77	2.54E-02	5.60E-06	2.36E-06	1.43E-04	1.30E-05
1332_1000_30@5.ais	3.75E-02	1.73E-04	3.51E-02	1.79E-04	3.55	1.65E-02	7.67E-05	9.37E-06	3.63E-04	3.18E-05
1332_1000_30@6.ais	3.57E-02	1.12E-04	3.35E-02	2.33E-04	3.41	2.14E-02	1.81E-04	1.78E-05	1.07E-03	1.42E-04
1332_1000_30@7.ais	3.37E-02	7.72E-05	3.32E-02	1.22E-04	3.47	2.35E-02	4.51E-04	2.53E-05	1.25E-03	7.61E-05
1332_1000_30@8.ais	3.55E-02	2.22E-04	3.28E-02	1.19E-04	3.74	2.11E-02	4.95E-06	1.20E-06	1.38E-04	8.92E-06
1332_1000_30@9.ais	3.30E-02	7.14E-05	3.39E-02	1.92E-04	3.73	1.65E-02	1.56E-04	8.38E-06	5.62E-04	2.44E-05
Avg	**3.70E-02**		**3.48E-02**		**3.66**		**9.96E-05**		**4.50E-04**	
s.d.	**3.11E-03**		**1.94E-03**		**0.15**		**1.39E-04**		**4.01E-04**	
s.d.%	**8.40**		**5.57**		**3.98**		**139.45**		**89.05**	

B.2: Normalized Ratios

Table B.2: Normalized Li/Ca, B/Ca, and Mg/Ca ratios (mmol/mol) for *E. viridis* spines. Li/Ca was normalized to HTP-CC standard, B/Ca was normalized to M93 standard, and Mg/Ca was normalized to NBS-19 standard (Appendix D). Values highlighted in red were omitted from the analysis because the Ca intensities (cps) were low (< 1.5E5 cps).

	Li/Ca mmol/mol	1 s.e	B/Ca mmol/mol	1 s.e	Mg/Ca mmol/mol	1 s.e
4222, 400 ppmv, 20C						
4222_400_20.ais	3.84E-02	1.33E-03	0.2656	2.52E-02	85.2	0.868
4222_400_20@1.ais	4.94E-02	1.72E-03	0.3313	3.14E-02	96.6	0.899
4222_400_20@2.ais	3.95E-02	1.39E-03	0.2882	2.74E-02	94.5	0.803
4222_400_20@3.ais	4.94E-02	1.72E-03	0.3469	3.29E-02	100.5	0.977
4222_400_20@4.ais	4.78E-02	1.66E-03	0.3204	3.03E-02	96.6	0.914
4222_400_20@5.ais	4.58E-02	1.59E-03	0.3177	3.01E-02	96.5	0.931
4222_400_20@6.ais	4.19E-02	1.48E-03	0.2632	2.50E-02	91.4	0.878
4222_400_20@7.ais	4.41E-02	1.52E-03	0.3216	3.05E-02	99.1	0.820
4222_400_20@8.ais	4.55E-02	1.59E-03	0.3120	2.96E-02	95.6	0.852
4222_400_20@9.ais	5.22E-02	1.81E-03	0.3757	3.56E-02	102.6	0.913
Avg	**4.54E-02**		**3.14E-01**		**95.9**	
s.d.	**1.42E-03**		**1.10E-02**		**1.5**	
4221, 400 ppmv, 20C						
4221_400_20.ais	4.82E-02	1.68E-03	0.3405	3.23E-02	99.7	0.909
4221_400_20@1.ais	4.01E-02	1.40E-03	0.2994	2.85E-02	98.9	0.929
4221_400_20@2.ais	4.16E-02	1.47E-03	0.3296	3.13E-02	100.8	1.072
4221_400_20@3.ais	4.77E-02	1.66E-03	0.3722	3.53E-02	97.4	0.874
4221_400_20@4.ais	4.62E-02	1.60E-03	0.3483	3.30E-02	96.0	0.873
4221_400_20@5.ais	4.72E-02	1.65E-03	0.3620	3.43E-02	95.8	0.934
4221_400_20@6.ais	4.82E-02	1.67E-03	0.3637	3.45E-02	100.1	0.966
4221_400_20@7.ais	4.16E-02	1.46E-03	0.3134	2.97E-02	86.7	0.940
4221_400_20@8.ais	4.76E-02	1.65E-03	0.3342	3.17E-02	101.4	1.066
4221_400_20@9.ais	4.37E-02	1.59E-03	0.3180	3.02E-02	97.2	0.992
4221_400_20@10.ais	4.45E-02	1.58E-03	0.3264	3.10E-02	98.0	1.126
Avg	**4.51E-02**		**3.37E-01**		**97.5**	
s.d.	**9.03E-04**		**6.89E-03**		**1.2**	

	Li/Ca mmol/mol	1 s.e	B/Ca mmol/mol	1 s.e	Mg/Ca mmol/mol	1 s.e
4213, 400ppm 20C						
4213_400_20.ais	1.95E-02	1.95E-02	0.2744	3.46E-01	90.3	2.791
4213_400_20@1.ais	2.04E-02	2.04E-02	0.2778	3.50E-01	90.6	2.802
4213_400_20@2.ais	2.17E-02	2.17E-02	0.2791	3.52E-01	83.0	2.567
4213_400_20@3.ais	2.04E-02	2.04E-02	0.2699	3.41E-01	85.6	2.647
4213_400_20@4.ais	2.30E-02	2.30E-02	0.3136	3.96E-01	91.9	2.841
4213_400_20@5.ais	2.05E-02	2.05E-02	0.2852	3.60E-01	83.7	2.588
4213_400_20@6.ais	1.94E-02	1.94E-02	0.3101	3.91E-01	85.5	2.645
4213_400_20@7.ais	1.95E-02	1.95E-02	0.3035	3.83E-01	84.3	2.606
4213_400_20@8.ais	1.85E-02	1.85E-02	0.3551	4.48E-01	97.1	3.001
4213_400_20@9.ais	2.07E-02	2.06E-02	0.2976	3.75E-01	84.0	2.597
Avg	**2.04E-02**		**2.97E-01**		**87.6**	
s.d.	**4.08E-04**		**8.12E-03**		**1.5**	
4233, 400ppmv, 20C						
4233_400_20.ais	2.16E-02	2.16E-02	0.3546	4.47E-01	91.0	2.813
4233_400_20@1.ais	2.21E-02	2.21E-02	0.3149	3.97E-01	87.9	2.717
4233_400_20@2.ais	2.07E-02	2.07E-02	0.3430	4.33E-01	91.7	2.834
4233_400_20@3.ais	2.04E-02	2.04E-02	0.3416	4.31E-01	91.4	2.827
4233_400_20@4.ais	2.08E-02	2.08E-02	0.3142	3.96E-01	89.6	2.770
4233_400_20@5.ais	1.84E-02	1.84E-02	0.2994	3.78E-01	82.8	2.559
4233_400_20@6.ais	1.77E-02	1.77E-02	0.3104	3.92E-01	89.3	2.760
4233_400_20@7.ais	1.97E-02	1.97E-02	0.3379	4.26E-01	92.8	2.870
Avg	**2.02E-02**		**3.27E-01**		**89.5**	
s.d.	**5.40E-04**		**6.94E-03**		**1.1**	
4312, 400 ppmv, 30C						
4312_400_30.ais	8.41E-02	2.91E-03	0.4563	4.32E-02	103.6	0.951
4312_400_30@1.ais	8.31E-02	2.88E-03	0.4499	4.26E-02	106.4	0.959
4312_400_30@2.ais	8.05E-02	2.81E-03	0.3982	3.79E-02	103.7	1.427
4312_400_30@3.ais	8.47E-02	2.93E-03	0.4244	4.02E-02	101.6	0.873
4312_400_30@4.ais	8.78E-02	3.04E-03	0.4373	4.15E-02	103.9	0.989
4312_400_30@5.ais	8.26E-02	2.86E-03	0.3955	3.75E-02	103.2	0.884
4312_400_30@6.ais	8.53E-02	2.99E-03	0.4196	3.97E-02	104.2	0.971
4312_400_30@7.ais	8.60E-02	3.12E-03	0.3927	3.73E-02	103.8	1.106
4312_400_30@8.ais	8.64E-02	2.99E-03	0.4271	4.05E-02	107.9	1.038
4312_400_30@9.ais	8.80E-02	3.05E-03	0.4566	4.32E-02	105.2	1.032
Avg	**8.49E-02**		**4.26E-01**		**104.3**	
s.d.	**7.47E-04**		**7.75E-03**		**0.6**	

	Li/Ca mmol/mol	1 s.e	B/Ca mmol/mol	1 s.e	Mg/Ca mmol/mol	1 s.e
4321, 400 ppmv, 30C						
4321_400_30.ais	8.39E-02	2.91E-03	0.4981	4.73E-02	111.9	0.977
4321_400_30@1.ais	8.58E-02	2.97E-03	0.5273	5.00E-02	107.2	1.048
4321_400_30@2.ais	8.75E-02	3.03E-03	0.5149	4.88E-02	104.9	0.936
4321_400_30@3.ais	8.89E-02	3.07E-03	0.5313	5.03E-02	109.9	1.033
4321_400_30@4.ais	8.60E-02	2.98E-03	0.4348	4.12E-02	115.0	1.139
4321_400_30@5.ais	8.26E-02	2.89E-03	0.4971	4.71E-02	109.9	1.070
4321_400_30@6.ais	8.47E-02	2.96E-03	0.4738	4.49E-02	110.9	1.030
4321_400_30@7.ais	8.69E-02	3.01E-03	0.4790	4.54E-02	113.2	1.038
4321_400_30@8.ais	8.61E-02	2.98E-03	0.4519	4.28E-02	115.5	1.126
4321_400_30@9.ais	8.79E-02	3.04E-03	0.4593	4.35E-02	113.9	1.054
Avg	**8.60E-02**		**4.87E-01**		**111.2**	
s.d.	**6.02E-04**		**1.03E-02**		**1.1**	
4311, 400 ppmv 30C						
4311_400_30.ais	3.72E-02	3.72E-02	0.4445	5.61E-01	119.4	3.693
4311_400_30@1.ais	3.32E-02	3.31E-02	0.3970	5.01E-01	118.1	3.651
4311_400_30@2.ais	3.66E-02	3.66E-02	0.4273	5.39E-01	119.9	3.706
4311_400_30@3.ais	*4.17E-02*	*4.17E-02*	*0.3486*	*4.40E-01*	*79.4*	*2.455*
4311_400_30@4.ais	3.08E-02	3.08E-02	0.4096	5.17E-01	108.3	3.349
4311_400_30@5.ais	3.20E-02	3.19E-02	0.4183	5.28E-01	107.0	3.308
4311_400_30@6.ais	3.30E-02	3.30E-02	0.3484	4.39E-01	98.8	3.055
4311_400_30@7.ais	3.35E-02	3.35E-02	0.4204	5.30E-01	117.3	3.627
4311_400_30@8.ais	3.12E-02	3.12E-02	0.3853	4.86E-01	121.6	3.761
4311_400_30@9.ais	3.40E-02	3.40E-02	0.4118	5.19E-01	122.0	3.773
Avg	**3.35E-02**		**4.07E-01**		**114.7**	
s.d.	**7.35E-04**		**9.25E-03**		**2.7**	
4332, 400ppmv, 30C						
4332_400_30.ais	2.82E-02	2.82E-02	0.2573	3.25E-01	81.1	2.509
4332_400_30@1.ais	2.75E-02	2.75E-02	0.2991	3.77E-01	86.8	2.684
4332_400_30@2.ais	3.14E-02	3.14E-02	0.3243	4.09E-01	102.0	3.155
4332_400_30@3.ais	2.49E-02	2.49E-02	0.3264	4.12E-01	81.1	2.508
4332_400_30@4.ais	3.39E-02	3.39E-02	0.3404	4.29E-01	105.2	3.254
4332_400_30@5.ais	3.53E-02	3.53E-02	0.3561	4.49E-01	101.9	3.149
4332_400_30@6.ais	3.49E-02	3.49E-02	0.3174	4.00E-01	100.4	3.105
4332_400_30@7.ais	3.71E-02	3.70E-02	0.3440	4.34E-01	102.9	3.183
Avg	**3.16E-02**		**3.21E-01**		**95.2**	
s.d.	**1.54E-03**		**1.10E-02**		**3.6**	

	Li/Ca mmol/mol	1 s.e	B/Ca mmol/mol	1 s.e	Mg/Ca mmol/mol	1 s.e
1211, 1000ppmv, 20C						
1211_1000_20.ais	2.56E-02	2.56E-02	0.2387	3.01E-01	85.9	2.657
1211_1000_20@1.ais	2.95E-02	2.95E-02	0.2682	3.38E-01	87.0	2.691
1211_1000_20@2.ais	2.74E-02	2.74E-02	0.2497	3.15E-01	86.4	2.670
1211_1000_20@3.ais	3.01E-02	3.01E-02	0.2797	3.53E-01	87.5	2.706
1211_1000_20@4.ais	2.40E-02	2.39E-02	0.2211	2.79E-01	85.1	2.630
1211_1000_20@5.ais	2.89E-02	2.89E-02	0.2613	3.30E-01	85.4	2.639
1211_1000_20@6.ais	2.89E-02	2.88E-02	0.2804	3.54E-01	88.0	2.720
1211_1000_20@7.ais	1.99E-02	1.99E-02	0.3029	3.82E-01	87.1	2.694
1211_1000_20@8.ais	2.28E-02	2.28E-02	0.3322	4.19E-01	89.5	2.767
1211_1000_20@9.ais	2.44E-02	2.44E-02	0.2544	3.21E-01	84.8	2.621
Avg	**2.61E-02**		**2.69E-01**		**86.7**	
s.d.	**1.06E-03**		**1.01E-02**		**0.5**	
1233, 1000ppmv, 20C						
1233_1000_20.ais	4.72E-02	4.72E-02	0.3313	4.18E-01	97.3	3.008
1233_1000_20@1.ais	4.69E-02	4.69E-02	0.3303	4.17E-01	95.2	2.943
1233_1000_20@2.ais	4.88E-02	4.88E-02	0.3465	4.37E-01	102.7	3.174
1233_1000_20@3.ais	4.83E-02	4.82E-02	0.3437	4.34E-01	98.9	3.059
1233_1000_20@4.ais	4.77E-02	4.77E-02	0.3356	4.23E-01	102.4	3.165
1233_1000_20@5.ais	4.98E-02	4.97E-02	0.3674	4.63E-01	101.4	3.134
1233_1000_20@6.ais	4.17E-02	4.17E-02	0.3401	4.29E-01	99.6	3.080
1233_1000_20@7.ais	4.46E-02	4.46E-02	0.3560	4.49E-01	108.7	3.362
Avg	**4.69E-02**		**3.44E-01**		**100.8**	
s.d.	**9.16E-04**		**1.27E-02**		**4.1**	
1213, 1000 ppmv, 20C						
1213_1000_20.ais	4.54E-02	1.58E-03	0.3334	3.16E-02	91.6	0.841
1213_1000_20@1.ais	4.70E-02	1.63E-03	0.3614	3.42E-02	90.5	0.956
1213_1000_20@2.ais	4.94E-02	1.71E-03	0.3418	3.24E-02	94.3	0.831
1213_1000_20@3.ais	4.77E-02	1.67E-03	0.3514	3.33E-02	87.5	0.918
1213_1000_20@4.ais	4.41E-02	1.60E-03	0.3360	3.19E-02	90.2	0.948
1213_1000_20@5.ais	4.65E-02	1.61E-03	0.3333	3.16E-02	88.9	0.855
1213_1000_20@6.ais	4.33E-02	1.50E-03	0.3009	2.85E-02	87.1	0.844
1213_1000_20@7.ais	3.73E-02	1.30E-03	0.3464	3.28E-02	87.2	0.862
1213_1000_20@8.ais	4.09E-02	1.42E-03	0.3145	2.98E-02	87.6	0.809
1213_1000_20@9.ais	4.49E-02	1.57E-03	0.3118	2.95E-02	89.4	0.851
Avg	**4.46E-02**		**3.33E-01**		**89.4**	
s.d.	**1.11E-03**		**5.99E-03**		**0.7**	

	Li/Ca mmol/mol	1 s.e	B/Ca mmol/mol	1 s.e	Mg/Ca mmol/mol	1 s.e
1221, 1000 ppmv, 20C						
1221_1000_20.ais	5.15E-02	1.80E-03	0.3733	3.54E-02	100.6	0.962
1221_1000_20@1.ais	4.25E-02	1.47E-03	0.3653	3.46E-02	98.4	0.941
1221_1000_20@2.ais	5.04E-02	1.79E-03	0.3965	3.76E-02	102.8	0.909
1221_1000_20@3.ais	5.08E-02	1.77E-03	0.3518	3.33E-02	96.8	0.949
1221_1000_20@4.ais	5.20E-02	1.80E-03	0.3601	3.41E-02	98.4	0.961
1221_1000_20@5.ais	4.64E-02	1.62E-03	0.3669	3.48E-02	98.5	0.918
1221_1000_20@6.ais	5.60E-02	1.94E-03	0.4212	3.99E-02	104.4	1.036
1221_1000_20@7.ais	5.56E-02	1.94E-03	0.4066	3.86E-02	105.0	1.094
1221_1000_20@8.ais	4.14E-02	1.48E-03	0.3035	2.87E-02	98.2	0.836
1221_1000_20@9.ais	5.79E-02	2.01E-03	0.3822	3.62E-02	106.0	1.013
1221_1000_20@10.ais	5.72E-02	6.92E-02	0.3684	3.49E-02	107.4	1.040
Avg	**5.11E-02**		**3.72E-01**		**101.5**	
s.d.	**1.71E-03**		**9.37E-03**		**1.1**	
s.d.%	**3.34**		**2.52**		**1.1**	
1311, 1000ppmv, 30C						
1311_1000_30.ais	4.17E-02	4.16E-02	0.3738	4.72E-01	112.8	3.486
1311_1000_30@1.ais	4.04E-02	4.04E-02	0.3879	4.89E-01	114.1	3.527
1311_1000_30@2.ais	4.15E-02	4.15E-02	0.3774	4.76E-01	113.8	3.519
1311_1000_30@3.ais	4.16E-02	4.16E-02	0.3868	4.88E-01	115.6	3.574
1311_1000_30@4.ais	4.19E-02	4.19E-02	0.3883	4.90E-01	108.1	3.343
1311_1000_30@5.ais	4.31E-02	4.31E-02	0.3845	4.85E-01	112.0	3.463
1311_1000_30@6.ais	4.07E-02	4.07E-02	0.3722	4.70E-01	109.7	3.392
1311_1000_30@7.ais	3.94E-02	3.94E-02	0.3659	4.62E-01	111.7	3.454
1311_1000_30@8.ais	3.97E-02	3.97E-02	0.3964	5.00E-01	110.1	3.403
1311_1000_30@9.ais	3.82E-02	3.82E-02	0.3663	4.62E-01	112.8	3.487
1311_1000_30@10.ais	3.73E-02	3.73E-02	0.3860	4.87E-01	115.7	3.577
Avg	**4.05E-02**		**3.81E-01**		**112.4**	
s.d.	**5.17E-04**		**3.00E-03**		**0.7**	
s.d.%	**1.28**		**0.79**		**0.6**	

	Li/Ca mmol/mol	1 s.e	B/Ca mmol/mol	1 s.e	Mg/Ca mmol/mol	1 s.e
1333, 1000 ppmv, 30C						
1333_1000_30.ais	3.46E-02	3.46E-02	0.3929	4.96E-01	103.1	3.189
1333_1000_30@1.ais	3.63E-02	3.62E-02	0.4311	5.44E-01	100.6	3.110
1333_1000_30@2.ais	3.24E-02	3.24E-02	0.3966	5.00E-01	96.7	2.991
1333_1000_30@3.ais	3.36E-02	3.36E-02	0.3689	4.65E-01	102.3	3.163
1333_1000_30@4.ais	3.38E-02	3.38E-02	0.3712	4.68E-01	102.9	3.180
1333_1000_30@5.ais	3.48E-02	3.48E-02	0.4105	5.18E-01	101.7	3.146
1333_1000_30@6.ais	3.53E-02	3.53E-02	0.3997	5.04E-01	104.3	3.225
1333_1000_30@7.ais	3.72E-02	3.72E-02	0.4052	5.11E-01	102.4	3.165
Avg	**3.47E-02**		**3.97E-01**		**101.8**	
s.d.	**5.42E-04**		**7.19E-03**		**0.8**	
1312, 1000 ppmv, 30C						
1312_1000_30.ais	8.60E-02	2.98E-03	0.3640	3.45E-02	102.4	1.009
1312_1000_30@1.ais	8.67E-02	3.01E-03	0.3698	3.50E-02	108.6	1.022
1312_1000_30@2.ais	8.97E-02	3.11E-03	0.3609	3.42E-02	110.7	1.127
1312_1000_30@3.ais	8.39E-02	2.92E-03	0.3513	3.33E-02	111.2	1.063
1312_1000_30@4.ais	8.43E-02	2.91E-03	0.3573	3.39E-02	107.7	1.080
1312_1000_30@5.ais	8.77E-02	3.05E-03	0.3715	3.53E-02	109.1	1.153
1312_1000_30@6.ais	8.71E-02	3.02E-03	0.3704	3.51E-02	110.5	1.108
1312_1000_30@7.ais	9.40E-02	3.25E-03	0.3887	3.68E-02	111.5	1.114
1312_1000_30@8.ais	7.80E-02	2.71E-03	0.3625	3.43E-02	106.3	0.957
1312_1000_30@9.ais	8.87E-02	3.10E-03	0.3911	3.71E-02	115.0	1.156
Avg	**8.66E-02**		**3.69E-01**		**109.3**	
s.d.	**1.32E-03**		**4.04E-03**		**1.1**	
1332, 1000 ppmv, 30C						
1332_1000_30.ais	4.43E-02	1.54E-03	0.2963	2.81E-02	100.1	0.982
1332_1000_30@1.ais	4.21E-02	1.46E-03	0.2836	2.69E-02	104.0	1.497
1332_1000_30@2.ais	5.13E-02	1.79E-03	0.3275	3.10E-02	104.8	0.946
1332_1000_30@3.ais	4.86E-02	1.71E-03	0.3205	3.04E-02	98.4	0.944
1332_1000_30@4.ais	4.82E-02	1.73E-03	0.3163	3.00E-02	103.0	0.957
1332_1000_30@5.ais	4.51E-02	1.57E-03	0.3010	2.85E-02	97.0	0.769
1332_1000_30@6.ais	4.30E-02	1.49E-03	0.2874	2.73E-02	93.2	0.837
1332_1000_30@7.ais	4.05E-02	1.40E-03	0.2854	2.70E-02	94.6	0.883
1332_1000_30@8.ais	4.28E-02	1.50E-03	0.2819	2.67E-02	102.1	0.873
1332_1000_30@9.ais	3.98E-02	1.38E-03	0.2911	2.76E-02	101.9	0.794
Avg	**4.46E-02**		**2.99E-01**		**99.9**	
s.d.	**1.18E-03**		**5.27E-03**		**1.3**	

Appendix C: Paleo-Echinoderm SIMS Data

C.1: Intensity Ratios

Table C.1: Intensity ratios ($^{6}Li/^{42}Ca$, $B/^{42}Ca$, $Mg/^{42}Ca$, $^{54}Fe/^{42}Ca$, and $Mn/^{42}Ca$) of various paleo-echinoderm samples. Values highlighted in red were omitted from the analysis because the Fe and Mn intensities (cps) were high.

	$^{6}Li/^{42}Ca$	1 s.e.	$B/^{42}Ca$	1 s.e.	$Mg/^{42}Ca$	1 s.e.	$^{54}Fe/^{42}Ca$	1 s.e.	$Mn/^{42}Ca$	1 s.e.
Paleo 62, 53 MA										
paleo62@1.ais	4.18E-02	2.49E-03	9.26E-02	7.24E-03	3.15	1.76E-01	1.68E-01	1.76E-02	5.59E-01	1.24E-01
paleo62@2.ais	3.63E-02	2.84E-04	6.48E-02	1.63E-03	2.84	3.21E-02	6.55E-02	1.39E-02	2.69E-01	8.82E-02
paleo62@11.ais	8.53E-02	6.67E-03	1.04E-01	3.47E-03	2.84	5.58E-02	3.69E-01	6.86E-02	4.31E-01	5.67E-02
Avg	**3.90E-02**		**7.87E-02**		**2.996**		**0.117**		**0.414**	
s.d.	**3.95E-03**		**1.96E-02**		**0.217**		**7.25E-02**		**0.205**	
s.d.%	**10.12**		**24.91**		**7.23**		**62.08**		**49.59**	
Paleo 29, 156 Ma										
paleo29@4.ais	*1.25E-01*	*2.57E-03*	*1.58E-01*	*2.36E-03*	*1.73*	*2.57E-02*	*2.36E+00*	*1.56E-01*	*4.18E-01*	*1.39E-02*
paleo29@5.ais	7.41E-02	4.02E-03	8.51E-02	3.40E-03	1.29	2.58E-02	6.68E-01	3.74E-02	4.65E-01	9.27E-03
paleo29@6.ais	*5.65E-02*	*1.39E-03*	*6.81E-02*	*1.87E-03*	*1.16*	*4.19E-03*	*1.60E+00*	*1.76E-01*	*5.43E-01*	*1.03E-02*
Avg	**7.41E-02**		**8.51E-02**		**1.29**		**0.668**		**0.465**	
s.d.	**4.02E-03**		**3.40E-03**		**2.58E-02**		**3.74E-02**		**9.27E-03**	
s.d.%	**5.42**		**3.99**		**2.01**		**5.59**		**1.99**	
Paleo 39, 156 Ma										
paleo39@6.ais	2.21E-02	1.94E-04	1.23E-01	6.74E-03	1.44	2.56E-02	5.83E-06	2.25E-06	7.51E-01	7.65E-03
paleo39@7.ais	1.49E-02	1.12E-04	2.44E-01	8.81E-03	2.60	2.43E-02	9.02E-01	1.91E-02	6.30E-02	2.55E-03
paleo39@12.ais	7.47E-02	3.94E-04	1.79E-01	5.98E-04	2.38	1.67E-02	6.93E-01	3.08E-02	6.71E-02	4.98E-04
Avg	**1.85E-02**		**1.83E-01**		**2.020**		**0.451**		**0.407**	
s.d.	**5.16E-03**		**8.54E-02**		**8.16E-01**		**0.638**		**4.87E-01**	
s.d.%	**2.79E+01**		**4.66E+01**		**4.04E+01**		**1.41E+02**		**1.20E+02**	
Paleo 38, 190 Ma										
paleo38@7.ais	5.60E-03	3.03E-04	9.84E-03	5.77E-04	1.01	1.92E-02	6.21E-01	2.63E-03	4.43E+00	1.64E-02
paleo38@8.ais	6.59E-03	3.76E-05	1.13E-02	5.42E-05	0.90	8.74E-03	5.86E-01	1.58E-03	4.43E+00	1.77E-02
paleo38@9.ais	4.51E-03	8.93E-05	4.03E-03	5.27E-05	0.93	4.22E-03	7.78E-01	3.52E-03	5.93E+00	3.51E-02
Avg	**5.57E-03**		**8.38E-03**		**0.948**		**0.661**		**4.93**	
s.d.	**1.04E-03**		**3.83E-03**		**5.99E-02**		**0.102**		**8.69E-01**	
s.d.%	**18.66**		**45.74**		**6.32**		**15.45**		**17.64**	

	$^{6}Li/^{42}Ca$	1 s.e.	$B/^{42}Ca$	1 s.e.	$Mg/^{42}Ca$	1 s.e.	$^{54}Fe/^{42}Ca$	1 s.e.	$Mn/^{42}Ca$	1 s.e.
Paleo 90, 220 Ma										
paleo90@13.ais	*4.28E-03*	*5.01E-05*	*3.21E-01*	*2.18E-02*	*4.78*	*7.57E-02*	*1.03E-01*	*8.80E-03*	*2.23E-02*	*4.38E-04*
paleo90@14.ais	3.68E-03	1.02E-04	3.25E-02	1.61E-03	3.74	7.58E-02	1.99E-01	6.44E-03	5.93E-01	8.19E-03
paleo90@15.ais	*9.47E-03*	*9.90E-04*	*5.91E-02*	*2.70E-03*	*1.74*	*1.40E-02*	*9.19E-01*	*1.54E-01*	*5.22E-01*	*5.55E-03*
Avg	**3.68E-03**		**3.25E-02**		**3.74**		**0.199**		**0.593**	
s.d.	**1.02E-04**		**1.61E-03**		**7.58E-02**		**6.44E-03**		**8.19E-03**	
s.d.%	**2.77**		**4.96**		**2.03**		**3.24**		**1.38**	
Paleo 97, 253 Ma										
paleo97@16.ais	1.76E-02	1.94E-04	3.39E-02	9.21E-04	2.44	7.13E-02	6.15E-01	2.03E-02	2.38E+00	7.03E-02
paleo97@17.ais	9.31E-03	6.18E-05	4.97E-02	3.30E-03	3.57	4.45E-02	4.71E-01	6.62E-03	2.31E+00	2.70E-02
paleo97@18.ais	5.88E-03	1.70E-04	1.56E-02	9.06E-04	2.63	5.36E-02	3.76E-01	8.94E-03	1.89E+00	2.33E-02
paleo97@19.ais	7.95E-03	7.11E-05	1.60E-02	1.18E-03	2.11	1.26E-02	7.79E-01	1.03E-02	3.25E+00	1.72E-02
Avg	**1.02E-02**		**2.88E-02**		**2.69**		**0.560**		**2.46**	
s.d.	**5.16E-03**		**1.64E-02**		**0.628**		**0.176**		**0.571**	
s.d.%	**50.63**		**56.80**		**23.37**		**31.40**		**23.24**	
Paleo 70, 326 Ma										
paleo70@8.ais	*2.58E-01*	*1.43E-02*	*1.36E-01*	*6.05E-03*	*2.96*	*5.54E-02*	*1.56E+00*	*1.16E-01*	*7.61E-01*	*2.44E-02*
paleo70@9.ais	2.79E-02	1.06E-03	5.91E-02	1.28E-03	2.11	2.85E-02	2.94E-01	4.85E-03	7.26E-01	8.95E-03
paleo70@10.ais	*1.72E-01*	*7.27E-03*	*5.71E-02*	*1.54E-03*	*1.73*	*1.76E-02*	*1.82E+00*	*9.26E-02*	*1.10E+00*	*2.41E-02*
Avg	**2.79E-02**		**5.91E-02**		**2.11**		**0.294**		**0.726**	
s.d.	**1.06E-03**		**1.28E-03**		**2.85E-02**		**4.85E-03**		**8.95E-03**	
s.d.%	**3.79**		**2.16**		**1.35**		**1.65**		**1.23**	
Paleo 68, 330 Ma										
paleo68@5.ais	2.75E-03	6.06E-05	6.40E-02	3.88E-03	3.42	2.97E-02	4.45E-01	1.83E-02	8.31E-01	2.34E-02
paleo68@6.ais	*1.22E-03*	*7.35E-05*	*4.14E-02*	*3.89E-03*	*2.81*	*9.30E-02*	*1.07E+00*	*6.65E-02*	*3.36E+00*	*1.72E-02*
paleo68@7.ais	1.46E-03	2.86E-05	4.64E-02	1.18E-03	3.12	6.69E-02	6.21E-01	7.56E-02	1.97E+00	1.16E-01
Avg	**2.11E-03**		**5.52E-02**		**3.2705**		**0.533**		**1.40**	
s.d.	**9.10E-04**		**1.25E-02**		**0.218**		**0.124**		**0.806**	
s.d.%	**43.22**		**22.65**		**6.67**		**23.26**		**57.52**	

	$^{6}Li/^{42}Ca$	1 s.e.	$B/^{42}Ca$	1 s.e.	$Mg/^{42}Ca$	1 s.e.	$^{54}Fe/^{42}Ca$	1 s.e.	$Mn/^{42}Ca$	1 s.e.
Paleo 40/41, 330 Ma										
paleo40@3.ais	4.64E-03	5.56E-05	5.87E-02	3.52E-03	3.19	2.81E-02	1.48E-01	6.79E-03	7.90E-02	1.62E-03
paleo40@4.ais	4.61E-02	1.08E-02	7.75E-02	1.39E-02	2.53	7.18E-02	3.67E-01	9.97E-03	1.99E-01	5.85E-03
paleo40@5.ais	9.62E-02	1.03E-02	8.10E-02	6.04E-03	2.30	1.70E-02	2.88E-01	2.96E-02	1.11E-01	5.87E-04
Avg	**4.90E-02**		**7.24E-02**		**2.67**		**0.268**		**0.129**	
s.d.	**4.59E-02**		**1.20E-02**		**0.467**		**0.111**		**6.21E-02**	
s.d.%	**93.63**		**16.57**		**17.46**		**41.43**		**47.96**	
Paleo 76, 354 Ma										
paleo76@16.ais	2.73E-02	2.23E-03	3.66E-02	2.22E-03	1.04	7.46E-03	5.24E-01	3.29E-02	4.01E+00	5.64E-02
paleo76@17.ais	1.53E-02	4.59E-04	4.80E-02	9.39E-03	1.31	1.70E-02	3.79E-01	2.61E-03	3.05E+00	1.35E-02
paleo76@18.ais	2.06E-02	1.22E-03	4.96E-02	2.58E-03	1.25	2.24E-02	3.65E-01	7.97E-03	2.80E+00	3.89E-02
Avg	**2.11E-02**		**4.88E-02**		**1.20**		**0.372**		**3.29**	
s.d.	**6.01E-03**		**1.08E-03**		**0.144**		**9.48E-03**		**0.636**	
s.d.%	**28.50**		**2.21**		**12.01**		**2.55**		**19.37**	
Paleo 77, 354 Ma										
paleo77@11.ais	1.33E-02	9.56E-05	2.11E-02	1.36E-03	1.28	9.17E-03	4.59E-01	5.29E-03	3.34E+00	8.05E-03
paleo77@12.ais	1.05E-02	6.01E-05	2.35E-02	1.98E-03	1.34	2.50E-02	3.56E-01	4.15E-03	3.09E+00	1.32E-02
paleo77@14.ais	1.90E-03	1.70E-04	3.61E-03	6.52E-04	0.398	1.75E-02	1.17E-01	2.98E-03	4.13E+00	1.05E-02
paleo77@15.ais	3.37E-03	1.43E-04	1.55E-02	1.43E-03	0.710	3.96E-02	1.68E-01	5.69E-03	4.36E+00	7.92E-02
Avg	**7.29E-03**		**1.59E-02**		**0.932**		**0.275**		**3.73**	
s.d.	**5.53E-03**		**8.89E-03**		**0.455**		**0.160**		**0.611**	
s.d.%	**75.83**		**55.75**		**48.82**		**58.13**		**16.35**	
Paleo 66, 354 Ma										
paleo66@1.ais	7.82E-03	1.97E-04	3.38E-02	2.04E-03	1.19E+00	1.53E-02	1.99E-01	2.85E-03	1.38E+00	3.29E-03
paleo66@2.ais	7.60E-03	3.17E-04	2.32E-02	1.38E-03	8.57E-01	1.03E-02	2.16E-01	3.86E-03	1.57E+00	2.80E-02
paleo66@3.ais	7.35E-03	4.47E-04	3.22E-02	3.23E-03	1.05E+00	1.29E-02	2.43E-01	2.98E-03	1.72E+00	9.55E-03
Avg	**7.59E-03**		**2.97E-02**		**1.03**		**0.219**		**1.56**	
s.d.	**2.35E-04**		**5.72E-03**		**0.165**		**2.21E-02**		**0.170**	
s.d.%	**3.09**		**19.25**		**16.00**		**10.08**		**10.90**	

	$^{6}Li/^{42}Ca$	1 s.e.	$B/^{42}Ca$	1 s.e.	$Mg/^{42}Ca$	1 s.e.	$^{54}Fe/^{42}Ca$	1 s.e.	$Mn/^{42}Ca$	1 s.e.
Paleo 26, 385 Ma										
paleo26@10.ais	4.05E-03	3.01E-05	1.72E-03	7.48E-05	1.17E+00	8.68E-03	2.92E-01	8.46E-04	1.49E+00	1.86E-03
paleo26@11.ais	1.13E-02	6.55E-04	4.97E-03	5.79E-04	1.21E+00	7.87E-03	4.50E-01	9.98E-03	2.01E+00	6.92E-03
paleo26@12.ais	7.71E-03	1.18E-04	6.88E-03	6.34E-04	1.84E+00	4.06E-02	4.55E-01	1.68E-02	1.72E+00	2.89E-02
Avg	**7.68E-03**		**4.52E-03**		**1.41**		**0.399**		**1.74**	
s.d.	**3.62E-03**		**2.61E-03**		**0.380**		**9.29E-02**		**0.261**	
s.d.%	**47.09**		**57.71**		**27.06**		**23.27**		**14.97**	

C.2 : Normalized Ratios

Table C.2: Normalized Li/Ca, B/Ca, and Mg/Ca SIMS values of various paleo-echinoderm samples. Li/Ca was normalized to HTP-CC standard, B/Ca was normalized to M93 standard, and Mg/Ca was normalized to NBS-19 standard (Appendix D). Normalized ratios for Fe/Ca and Mn/Ca were omitted because there were no available standards to normalize the data. Values highlighted in red were omitted from the analysis because the Fe and Mn intensities (Appendix C.1) were high.

	Li/Ca mmol/mol	1 s.e	B/Ca mmol/mol	1 s.e	Mg/Ca mmol/mol	1 s.e
Paleo 62, 53 MA						
paleo62@1.ais	5.04E-02	2.51E-02	0.795	0.0976	85.96	4.82
paleo62@2.ais	4.36E-02	2.38E-02	0.557	0.0545	77.60	1.01
paleo62@11.ais	1.03E-01	2.58E-02	0.891	0.0895	77.49	1.60
Avg	**4.70E-02**		**0.676**		**81.78**	
s.d.	**3.36E-03**		**0.119**		**4.18**	
s.d.%	**7.15**		**17.62**		**5.11**	
Paleo 29, 156 Ma						
paleo29@4.ais	*1.50E-01*	*6.04E-03*	*1.36E+00*	*1.18E-02*	*47.24*	*0.76*
paleo29@5.ais	8.92E-02	5.73E-03	7.31E-01	9.18E-03	35.11	0.74
paleo29@6.ais	*6.80E-02*	*2.88E-03*	*5.85E-01*	*4.05E-03*	*31.64*	*0.23*
Avg	**8.92E-02**		**7.31E-01**		**35.11**	
s.d.	**5.73E-03**		**9.18E-03**		**0.739**	
s.d.%	**6.42**		**1.26**		**2.11**	
Paleo 39, 156 Ma						
paleo39@6.ais	2.67E-02	2.35E-02	1.055	0.1154	39.38	0.74
paleo39@7.ais	1.79E-02	2.32E-02	2.092	0.2120	70.88	0.80
paleo39@12.ais	8.98E-02	2.41E-02	1.536	0.1455	64.99	0.62
Avg	**4.48E-02**		**1.56**		**58.42**	
s.d.	**2.27E-02**		**0.299**		**9.67**	
s.d.%	**50.61**		**19.19**		**16.55**	
Paleo 38, 190 Ma						
paleo38@7.ais	6.74E-03	4.33E-04	8.45E-02	1.80E-04	27.66	0.55
paleo38@8.ais	7.93E-03	2.77E-04	9.67E-02	1.94E-05	24.45	0.29
paleo38@9.ais	5.43E-03	2.16E-04	3.46E-02	6.74E-06	25.51	0.20
Avg	**6.70E-03**		**7.19E-02**		**25.87**	
s.d.	**1.25E-03**		**3.29E-02**		**1.64**	
s.d.%	**18.66**		**45.74**		**6.32**	
Paleo 90, 220 Ma						
paleo90@13.ais	*5.15E-03*	*1.88E-04*	*2.76E+00*	*2.23E-01*	*130.41*	*2.23*
paleo90@14.ais	4.43E-03	1.96E-04	2.79E-01	1.67E-03	102.06	2.17
paleo90@15.ais	*1.14E-02*	*1.25E-03*	*5.07E-01*	*5.07E-03*	*47.61*	*0.49*
Avg	**4.43E-03**		**0.279**		**102.06**	
s.d.	**1.96E-04**		**1.67E-03**		**2.17**	
s.d.%	**4.43**		**0.60**		**2.13**	

	Li/Ca mmol/mol	1 s.e	B/Ca mmol/mol	1 s.e	Mg/Ca mmol/mol	1 s.e
Paleo 97, 253 Ma						
paleo97@16.ais	2.12E-02	7.69E-04	2.91E-01	9.93E-04	66.64	1.99
paleo97@17.ais	1.12E-02	3.94E-04	4.27E-01	5.20E-03	97.50	1.37
paleo97@18.ais	7.07E-03	3.18E-04	1.34E-01	4.48E-04	71.88	1.53
paleo97@19.ais	9.57E-03	3.41E-04	1.37E-01	5.98E-04	57.49	0.50
Avg	**1.23E-02**		**0.247**		**73.38**	
s.d.	**6.21E-03**		**0.140**		**17.15**	
s.d.%	**50.63**		**56.80**		**23.37**	
Paleo 70, 326 Ma						
paleo70@8.ais	*3.11E-01*	*2.03E-02*	*1.17E+00*	*2.61E-02*	*80.70*	*1.60*
paleo70@9.ais	3.35E-02	1.72E-03	5.07E-01	2.40E-03	57.48	0.86
paleo70@10.ais	*2.07E-01*	*1.13E-02*	*4.90E-01*	*2.78E-03*	*47.25*	*0.57*
Avg	**3.35E-02**		**0.507**		**57.48**	
s.d.	**1.72E-03**		**2.40E-03**		**0.860**	
s.d.%	**5.13**		**0.47**		**1.50**	
Paleo 68, 330 Ma						
paleo68@5.ais	3.31E-03	1.36E-04	5.50E-01	7.89E-03	93.66	1.01
paleo68@6.ais	*1.47E-03*	*1.02E-04*	*3.56E-01*	*5.11E-03*	*76.75*	*2.59*
paleo68@7.ais	1.76E-03	6.98E-05	3.98E-01	1.73E-03	85.07	1.91
Avg	**2.53E-03**		**0.4739**		**89.36**	
s.d.	**1.10E-03**		**0.107**		**6.08**	
s.d.%	**43.22**		**22.65**		**6.80**	
Paleo 40/41, 330 Ma						
paleo40@3.ais	5.58E-03	2.29E-02	0.504	0.0428	87.21	0.91
paleo40@4.ais	5.55E-02	2.59E-02	0.665	0.1219	69.03	2.03
paleo40@5.ais	1.16E-01	2.59E-02	0.695	0.0616	62.65	0.63
Avg	**5.89E-02**		**0.621**		**72.97**	
s.d.	**3.19E-02**		**5.95E-02**		**7.36**	
s.d.%	**54.06**		**9.57**		**10.08**	
Paleo 77, 354 Ma						
paleo77@11.ais	1.61E-02	5.66E-04	1.81E-01	9.14E-04	35.04	0.34
paleo77@12.ais	1.27E-02	4.44E-04	2.02E-01	1.48E-03	36.45	0.72
paleo77@14.ais	2.29E-03	2.19E-04	3.10E-02	7.46E-05	10.87	0.48
paleo77@15.ais	4.06E-03	2.22E-04	1.33E-01	7.07E-04	19.38	1.09
Avg	**8.77E-03**		**0.137**		**25.44**	
s.d.	**3.33E-03**		**3.82E-02**		**6.21**	
s.d.%	**37.92**		**27.88**		**24.41**	

	Li/Ca mmol/mol	1 s.e	B/Ca mmol/mol	1 s.e	Mg/Ca mmol/mol	1 s.e
Paleo 76, 354 Ma						
paleo76@16.ais	3.29E-02	2.92E-03	3.14E-01	2.58E-03	28.26	0.27
paleo76@17.ais	1.85E-02	8.43E-04	4.12E-01	1.43E-02	35.67	0.52
paleo76@18.ais	2.48E-02	1.70E-03	4.26E-01	4.05E-03	34.23	0.65
Avg	**2.54E-02**		**0.384**		**32.72**	
s.d.	**7.23E-03**		**0.06**		**3.93**	
s.d.%	**28.50**		**15.83**		**12.01**	
Paleo 66, 354 Ma						
paleo66@1.ais	9.41E-03	4.02E-04	2.90E-01	2.19E-03	32.35	0.47
paleo66@2.ais	9.14E-03	4.96E-04	1.99E-01	1.02E-03	23.39	0.32
paleo66@3.ais	8.84E-03	6.19E-04	2.76E-01	3.31E-03	28.57	0.40
Avg	**9.13E-03**		**0.255**		**28.10**	
s.d.	**2.82E-04**		**4.91E-02**		**4.50**	
s.d.%	**3.09**		**19.25**		**16.00**	
Paleo 26, 385 Ma						
paleo26@10.ais	4.87E-03	1.72E-04	1.48E-02	4.09E-06	31.88	0.31
paleo26@11.ais	1.36E-02	9.18E-04	4.27E-02	9.14E-05	32.90	0.30
paleo26@12.ais	9.28E-03	3.50E-04	5.91E-02	1.38E-04	50.35	1.15
Avg	**9.24E-03**		**3.88E-02**		**38.38**	
s.d.	**4.35E-03**		**2.24E-02**		**10.38**	
s.d.%	**47.09**		**57.71**		**27.06**	

Appendix D: Reference Material SIMS Data

D.2: Intensity Ratios

Table D.2: Intensity ratios (Li/Ca, B/Ca, Mg/Ca, Fe/Ca, and Mn/Ca) of the standards used to normalize the cultured sea urchins and paleo-echinoderm data.

	$^{6}Li/^{42}Ca$	1 s.e.	$B/^{42}Ca$	1 s.e.	$Mg/^{42}Ca$	1 s.e.	$^{54}Fe/^{42}Ca$	1 s.e.	$Mn/^{42}Ca$	1 s.e.
M93 (Boron Standard)										
M93@14.ais	3.37E-03	2.15E-05	3.65E-02	1.12E-04	1.44E-01	5.16E-04	2.74E-05	4.68E-06	3.88E-04	1.37E-05
M93@16.ais	4.08E-03	2.37E-05	4.09E-02	1.20E-04	2.07E-01	1.77E-03	3.19E-05	7.67E-06	3.66E-04	1.22E-05
M93@17.ais	3.51E-03	2.63E-05	4.42E-02	1.97E-04	1.69E-01	1.03E-03	1.77E-05	5.39E-06	2.90E-04	1.22E-05
M93@18.ais	3.88E-03	2.34E-05	4.09E-02	9.82E-05	2.02E-01	1.09E-03	2.38E-05	5.76E-06	4.76E-04	1.35E-05
M93@19.ais	4.09E-03	2.82E-05	3.98E-02	1.09E-04	2.01E-01	1.36E-03	2.77E-05	5.20E-06	2.73E-04	1.74E-05
M93@20.ais	4.07E-03	2.36E-05	5.06E-02	1.76E-04	1.69E-01	1.23E-03	2.38E-05	2.53E-06	3.45E-04	1.08E-05
M93@21.ais	4.06E-03	2.36E-05	4.47E-02	1.40E-04	1.92E-01	1.99E-03	2.05E-05	3.53E-06	3.57E-04	1.62E-05
M93@22.ais	3.61E-03	2.52E-05	4.40E-02	1.58E-04	1.55E-01	6.72E-04	2.98E-05	4.74E-06	4.65E-04	2.10E-05
M93@23.ais	4.32E-03	3.00E-05	4.02E-02	2.59E-04	1.84E-01	6.57E-04	2.66E-05	3.68E-06	4.08E-04	1.97E-05
Avg			**4.24E-02**							
s.d.			**4.02E-03**							
s.d.%			**9.47**							
CAL-HTP (Lithium Standard)										
HTP@25.ais	2.48E-02	7.91E-05	4.33E-04	1.97E-05	2.22E-04	2.29E-05	8.05E-06	1.54E-06	9.53E-05	1.36E-05
HTP@26.ais	2.27E-02	6.51E-05	2.89E-04	1.77E-05	1.98E-04	2.19E-05	8.90E-06	1.83E-06	6.78E-07	6.55E-07
HTP@27.ais	2.40E-02	1.02E-04	2.99E-04	1.74E-05	1.84E-04	1.02E-05	6.11E-06	1.50E-06	3.30E-06	1.58E-06
HTP@28.ais	2.46E-02	6.12E-05	3.46E-04	1.97E-05	2.54E-04	1.52E-05	4.06E-06	1.53E-06	7.35E-05	1.06E-05
HTP@29.ais	2.39E-02	1.08E-04	3.19E-04	2.23E-05	1.86E-04	1.00E-05	5.13E-06	1.77E-06	5.10E-06	3.24E-06
Avg	**2.40E-02**									
s.d.	**8.28E-04**									
s.d.%	**3.45**									

	$^{6}Li/^{42}Ca$	1 s.e.	$B/^{42}Ca$	1 s.e.	$Mg/^{42}Ca$	1 s.e.	$^{54}Fe/^{42}Ca$	1 s.e.	$Mn/^{42}Ca$	1 s.e.
UCI-CC (Magnesium Standard)										
UCI.ais	8.56E-07	4.20E-07	1.12E-04	1.75E-05	0.127	1.40E-03	1.06E-05	1.70E-06	1.17E-01	3.43E-04
UCI@1.ais	0.00E+00	0.00E+00	7.14E-05	1.18E-05	0.126	9.73E-04	7.53E-06	2.28E-06	1.16E-01	6.07E-04
UCI@2.ais	1.31E-06	4.23E-07	5.59E-05	8.78E-06	0.126	1.10E-03	7.53E-06	1.66E-06	1.16E-01	6.84E-04
UCI@3.ais	3.43E-06	6.83E-07	4.77E-05	6.86E-06	0.126	1.06E-03	8.61E-06	2.56E-06	1.16E-01	5.44E-04
UCI@4.ais	1.21E-06	4.21E-07	6.66E-05	9.67E-06	0.127	1.23E-03	7.85E-06	1.88E-06	1.17E-01	4.74E-04
Avg					**0.126**					
s.d.					**8.10E-04**					
s.d.%					**0.64**					
NBS19 (Magnesium Standard)										
NBS19.ais	8.45E-05	4.19E-06	1.11E-04	1.87E-05	0.607	4.84E-03	5.10E-05	1.20E-05	1.43E-02	8.41E-05
NBS19@1.ais	6.51E-05	3.00E-06	3.45E-05	4.43E-06	0.654	4.87E-03	9.98E-05	8.63E-06	1.11E-02	1.16E-04
Avg					**0.631**					
s.d.					**3.29E-02**					
s.d.%					**5.21**					
LAS 20 (High Magnesium Standard)										
LAS20@1.ais	2.15E-02	7.67E-05	1.73E-04	2.23E-05	1.46	1.19E-02	6.95E-06	2.56E-06	1.51E-04	9.17E-06
LAS20@2.ais	2.17E-02	5.73E-05	1.81E-04	2.00E-05	1.45	9.96E-03	4.14E-06	2.05E-06	1.50E-04	6.68E-06
Avg					**1.45**					
s.d.					**1.45E-03**					
s.d.%					**0.10**					

References

Anderson, A. J., F. T. Mackenzie, and A. Lerman. "Coastal Ocean and Carbonate Systems in the High-CO_2 World of the Anthropocene." *American Journal of Science*, 2005: 875-918.

Barnes, Robert D. *Invertebrate Zoology.* Philadelphia: W.B. Saunders Company, 1963.

Beniash, Elia, Joanna Aizenberg, Lia Addadi, and Stephen Weiner. "Amorphous calcium carbonate transforms into calcite during sea urchin larval spicule growth." *The Royal Society*, 1997: 461-465.

Benninghoven, A., F.G. Rudenauer, and H.W. Werner. *Secondary ion mass spectrometry : basic concepts, instrumental aspects, applications, and trends.* New York: John Wiley & Sons, Inc., 1987.

Berner, Robert A., Antonio C. Lasaga, and Robert M. Garrels. "The Carbonate-Silicate Geochemical Cycle and Its Effect on Atmospheric Carbon Dioxide over the Past 100 Million Years." *American Journal of Science*, 1983: 641-683.

Brockington, Simon, and Andrew Clarke. "The relative influence of temperature and food on the metabolism of a marine invertebrate." *Journal of Experimental Marine Biology and Ecology*, 2000: 87-99.

Broecker, W. S., and T. H. Peng. *Tracers in the Sea.* Palisades, NY: El-Digio Press, 1982.

Broecker, Wally, and Jimin Yu. "What do we know about the evolution of Mg/Ca ratios in seawater?" *Paleoceanography*, 2011: 1-8.

Byrne, Maria, Melanie Ho, Paulina Selvakumaraswamy, Hong D. Nguyen, Symonl Dqorjanyn, and Andy R. Davis. "Temperature, but not pH, compromises sea urchin fertilization and early development under near-future climate change scenarios." *The Royal Society*, 2009: 1883-1888.

Chave, Keith E. "Aspects of the Biogeochemistry of Magnesium 2. Calcareous Sediments and Rocks." *The Journal of Geology*, 1954: 587-599.

Chester, Roy. *Marine Geochemistry .* London: Blackwell Science Ltd., 2000.

Courtney, Travis, Westfield, Isaac, Ries, Justin. "*Echinometra viridis* exhibits seasonal response in calcification rates to predicted end of 21st century CO_2-induced ocean acidification." *Journal of Experimental Marine Biology and Ecology*, 2013: 169-175.

Cutress, Bertha M. "Observations on Growth in *Eucidaris Tribuloides* (Lamarck), with Special Reference to the Origin of the Oral Primary Spines ." *Bulletin of Marine Science*, 1965: 797-833.

Delaney, Margaret Lois, Allan W. Be, and Edward A. Boyle. "Li, Sr, Mg, and Na in foraminiferal calcite shells from laboratory culture, sediment traps, and sediment cores." *Geochimica et Cosmochimica Acta*, 1985: 1327-1341.

Dickson, J.A.D. "Diagenesis and crystal caskets: echinoderm Mg calcite transformation, dry canyon, New Mexico, U.S.A." *Journal of Sedimentary Research*, 2001: 764-777.

Dickson, J.A.D. "Echinoderm skeletal preservation: calcite–aragonite seas and the Mg/Ca ratio of phanerozoic oceans." *Journal Sedimentary Research*, 2004: 355-365.

Dissard, D, G. Nehrke, G.J. Reichart, and J. Bima. "Impact of seawater pCO_2 on calcification and Mg/Ca and Sr/Ca ratios in benthic foraminfera caclite: results from culturing experiments with Ammonia tepida." *Biogeosciences*, 2010: 81-93.

Ebert, Thomas A. "Growth rates of the sea urchin *strongylocentrotus purpuratus* related to food availablity and spine abrasion." *Ecological Society of America*, 1968: 1075-1091.

Fabry, Victoria J., Brad A. Seibel, Richard A. Feely, and James C. Orr. "Impacts of ocean acidification on marine fauna and ecosystem process." *International Council for Exploration of the Sea*, 2008: 414-432.

Feely, R. A., S. C. Doney, and S. R. Cooley. "Ocean Acidification: Present Conditions and Future Changes in a High-CO_2 World." *Oceanography*, 2009: 36-47.

Foster, G.L. "Seawater pH, pCO_2 and [CO_2^{-3}] variations in the Caribbean Sea over the last 130 kyr: A boron isotope and B/Ca study of planktonic foraminifera." *Earth and Planetary Science Letters*, 2008: 254-266.

Furst, Marian, H.A. Lowenstam, and D.S. Burnett. "Radiographic Study of the Distribution of Boron in Recent Mollusc Shells." *Geochimica et Cosmochimica Acta*, 1976: 1381-1386.

Gilbert, P.U.P.A, and Fred H. Wilt. "Molecular Aspects of Biomineralization of the Echinoderm Endoskeleton." In *Molecular Biomineralization, Progress in Molecular and Subcellular Biology, Vol. 52*, by Werner Müller, 199-223. Berlin: Springer-Verlag, 2011.

Hall, Jenney M., and L-H Chan. "Li/Ca in multiple species of benthic and planktonic foraminifera: Thermocline, latitudinal, and glacial-interglacial variation." *Geochimica et Cosmochimica Acta*, 2004: 529-545.

Hardie, L.A. "Secular variation in seawater chemistry: An explanation for the coupled secular variation in the mineralogies of marine limestones and potash evaporites over the past 600 my." *Geology*, 1996: 279-283.

Hemming, Gary N., Richard J. Reeder, and Stanley R. Hart. "Growth-step-selective incorporation of boron on the calcite surface." *Geochimica et Cosmochimica Acta*, 1998: 2915-2922.

Hemming, N. G., and G. N. Hanson. "Boron Isotopic Composition and Concentration in Marine Carbonates." *Geochimica Et Cosmochimica Acta 56*, 1991: 537-534.

Hemming, N.G., R.J. Reeder, and G.N. Hanson. "Mineral-fluid partitioning and isotopic fractionation of boron in synthetic calcium carbonate." *Geochimica et Cosmochimica Acta*, 1994: 371-379.

Hendler, Gordon, John E Miller, David L. Pawson, and Porter M. Kier. *Sea Stars, Sea Urchins, and Allies: Echinoderms of Florida and the Caribbean.* Smithsonian, 1995.

Hershey, J. Peter, Marino Fernandez, Peter J. Milne, and Frank J. Millero. "The ionization of boric acid in NaCl, Na-Ca-Cl and Na-Mg-Cl solutions at 25C." *Geochimica et Cosmochimica Acta*, 1986: 143-148.

Hess, Hans, William I. Ausich, Carlton E. Brett, and Michael J. Simms. *Fossil Crinoids.* Cambridge: Cambridge Press, 1999.

Hinton, Richard W. "NIST SRM 610, 611 and SRM 612, 613 Multi-Element Glasses: Constraints from Element Abundance Ratios Measured by Microprobe Techniques." *Geostandards and Geoanalytical Research*, 1999: 197-207.

Honisch, Barbel, et al. "The Geological Record of Ocean Acidification." *Science*, 2012: 1058-1063.

Honisch, Barbel, N. Gary Hemming, David Archer, Mark Siddall, and Jerry F. McManus. "Atmospheric Carbon Dioxide Concentration Across the Mid-Pleistocene Transition." *Science*, 2009: 1551-1554.

Horita, J., H. Zimmermann, and H.D. Holland. "Chemical evolution of seawater during the Phanerozoic: Implications from the record of marine evaporites." *Geochimica et Cosmochimica Acta*, 2002: 3733-3756.

Huh, Youngsook, Lui-Heung Chan, Libo Zhang, and John M. Edmond. "Lithium and its isotopes in major world rivers: Implications for weathering and the oceanic budget." *Geochimica et Cosmochimica Acta*, 1998: 2039-2051.

Intergovernmental Panel on Climate Change. "Climate Change 2001: Synthesis Report." Wembley, 2001.

Jorgensen, Bo Barker, Johnathan Erez, Niels Peter Revsbech, and Yehuda Cohen. "Symbiotic photosynthesis in a planktonic foraminifera, *Globigerinoides sacculifer* (Brady), studied with microelectrodes." *American Society of Limnology and Oceanography, Inc.*, 1985: 1253-1267.

Kasemann, Simone A., Alistair B. Jeffcoate, and Tim Elliott. "Lithium Isotope Composition of Basalt Glass Reference Material." *Analytical Chemistry*, 2005: 5251-5257.

Kasemann, Simone A., Daniela N. Schmidt, Jelle Bijma, and Gavin L. Foster. "In situ boron isotope analysis in marine carbonates and its application for foraminifera and paleo-pH." *Chemical Geology*, 2009: 138-147.

Katz, Amitai. "The interaction of magnesium with calcite during crystal growth at 25–90°C and one atmosphere." *Geochimica et Cosmochimica Acta*, 1973: 1563-1586.

Katz, Miriam E., Zoe V. Finkel, Daniel Grzebyk, Andrew H. Knoll, and Paul G. Falkowski. "Evolutionary Trajectories and Biogeochemical Impacts of Marine Eukaryotic Phytoplankton." *Annual Review of Ecology, Evolution, and Systematics*, 2004: 523-556.

Kozloff, Eugene N. *Invertebrates.* Orlando: Saunders College Publishing, 1990.

Langer, Gerald, et al. "Species-specific responses of calcifying algae to changing seawater carbonate chemistry." *American Geophysical Union*, 2006: 1-12.

Laurent, Augustin, et al. "Eight glacial cycles from an Antarctic Ice core." *Nature*, 2004: 623-628.

Lawrence, John. *A Functional Biology of Echinoderms.* Baltimore: The John Hopkins University Press, 1987.

Lea, David W., Tracy A. Mashiotta, and Howard J, Spero. "Controls on magnesium and strontium uptake in planktonic foraminifera determined by live culturing." *Geochimica et Cosmochimica Acta*, 1999: 2369-2379.

Lear, Caroline H., and Yair Rosenthal. "Benthic Foraminiferal Li/Ca: Insights into Cenozoic seawater carbonate saturation state." *Geology*, 2006: 985-988.

Markel, K., and Ursula Roser. "The Spine Tissues in the Echinoid *Eucidaris tribuloides*." *Zoomorphology*, 1983: 25-41.

Marriott, Caedmon S., Gideon M. Henderson, Nick S. Belshaw, and Alexander W. Tudhope. "Temperature dependence of δ^7Li, δ^{44}Ca and Li/Ca during growth of calcium carbonate." *Earth and Planetary Science Letters*, 2004a: 615-624.

Marriott, Caedmon S., Gideon M. Henderson, Rebecca Crompton, Michael Staubwasser, and Sam Shaw. "Effect of mineralogy, salinity, and temperature on Li/Ca and Li isotope composition of calcium carbonate." *Chemical Geology*, 2004b: 5-15.

Michard, Annie, and Francis Albarede. "The REE Content of Some Hydrothermal Fluids." *Chemical Geology*, 1986: 51-60.

Miles, Hayley, Stephen Widdicombe, John I. Spicer, and Jason Hall-Spencer. "Effects of anthropogenic seawater acidification on acid–base balance in the sea urchin Psammechinus miliaris." *Marine Pollution Bulletin*, 2007: 89–96.

Montanez, Isabel P. "Biological skeletal carbonate records changes in major-ion chemistry of paleo-oceans." *PNAS*, 2002: 15852-15854.

Nooijer De, Lennart, Takashi Toyofuku, and Hiroshi Kitazato. "Foraminifera Promote Calcification by Elevating Their Intracellular pH." *PNAS* , 2009: 1-5.

Nurnberg, Dirk, Jelle Bijma, and Christoph Hemleben. "Assessing the reliability of magnesium in foraminferal calcite as a proxy for water mass temperatures." *Geochimica et Cosmochimica Acta*, 1996: 803-814.

Okumura, Minoru, and Yasushi Kitano. "Coprecipitation of alkali metal ions with calcium carbonate." *Geochimica et Cosmochimica Acta*, 1986: 49–58.

Onuma, N., F. Masuda, M. Hirano, and K. Wada. "Crystal structure control on trace element partition in molluscan shell formation." *Geochimica et Cosmochimica Acta*, 1979: 187-189.

Paul, C.R.C., and A.B Smith. "The Early Radiation and Phylogeny of Echinoderms." *Biology Review*, 1984: 443-481.

Petit, J.R., et al. "Climate and atmospheric history of the past 420,000 years from the Vostok ice core, Antarctica." *Nature*, 1999: 429-413.

Politi, Yael, Talmon Arad, Eugenia Klein, Steve Weiner, and Lia Addadi. "Sea Urchin Spine Calcite Forms via a Transient Amorphous Calcium Carbonate Phase." *Science*, 2004: 1161-1164.

Ries, Justin B. "Skeletal mineralogy in a high-CO_2 world." *Journal of Experimental Marine Biology and Ecology*, 2011: 54-64.

Ries, Justin B., Anne L. Cohen, and Daniel C. McCorkle. "Marine Calcifiers exhibit mixed responses to CO_2-induced ocean acidification." *Geological Society of America*, 2009: 1131-1134.

Rollion-Bard, C., and J. Erez. "Intra-shell boron isotope ratios in the symbiont-bearing benthic foraminiferan Amphistegina lobifera: implications for $\delta^{11}B$ vital effects and paleo-pH reconstructions." *Geochimica et Cosmochimica Acta*, 2010: 1530-1536.

Rosenthal, Yair, Edward A. Boyle, and Niall Slowey. "Temperature control on the incorporation of magnesium, strontium, fluorine, and cadmium into benthic foraminiferal shells from Little Bahama Bank: Prospects for thermocline paleoceanography." *Geochimica et Cosmochimica Acta*, 1997: 3633-3643.

Russell, Ann D., Barbel Honisch, Howard J. Spero, and David W. Lea. "Effects of seawater carbonate ion concentration and temperature on shell U, Mg, and Sr in cultured planktonic foraminifera." *Geochimica et Cosmochinica Acta*, 2004: 4347-4361.

Sarmiento, Jorge L., and Nicolas Gruber. *Ocean Biogeochemical Dynamics.* Princeton: Princeton University Press, 2006.

Schneider, Kenneth, and Johnathan Erez. "The effect of carbonate chemistry on calcification and photosynthesis in the hermatypic coral *Acropora eurystoma*." *The American Society of Limnology and Oceanography, Inc.*, 2006: 1284-1293.

Shirayama, Y., and H. Thorton. "Effect of increased atmospheric CO_2 on shallow water marine benthos." *Journal of Geophysical Research*, 2005: 1-7.

Siikavuopio, Sten I., Jørgen S. Christiansen, and Trine Dale. "Effects of temperature and season on gonad growth and feed intake in the green sea urchin (*Strongylocentrotus droebachiensis*)." *Aquaculture*, 2006: 389-394.

Spicer, J.I. "Oxygen and acid-base status of the sea urchin *Psammechinus miliaris* during environmental hypoxia." *Marine Biology*, 1995: 71-76.

Stanley, Steven M., Justin B. Ries, and Lawrence A. Hardie. "Low-magnesium calcite produced by coralline algae in seawater of Late Cretaceous composition." *PNAS*, 2002: 15323–15326.

Stoll, Heather, Gerald Langer, Nobumichi Shimizu, and Kinuyo Kanamaru. "B/Ca in coccoliths and relationship to calcification vesicle pH and dissolved inorganic carbon concentrations." *Geochimica et Cosmochimica*, 2011.

Su, X., S. Kamat, and A.H. Heuer. "The structure of sea urchin spines, large biogenic single crystals of calcite." *Journal of Material Science*, 2000: 5545-5551.

Taylor, S.R., and S.M McLennan. *The continental crust: Its composition and evolution.* Palo Alto: Blackwell Scientific, 1985.

Tripati, Aradhna K., Christopher D. Roberts, and Robert A. Eagle. "Coupling of CO_2 and Ice Sheet Stability Over Major Climate Transitions of the Last 20 Million Years." *Science*, 2009: 1394-1397.

Tripati, Aradhna K., Roberts, Christopher D., Eagle, Robert A., Li, Gaojun. "A 20 million year record of planktonic foraminiferal B/Ca ratios: Systematics and uncertainties in pCO_2 reconstructions." *Geochimica et Cosmochimica Acta*, 2011: 2582-2610.

Tunusoglu, O., T. Shahwan, and A. E. Eroglu. "Retention of aqueous Ba^{2+} ions by calcite and aragonite over a wide range of concentrations: Characterization of the uptake capacity, and kinetics of sorption and precipitate formation." *Geochimical Journal*, 2007: 379-389.

Turekian, Karl K. *Oceans.* Michigan: Prentice-Hall, 1968.

Vigier, Nathalie, Claire Rollion-Bard, Silvia Spezzaferri, and Fabrice Brunet. "*In situ* measurements of Li isotopes in foraminifera." *Geochemistry, Geophysics, and Geosystems*, 2007: 1-9.

Wilkinson, B.H., and T.J. Algeo. "Sedimentary carbonate record of calcium–magnesium cycling." *American Journal of Science*, 1989: 1158-1194.

Wilt, Fred, and Steve Benson. "Development of the endoskeletal spicule of the sea urchin embryo." *Self-assembling architecture*, 1988: 203-227.

Wood, Hannah L., John I. Spicer, and Stephen Widdicombe. "Ocean acidification may increase calcification rates, but at a cost." *Proceedings of the Royal Society Biological Sciences*, 2008: 1767-1773.

Yokota, Y. "Introduction to Sea Urchin Biology." In *The Sea Urchin: From Basic Biology to Aquaculture*, by Yukio Yakota, Valeria Matranga, & Zuzana Smolenicka, 1-10. Lisse: A.A. Balkema Publishers, 2002.

Yu, Jimin, Gavin L. Foster, Henry Elderfeld, WAllace S. Broecker, and Elizabeth Clark. "An evaluation of benthic foraminiferal B/Ca and ^{11}B for deep ocean carbonate ion and pH reconstructions." *Earth and Planetary Science Letters*, 2011: 1-7.

Yu, Jimin, Henry Elderfield, and Barbel Honisch. "B/Ca in Planktonic Foraminifera as a Proxy for Surface Water pH." *Paleoceanography*, 2007: 1-17.

Zeebe, Richard E., Jelle Bijma, Barbel Honisch, Abhijit Sanyal, Howard J. Spera, and Dieter A. Wold-Gladrow. "Vital effects and beyond: a modeling perspective on developing palaeoceanographic proxy relationship in foraminifera." *Geological Society of London*, 2008: 45-58.

.